Extraction of bioactive compounds from *Ficus auriculata* leaves and its application

Thesis submitted in partial fulfillment of the requirements

for the degree of

DOCTOR OF PHILOSOPHY

by

Thangsei Nengneilhing Baite

Roll No.: 176107031

Department of Chemical Engineering

Indian Institute of Technology Guwahati

Guwahati 781039, India

August 2023

Extraction of bioactive compounds from *Ficus auriculata* leaves and its application

Thangsei Nengneilhing Baite

Dedicated to my Parents for their sacrifices, faith, love and support

Department of Chemical Engineering
Indian Institute of Technology Guwahati
Guwahati 781039, India

STATEMENT

I hereby declare that the content embodied in the thesis entitled "**Extraction of bioactive compounds from *Ficus auriculata* leaves and its application**" is the result of investigations carried out by me at the Department of Chemical Engineering, Indian Institute of Technology Guwahati, India, under the guidance of Prof. Bishnupada Mandal and Prof. Mihir Kumar Purkait. In keeping with the general practice of reporting scientific observations, due acknowledgements have been made wherever the work described is based on the findings of other investigators.

Thangsei Nengneilhing Baite

Department of Chemical Engineering

Indian Institute of Technology Guwahati

Guwahati 781039, India

CERTIFICATE

It is certified that the work reported in the thesis entitled "**Extraction of bioactive compounds from *Ficus auriculata* leaves and its application**", by **Thangsei Nengneilhing Baite**, has been carried out under our supervision. The work documented in this thesis has not been submitted to any other University or Institute for the award of any degree or diploma.

This thesis in our opinion, has reached the standard fulfilling the requirements for the award of the degree of Doctor of Philosophy in accordance with the regulations of the institute.

Dr. Bishnupada Mandal

Professor

Department of Chemical Engineering

Indian Institute of Technology Guwahati

Guwahati 781039, India

Dr. Mihir Kumar Purkait

Professor

Department of Chemical Engineering

Indian Institute of Technology Guwahati

Guwahati 781039, India

Acknowledgements

This thesis becomes a reality with the kind support and help of many individuals. It is a genuine pleasure to express my deep sense of thanks and gratitude to all who helped me in the completion of this thesis.

First and foremost, I would like to thank ***God*** *for giving me strength and encouragement throughout all the challenging moments of completing this thesis. I am truly grateful for His unconditional and endless love, mercy, and grace.*

I wish to express my deepest gratitude and appreciation for my supervisors, ***Prof. Bishnupada Mandal*** *and* ***Prof. Mihir Kumar Purkait*** *for providing me invaluable guidance throughout the various stages of my research journey. I am indebted to them for their positive inputs and constant encouragement throughout my entire journey. I am grateful to them for their great support in every way which helped me to finish this work.*

I would like to extend my sincere gratitude to my doctoral committee members ***Prof. G. Pugazhenthi*** *(Department of Chemical Engineering),* ***Prof. Chandan Das*** *(Department of Chemical Engineering) and* ***Prof. Lal Mohan Kundu*** *(Department of Chemistry) for their valuable suggestions and constructive criticism during the project evaluations, which helped me to make necessary improvements in various stages of my research work.*

I am extremely grateful to my ***thesis examiners*** *for their insightful advice that helped me improve the quality of the thesis.*

I would like to acknowledge all the centres for providing me various facilities required for my analysis and characterization during the research work specifically, ***Analytical Lab Facility*** *(Department of Chemical Engineering),* ***Central Instrument Facility*** *(IITG), Centre for the Environment (IITG), Centre for Nanotechnology (IITG), and* ***Department of Chemistry*** *(IITG). I would also like to thank* ***Guwahati Biotech Park*** *for allowing me to conduct my analysis. Further, I would like to acknowledge* ***North East Institute of Science and Technology****, Jorhat, for providing the XPS facility required for the thesis work.*

I am also grateful to all the ***faculty*** *and* ***staff*** *members of the Department of Chemical Engineering for helping and providing me the necessary facilities and resources.*

Acknowledgements

*I would like to thank my **seniors** (Dr. Babul Prasad, Dr. Rajashree Borgohain, Dr. Pradip Das, Dr. Murchana Changmai, Dr. Abhik Bhattacharjee, Dr. Piyal Mondal, Mr. Saptarshi Gupta, Dr. Debarati Mukherjee and Dr. Sukanya Kundu) and **colleagues** (Geetanjali, Ida, Deepti, Anweshan, Pranjal, Simons, Ankush, Niladri, Purnima, Shikha, Aviti, Shubham, Ahana, Shashi, Kumari, Nagaphani, Mukesh, and Satish) for always being there when I need them.*

*I am immensely grateful to my **friends** (Moite, Emily, Serena, Christy, Jenifer, and Punam) who are a constant source of support through all my ups and downs. I can never thank them enough for all the ways they have supported me and stood by me each and every step of the way.*

*I would like to express my utmost gratitude towards **Mr. T. T. Haokip** (Joint Registrar, IITG) and his family for all their love and support and for providing me with a feeling of home during the course of my PhD journey. I am very thankful to my relatives and all my well-wishers who are directly or indirectly involved in my research journey.*

*My final words go to my family whom I am abundantly blessed with for all their unconditional love, sacrifices and encouragement. I am greatly indebted to my **mom (Nemjalam)** and **dad (Seikholet), siblings (Kimboi, Nei Prescilla, Haopu,** & **Mordecai), sisters- (Rachel** & **Chingboi)** and **brothers-in-law (Haopu** & **Hemin), nephews (Goulun, Christopher, Goulen** & **Asher)** and **nieces (Khanthem, Hazel,** & **Grace)**, whose unwavering support made it possible for me to come so far.*

Thangsei Nengneilhing Baite

Abstract

The primary objective of this thesis is the extraction of bioactive compounds from *Ficus auriculata* leaves and exploration of its potential application. Gallic acid was extracted from *F. auriculata* leaves using green process. The gallic acid – rich extract was used as an additive for coating of green bananas to delay the ripening process. The extract was also used as the active ingredient in the preparation of antioxidant formulations. The by-product obtained after extraction was used for synthesis of valuable biomaterial and studied for its potential application in food packaging. The abstract of this work is shown below.

Gallic acid is a well-known antioxidant ascribed to various beneficial health effects and is found in a variety of plants. At first, gallic acid was extracted from *F. auriculata* leaves using ultrasound assisted extraction and the process parameters were optimized. The influence of time (5 – 60 min), temperature (30 – 75 °C), sonication level (30 – 70%) and solid to solvent ratio (1:5 – 1: 40 g/mL) on gallic acid extraction was investigated. Maximum extraction was obtained after 30 min at 50% sonication level, 1:10 g/mL solid to solvent ratio and pH 8 at 50 °C. Among the various solvents, 50% methanol resulted in highest extraction followed by alkaline water and 50% ethanol where gallic acid content in the extract was found to be 329.46 mg/L, 312.92 mg/L and 183.74 mg/L, respectively. Sonication bath was found to perform better in extracting and retaining extracted gallic acid as compared to probe sonication. The kinetics of the extraction was studied and Peleg model was found to have the best correlation with highest R^2 value (0.99). The extracted gallic acid was purified using reverse osmosis and HPLC.

The gallic acid (antioxidant) rich leaf extract of *F. auriculata* was then incorporated into polyvinyl alcohol (PVA) and utilized as a coating to delay the ripening of green bananas. The

films exhibited low opacity of 0.86 ± 0.014 for pure PVA (PP) and 0.92 ± 0.019, 0.99 ± 0.020 and 1.18 ± 0.029 for PVA+1% extract (PE1), PVA+5% extract (PE5), and PVA+10% extract (PE10), respectively, signifying excellent transparency. The weight loss was higher in the uncoated group than in any coated fruits. The reduction in titratable acidity and the increase in total soluble sugars was slower in all the coated samples, as compared to the uncoated ones. The fruits without any treatment attained complete maturity on the 9th day where the ion leakage was 85.61±2.33% while that of PP was 56.36±2.95% and that of PE1, PE5, and PE10 remained below 30%. The coated samples showed better retention and consequently slower degradation of chlorophyll. The fruits coated with pure PVA as well as 10% extract incorporated PVA remained acceptable till day 15, while the ones with 1% and 5% of extract reached full ripeness on the18th day.

The extracted gallic acid was further used as the active ingredient for the preparation of antioxidant formulations. The excipients were derived from commonly available raw materials such as starch, sucrose, and glucose, and the formulations were prepared by varying the amount of each component. Six formulations were prepared and denoted as F1, F2, F3, F4, F5, and F6. Out of the six formulations prepared, F1, F5, and F6 were obtained as free flowing powders and were found to be suitable for tabletting. The formulations F2, F3, and F4 remained sticky due to higher content of hygroscopic components. The free-flowing formulations were formed into tablets using a hand-operated pellet maker. All the tablets had disintegration times below 15 min, which meet the standards of the Indian Pharmacopeia. The antioxidant activity of the formulations was found to increase with an increase in the gallic acid-rich extract content where the activity for F1, F5, and F6 were found to be

83.78%, 33.51%, and 78.92%, respectively. The formulations were found to be stable at pH 2.5 and 8.5, signifying a good stability in the gastrointestinal tract.

Further, lignin was extracted from the waste leaves of *F. auriculata* obtained after separation of gallic acid. The synthesized lignin was incorporated into PVA films. The neat and blend PVA films were characterized using different techniques. The lignin blend films showed sufficient transparency for their use in food packaging. Lignin addition improved the UV-shielding, thermal, antioxidant and mechanical property of PVA films. The water solubility decreased from 31.86% to 12.19 ± 3.13%, 11.21 ± 2.67% and 7.14 ± 1.94%, while the water vapour permeability increased from 3.85 ± 0.21 $\times 10^{-7}$ g.m.h^{-1}Pa^{-1} to 3.92 ± 0.15, 5.16 ± 0.18 and 7.84 ± 0.64 $\times 10^{-7}$ g.m.h^{-1}Pa^{-1} for pure PVA and films containing 1%, 3%, and 5% lignin, respectively. The prepared films showed a much better performance than commercial packaging films in inhibiting mold growth during storage of preservative – free bread storage. The bread samples packed with commercial package showed signs of mold growth on the 3rd day while the growth was completely inhibited till 15th day for PVA film containing 1% lignin. The pure PVA film and the ones containing 3% and 5% of lignin inhibited growth till the 12th and 9th day, respectively. Findings from the current study shows that safe, cheap and eco – friendly biomaterials can inhibit the growth of spoilage microorganisms and thus potentially be used in food packaging.

Research Publications

Published

1. **Baite, T. N**., Mandal, B., and Purkait, M. K., 2021. Ultrasound assisted extraction of gallic acid from *Ficus auriculata* leaves using green solvent. *Food and Bioproducts Processing*. https://doi.org/10.1016/j.fbp.2021.04.008
2. **Baite, T.N**., Mandal, B., and Purkait, M.K., 2022. Antioxidant-Incorporated Poly (vinyl alcohol) Coating: Preparation, Characterization, and Influence on Ripening of Green Bananas. *ACS Omega*. https://doi.org/10.1021/acsomega.2c05271
3. **Baite, T.N.,** Mandal, B., and Purkait, M.K., 2023. Lignin synthesis from waste leaves and its potential application for bread packaging: A waste valorization approach. *International Journal of Biological Macromolecules*. https://doi.org/10.1016/j.ijbiomac.2023.123880

Communicated

4. **Baite, T.N.,** Mandal, B., and Purkait, M.K. Ultrasound based hybrid extraction techniques of phenolic compounds from agricultural sources: A review.

Conference/Presentations

1. Baite, T. N., Mandal, B., and Purkait, M. K.; A study on green extraction method for gallic acid from Ficus auriculata leaves, CHEMCON – 2020, 27 – 29 December, 2020 (Virtual mode).
2. Baite, T. N., Mandal, B., and Purkait, M. K.; Plant extract mediated green synthesis of zinc oxide nanoparticles as a food packaging additive. International Conference on Sustainable Approaches in Food Engineering and Technology, 24-25 June, 2021 at Tezpur University, Assam, India.
3. Baite, T. N., Mandal, B., & Purkait, M. K.; Synthesis and Characterization of Lignin Nanoparticles for Functional Property Enhancement of Biopolymers, Advances in Chemical and Material Sciences, 14 – 16 April, 2022 at Heritage Institute of Technology, Kolkata, West Bengal, India.
4. Baite, T. N., Mandal, B., & Purkait, M. K.; Utilization of extract and by-products of *Ficus auriculata* leaves, Research and Industrial Conclave, 14 – 16 May, 2023 at Indian Institute of Technology Guwahati, Assam, India.

CONTENTS

CONTENTS

LIST OF FIGURES

LIST OF FIGURES

LIST OF TABLES

Nomenclature

Notations

D_B	Bulk density
D_T	Tapped density
h	Height
k_1	initial rate (1/min)
k_2	const. related to maximum extraction yield (1/min)
k_3	rate constant (min^{-n})
k_4	initial yield
k_5	diffusion coefficient
k_6	washing coefficient
k_7	rate constant
m/z	Mass-to-charge ratio
n	diffusional exponent
Θ	Angle of repose
r	Radius
V_0	Initial volume
V_F	Final volume/ Filtrate volume
W_f	Final weight after drying
W_i	Initial weight before drying
ε	Extinction coefficient

Abbreviations

A	Absorbance
AA	Antioxidant activity

AFM	Atomic force microscopy
AIL	Acid insoluble lignin
ANOVA	Analysis of variance
API	Active pharmaceutical ingredient
ASL	Acid soluble lignin
ATR	Attenuated total reflectance
Bx	Brix
CAE	Constant analyzer energy
CHNS	Carbon, hydrogen, nitrogen, and sulphur
cm	Centimetres
DF	Dilution factor
DPPH	2,2-diphenyl-1-picrylhydrazyl
DTG	Differential thermogravimetry
EA	Elemental analyzer
FC	Folin – Ciocalteu
FESEM	Field emission scanning electron microscope
FFS	Film-forming solution
FTIR	Fourier- transform infrared spectroscopy
g	Grams
GAE	Gallic acid equivalents
GPD	Gallons per day
GRAS	Generally Recognized As Safe
h	Hour
H_2SO_4	Sulphuric acid
HCl	Hydrochloric acid

HNO_3	Nitric acid
HPLC	High Performance Liquid Chromatography
KBr	Potassium bromide
kHz	Kilo Hertz
L	Litres
LCMS	Liquid Chromatography Mass Spectrometer
m	Metre
M	Molar
M.W.	Molecular weight
mg	Milligrams
min	Minute
mL	Millilitres
mm	Millimetres
mM	Millimolar
MSI	Membrane stability index
MTT	3-(4,5-dimethylthiazol-2-yl)-2,5-diphenyltetrazolium bromide
NaOH	Sodium hydroxide
nm	Nanometres
NMR	nuclear magnetic resonance
Pa	Pascal
ppm	Parts per million
PVA	Poly(vinyl alcohol)
RH	Relative humidity
RI	Refractive index
RMS	Root mean square

RO	Reverse osmosis
RPM	Rotations per minute
s	Seconds
SD	Standard deviation
SDS	Sodium dodecyl sulfate
SR	Solid residue
TA	Titratable acidity
TGA	Thermogravimetric analyzer
TOF	Time-of-flight
TPC	Total phenolic content
TSS	Total soluble solids
UV – Vis	UV – Visible
UV	Ultra-violet
WL	Weight loss
WVP	Water vapour permeability
WVTR	Water vapour transmission rate
XPS	X-ray photoelectron spectroscopy

Chapter 1

Introduction, Literature Review, Objectives and Organization of the Thesis

Chapter 1

Introduction, Literature Review, Objectives and Organization of the Thesis

This chapter discusses a brief summary of the fundamentals of plant based natural antioxidants. The state-of-the art literature on extraction of bioactive compounds from plants using green extraction methods is summarized. The potential application of extracted bioactive compounds from plants in preserving shelf life of perishable produces are explored here. The path for easy development of antioxidant formulation is also described. Furthermore, the utilization of extraction by-product as raw material for recovery of valuable biomaterial and its application is elaborated. Finally, the objectives of the present work and the outline of the thesis work is highlighted.

1.1. Background

Antioxidants are known to exhibit health related benefits by inhibition of various undesirable changes that lead to cell deterioration and consequently potential ailments. Owing to the associated beneficial effects on health, antioxidants have gained popularity for use in food and pharmaceutical industries. Antioxidants are present in varying quantities in a wide range of natural sources and plant parts such as fruits and leaves. Phenolic compounds are defined as substances with one or more hydroxyl groups joined to one or more benzene rings, depending on the compound. The components that link these rings together and the number of phenolic groups in these compounds are used to classify them. Their structure can range from straightforward molecules like phenolic acids to more intricate ones like condensed tannins. Phenolic acids, stilbenes, lignans, and flavonoids are the most prevalent classes of polyphenols and make up the largest number of compounds. The two subclasses of phenolic acids—which represent the group with a simpler structure—are hydroxybenzoic acids and cinnamic acids. The most prevalent secondary metabolite found in plants, phenolics are thought to be produced as a defence mechanism against pathogens and harsh environmental conditions. They exhibit significant positive health effects and are recognised as

powerful antioxidants with a key role in a variety of pharmacological functions. They are crucial in different stages of plant growth and development. However, phenolic compounds frequently interact with other food ingredients, making it more difficult to fully understand them.

The present study aims to use the traditionally used medicinal plant, Roxburgh Fig (*Ficus auriculata*), as a source to extract gallic acid. The Roxburgh fig tree (*Ficus auriculata* Lour.) is a small tree whose different parts have been used for ages, both for culinary and medicinal purposes. The leaf and fruit parts of *F. auriculata* are reported to have antioxidant, anti-inflammatory and antibacterial activities (Al Fishawy et al., 2011). Use of leaf parts and paste as well as stem bark for treatment of diabetes, diarrhoea, dysentery, cuts and wounds have also been reported (Gaire et al., 2011; Shrestha and Dhillion, 2003). The analysis of the stem extract of *F. auriculata* showed the presence of flavonoids, phytosterols, resins, alkaloids, glycosides, diterpenes, carbohydrates, saponins, proteins, amino acids, phenols and tannins. The use of various parts of this tree for medicinal purposes is attributed to the presence of bioactive compounds. The methanolic fruit extract of *F. auriculata* is reported to contain a significant gallic acid content of 23.93 mg/100 g of fruit weight (Saini et al., 2012). The analysis of the leaf extract showed a high total phenolic and flavonoid content resulting in high antioxidant activity (Thingbaijam et al., 2012).

1.2. Extraction of phenolic compounds from natural sources

Currently, extraction and chemical synthesis are the main methods used to produce phenolic compounds on a large scale for various applications. Although extraction is still the most popular method, the high cost of solvents used, the higher energy requirement, and the negative effects on the environment, are the major drawbacks. The effectiveness of extraction process is greatly influenced by the choice of suitable extraction techniques. This depends on a number of variables, the most important of which are the type of extraction method, sample matrix, and solvent. Regarding their ability to be extracted, phenolic compounds can be divided into two groups: the ones

that can be extracted using water or aqueous organic solvent mixtures, and the others that cannot be extracted and remain on the feed. Different kinds of bioactive compounds are extracted using conventional and non-conventional methods. The traditional or conventional methods involve the use of sizable amounts of organic solvents, high temperatures, and agitation. The shortcomings of conventional methods can be overcome by safer and cleaner non-conventional techniques. The polarity of the target compounds, their heat sensitivity as well as the intended end use may have an impact on the extraction method selection. Following extraction, the extracts are screened using a number of analytical characterization techniques for determination and identification of the phenolic contents. High–performance liquid chromatography (HPLC) coupled with UV– spectrophotometry is an easy analytical method for analysis of phenolics, however, it cannot sufficiently identify the compounds (Chen et al., 2001). Liquid chromatography–mass spectrometry (LC-MS) is widely used since it combines the separation ability of LC with confirmation and identification power of MS. Gas chromatography – mass spectrometry (GC-MS) is commonly used for the analysis of volatile samples, however, the analysis of non – volatile samples necessitate an additional step of chemical derivatization (Deng and Zito, 2003). LC coupled with diode array detector (DAD) and MS is being increasingly used for characterization of bioactive compounds in biological sources and food systems (Harnly et al., 2007).

The separation and recovery of phenolic compounds from different agricultural sources have been the focus of many studies. Gallic acid is a phenolic acid present in a wide range of plant families including *F. auriculata* as mentioned above. It is a well-known antioxidant compound, which has been claimed to improve cardiac dysfunction and fibrosis in certain cases of heart failure (Jin et al., 2018; Kang et al., 2015; Shi et al., 2011; Variya et al., 2020). Phenolic acids as free radical scavengers has also been reported to perform better than other antioxidant enzymes (Chen et al., 2020). The extraction of gallic acid from different agricultural sources and industrial wastes has previously been studied by different researchers. However, most of the studies used conventional hydro alcoholic solvents, pressurised liquid or ionic-liquid based solvents (Lin et al., 2017). The conventional techniques also include enzyme assisted extraction,

maceration extraction, reactive extraction, adsorption and membrane separation (Athankar et al., 2016; Dhadge et al., 2019; Ena et al., 2012; Mushtaq et al., 2015). Separation methods like ultrasound based emulsification (Becerril-Bravo et al., 2010), solid-phase micro-extraction (Asfaram et al., 2017) and cloud point extraction (Purkait et al., 2009, 2006) have also been studied for separation of non – food components. The traditional methods involve high temperature, complex experimental requirement, longer extraction duration and usage of large quantities of organic solvents. This in turn leads to possible destruction of heat sensitive compounds, higher energy consumption and a negative environmental impact from the disposal of the chemicals. Additionally, even a trace amount of organic solvent could pose a problem of toxicity if present in the end product, especially in the applications in food systems. To overcome the shortcomings of conventional methods, some emerging methods have also been employed including pressurised liquid extraction (Souza et al., 2020), microwave assisted extraction (Li et al., 2016; Liu et al., 2016) and ultrasound assisted extraction (Cláudio et al., 2012; Plazzotta et al., 2020).

1.3. Coating of fruits as a means of preservation

Global food waste has increased as a result of the growing demand for agricultural products, the ongoing population growth, and the growing consumption of agricultural products despite technological advancements. Fruits and vegetables serve as the major sources of vitamins and minerals. According to the Food and Agriculture Organization (FAO), fruit and vegetable waste occurs throughout the entire food supply chain globally at a rate of 40% to 50% (Parsafar et al., 2023). That is to say, more than a third of the fruits and vegetables that are produced globally are lost before they are consumed (Yavari et al., 2022). This equates to 28 million tonnes of waste (Abadi et al., 2021). Average fruit and vegetable wastes have been reported to be between 2% and 20% and 24% and 40%, respectively, in both developed and developing nations (Golshan et al., 2017). Several factors contribute to the large amounts of produce that are wasted in supermarkets and among their suppliers. Short shelf lives, transportation and packaging issues, poor demand forecasting, and high quality standards that prioritise a product's

aesthetic appearance are a few of them (Teller et al., 2018; Tromp et al., 2016). Hence, there is an increased need for reducing food losses using cheap and sustainable processes.

The abrupt changes in the majority of metabolic processes that occur before and after fruit ripening have a significant impact on senescence, and this has received a lot of attention. When ethylene production peaks during ripening, it is common to notice an increase in respiration rate, which is a sign of climateric ripening (Jafarzadeh et al., 2021). When describing climacteric fruits, which reach full physiological maturity at a specific developmental stage even after being removed from the tree or plant, the patterns of CO_2 and ethylene productions are typically used as criteria (Zhang et al., 2018). By converting starch into sugar, climateric fruits like plums, peaches, bananas, cantaloupe, kiwi, and pears continue to develop flavour and get sweeter. They are extremely vulnerable to the ethylene gas that is produced. Therefore, it's crucial to use some preventive methods to control ethylene and CO_2 production, microbial safety, and sensory quality of climacteric fruits during the storage period.

The application of coating to extend the commercial shelf stability of various types of foods has gained substantial research interest in the recent past. They are particularly successful in the preservation of fresh fruits. Coatings aid in improving the shelf stability of fruits by creating a semi-permeable barrier and a modified atmosphere with a controlled exchange of moisture and metabolic gases such as oxygen, carbon dioxide, and ethylene. This consequently prolongs the shelf life by delaying the ripening and inhibiting the activity of spoilage-causing microorganisms (Wantat et al., 2021).

Banana is amongst the most widely consumed and popular fruits in the world that act as a staple food for many communities owing to its nutritional content and taste (Soradech et al., 2017). Banana is a climacteric fruit with a high moisture content which makes it highly perishable due to rapid postharvest physicochemical changes (Yang et al., 2022). Despite the large popularity, the low shelf life of bananas poses a significant commercial loss, especially where provisions for low-temperature storage are absent or less (Peroni-Okita et al., 2013). The commonly practiced post-harvest treatment of

bananas includes controlled atmosphere storage, low-temperature storage, and the application of ethylene inhibitors (Deng et al., 2017; Zhu et al., 2015). However, their application may be limited by chilling injury resulting from cold storage, non-uniform ripening, and high processing cost, among others, which make them infeasible for the majority of the banana-producing population (Deng et al., 2017). This necessitates the development of a simple and economical yet effective technique for the preservation of bananas and other perishable products.

1.4. Antioxidant formulations

Every culture throughout history has used herbal products. For the diagnosis, prevention, and treatment of numerous diseases, many traditional herbal medical practises have been adopted. The presence of the bioactive compounds discovered having antioxidant, anti-inflammatory, and antibacterial properties of *F. auriculata*'s leaf and fruit parts may be accredited for the various uses of this tree's medicinal parts. Gallic acid is a phenolic acid found in a variety of plant families, including *F. auriculata*. It is a well-known antioxidant substance that has been credited with reducing cardiac fibrosis and dysfunction in some heart failure patients. This means that increasing the intake of gallic acid—either through diet in small amounts or in concentrated forms—may aid in the prevention of cancer-related diseases and the treatment of specific types of cancer. Additionally, gallic acid has demonstrated promise in the treatment of conditions like diabetes by improving insulin sensitivity, reducing the risk of cardiovascular disease, and preventing weight gain thanks to better cholesterol metabolism. These days, there are numerous formulations of herbal medicine products. Liquid, powder, capsules, or tablets can all be used to prepare it. Along with other qualities related to the powdered herbs and plants, a herbal extract/powder combination has the typical characteristics of a viscous plant extract. Among oral solid pharmaceutical dosage forms, tablets are the most widely used and convenient type (Nguyen et al., 2013). Direct compression has advantages over other tableting methods like wet granulation because it processes materials more quickly, uses fewer excipients, and poses less of a stability risk. Mostly made up of carbohydrates,

dried herbal extracts are amorphous and have a high hygroscopicity because of their high affinity for the surrounding water vapour. These characteristics may negatively impact the manufacturing process as well as the final product's quality (Tong et al., 2008). When herbal tablets are prepared by wet granulation using aqueous granulation fluid, an agglomeration of granules frequently occurs because of the high aqueous viscosity of the extract portion. As a result, ethanol is a more commonly used non-aqueous binder (Colorcon, 2017).

Over the past decades, chewable tablets have gained considerable attention as a preferred alternative to conventional tablets and capsules due to better consumer compliance. Maximum acceptability with chewable tablets is seen if they provide pleasant taste and mouth feel. To provide this property in tablets, various sweeteners and flavors are employed. Usually, sugar-based excipients are used as they are highly water soluble and dissolve quickly in saliva and provide pleasant taste and mouth feel to the final product.

1.5. Synthesis of biomaterials from biomass

Research efforts are constantly being directed toward the utilization of various biopolymers in diverse applications, including food packaging. This is driven by the need to use environment and eco – friendly resources in place of the conventional non – biodegradable plastics (Yang et al., 2016b). In addition to first-generation biomass, lignocellulose from biowastes such as agricultural waste and other biowastes provides a renewable feedstock for the creation of biobased and sustainable packaging materials. These materials do, however, typically exhibit poor mechanical properties and are sensitive to environmental factors. Consequently, numerous efforts have put into producing films with enhanced properties by using either mixtures of biopolymers or containing natural plasticizers and reinforcements for use in packaging. One of the main requirements for a good food packaging material is that it should be resistant to water and have good barrier properties against oxygen and other related gases to keep the food products safe. Therefore, it is essential to investigate environmentally friendly methods

for improving the hydrophobic properties of biopolymers. Future leading candidates for creating packaging films based on nanocomposite materials include modified nanocellulose and lignin nanoparticles.

Lignin is regarded as one of the major readily available renewable resources because it is the second most prevalent component of biomass. Agricultural lands are major producers of dry biomass, which is the primary source of lignin. The sugar, pulp, and paper industries are additional sources of lignocellulosic waste with high lignin content. In recent years, lignin valorisation has been strongly encouraged due to its abundance and low cost. Traditionally, lignin has only been used for low-quality solid fuels; however, due to its composition, which is rich in aromatic compounds, new opportunities for its monetization include the production of value-added goods and biofuels (González-González et al., 2022). In this way, the incorporation of lignin-derived products will result in profitable and sustainable industries built on the principles of the circular economy. The structure of lignin, which is rich in aromatics and phenolic hydroxyls, has drawn attention for a variety of new uses. Fuels, adhesives, paper coating, controlled release agents (agrochemicals), health (drug encapsulation and delivery, obesity, diabetes, cancer), cosmetics, coating for furniture, are some of the emerging application areas for lignin (Mujtaba et al., 2022). Despite all these intriguing uses, lignin's effective use as a high-value material is severely constrained by its larger particle size, heterogeneity, slow rate of dispersibility, and asymmetrical morphology. Various chemical processes are used to convert lignin into nanoparticles for this purpose. Nano-sized lignin materials have a number of benefits, including uniform size, high surface area, dispersibility, and degradability (Schneider et al., 2021). Its antioxidant, biodegradability, non-toxicity, good thermal stability, and UV- barrier properties have drawn uncharacteristic attention. Lignin is well suited for use in food packaging, medicine, and other industries owing to these aforementioned properties. Because of its phenolic content and functional groups, lignin has good antimicrobial properties which is an additional significant characteristic of a food packaging material (Yang et al., 2016a). Recent interest has been generated by the incorporation of lignin to a variety of commercial products. Lignin-based nanocomposites have also garnered a lot

of interest for different applications owing due to the favorable properties. It has been incorporated into polymers to produce composite materials with enhanced physical and chemical properties (Xie et al., 2021; Zhang et al., 2021). Additionally, there is a rising attention towards the development of lignin-derived resins, adhesives, and carbon fibres (Idumah et al., 2019).

1.6. State of the art literature review

With a brief overview of the contemporary research, this section outlines the outcome of various literatures so as to identify few promising areas of research that needs to be addressed in this thesis. The state-of-the-art literature has been presented for extraction and utilization of bioactive compounds from *Ficus auriculata* leaves.

1.6.1. Extraction of bioactive compounds using green technique and solvent

The food, pharmaceutical, pigment, and cosmetic industries use gallic acid, also known as 3,4,5-trihydroxy benzoic acid, extensively as a chemical of significant industrial importance. In light of its recovery from industrial downstream processes, its antioxidant, antifungal, anti-inflammatory, and antiviral properties attract a great deal of interest from researchers. Gallic acid is typically found in a variety of foods and drinks, including oak bark, walnuts, apples, blueberries, olives, tea, and wine. Microbial fermentation is a commonly used method for production of gallic acid (Puoci et al., 2012; Treviño-Cueto et al., 2007). Extraction method has also been explored for recovery of gallic acid from different processing wastes (Puoci et al., 2012). Adsorption using surface functionalized polymers and metal organic frameworks have been studied for separation of gallic acid from food and non – food sources (Bagheri and Ghaedi, 2020; Bhawani et al., 2018). Pressurized liquid extraction is another green method used for gallic acid recovery with high yield (Souza et al., 2020). Ultrasound-assisted extraction (UAE) is found to enhance the yield of gallic acid and antioxidant activity during the study on *Syzygium cumini* seed kernel. However, despite the huge potential for extraction with good efficiency, the application of UAE for gallic acid is scant.

Ultrasound-assisted extraction is an emerging separation technique, efficient for a broad range of compounds from different types of matrices and sources (Chemat et al., 2011; Dastkhoon et al., 2017). Ultrasonic extraction is a widely used technique for obtaining different kinds of bioactive compounds from various types of biological sources owing to its efficiency and rapidity. The main driving force for ultrasound-assisted extraction is acoustic cavitation (**Fig. 1.1**). The passage of a sound wave between 20 kHz and 10 MHz through a liquid medium generates alternate cycles of compression and rarefaction.

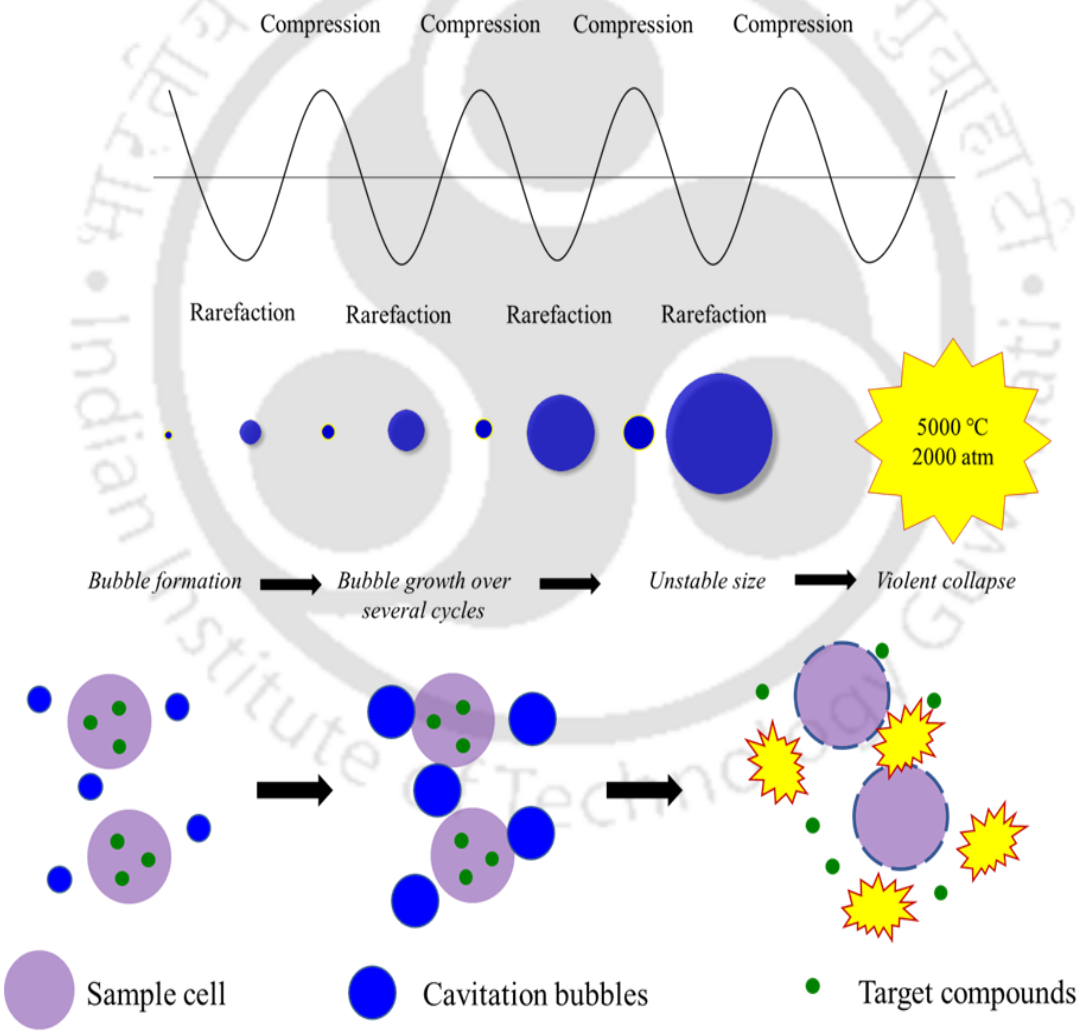

Figure 1.1 Acoustic cavitation process during ultrasound-assisted extraction

This results in the formation, growth, and ultimately violent implosion of microbubbles (Azmir et al., 2013), which can produce temperature and pressure as high as 5000 K and 1000 atm, respectively. This violent collapse consequently leads to the disintegration of the cell wall, causing an enhanced solvent diffusion into the plant matrix and subsequent leaching out of the target compounds. This results in an intensification of the mass transfer process by intensifying diffusion or by damaging the cell walls of the plants (Ardekani et al., 2017; Esclapez et al., 2011; Luque de Castro et al., 2011). The extraction process may be influenced by several parameters including the solvent type, solvent and sample ratio, frequency, amplitude, temperature, and time. UAE has the advantages of reduced extraction time and temperature, lesser energy and solvent, increased mass transfer, enhanced kinetics, improved yield, simpler system, and process (Baite et al., 2021; Riera et al., 2004). However, the production of highly reactive radicals at higher energy and power levels may lead to the oxidation and degradation of extracted phenolic compounds. Hence, prolonged sonication should be avoided. Ultrasound also helps in retaining the quality of heat sensitive components because of the feasibility of extraction at lower temperatures. Additionally, the ease of operation, safety and inexpensive system requirement make it a better alternative against conventional extraction techniques (Setyaningsih et al., 2019; Vieira et al., 2013). Different solvents, such as water, alcohols, acetone, and others, have been used to extract various compounds during the UAE. The type of solvent, the amount of solvent and concentration, and the ratio of solvent to solute are all variables that can affect how effective ultrasound extraction is. It has long been common practise to extract phenolic compounds from plant materials using alcohols and acetone with varying amounts of water. Since ethanol has been found to have the highest affinity for phenolics in many systems that have been studied, it is the preferred solvent for extracting phenolic compounds from fruit and vegetable matrices (Ramić et al., 2015).

An increase in ethanol concentration increases the yield of phenolic compounds up to certain point before it starts to decrease the yield (Garcia-Castello et al., 2015; Pan et al., 2012). This tendency may be caused by the phenolic compound becoming more solubilized and diffusive as a result of the solvent's decreasing dielectric constant as

ethanol concentration increased. The plant tissue becomes less hydrated and the protein becomes denaturized when ethanol concentrations near 100% are used as a solvent, which reduces yield (Kumar et al., 2021). The current research has only been able to reduce the volume of ethanol used for extraction using UAE, despite the fact that the ultimate goal is to completely eliminate its use.

Possible scope for further research on the extraction of bioactive compounds

It is envisaged from the state of art literatures that most of the extraction methods use organic solvents, which contributes to high cost of extracted product and pose negative impact on health and the environment. Use of green solvent like water in appropriate condition to extract the gallic acid from agricultural sources is rarely reported in the literature. Further, there is no reported work on the extraction of gallic acid from *F. auriculata* leaves. Hence, there is a scope for extraction of bioactive compound such as gallic acid from *F. auriculata* leaves using green solvent based non-conventional technique and optimization of the process parameters.

1.6.2. Enhancement of shelf life of perishable fruits using natural antioxidants-based coating

Most fruits and vegetables release ethylene, one of the most basic phytohormones, after being harvested. Ethylene starts the ripening process, softens and degrades chlorophyll, and ultimately speeds up the deterioration of fresh goods. This phytohormone hastens the ripening and senescence of fresh produce, degrading the products' quality, vital minerals, and viability as a commercial commodity (Álvarez-Hernández et al., 2018). As a result, numerous initiatives have been undertaken to reduce the rate at which fresh produce deteriorates as a result of ethylene, including the use of ethylene absorbers, ethylene oxidising agents, ethylene inhibitors based on chemicals and nanomaterials (Gaikwad et al., 2020). One of the most commonly used ethylene scavengers is potassium permanganate ($KMnO_4$), an ethylene-reacting broad-spectrum oxidising agent however, it cannot be used in direct food contact due to its toxicity. To avoid direct food contact in this situation, KMnO4 may be used impregnated or encapsulated

into a solid base (nanoparticles, waxes, polymers, etc.) (Miranda et al., 2021). It has been widely reported that ethylene scavengers like zeolite, titanium dioxide, and transition metals are sometimes enclosed in a tiny sachet placed inside a package or incorporated into packaging films (Mariah et al., 2022). When compared to other food products, fresh produce has relatively low costs. The commercial use of new ethylene scavenging packaging could result in an increase in unit costs and prices for individual products, which could have an indirect impact on consumer behaviour and product acceptance. In addition to ethylene scavengers, there are other techniques that have caught the attention of researchers for delaying the ripening process such as by controlling the mass transfer between the product and the environment.

Even after harvest, fruits and vegetables continue to breathe, using up the oxygen present. This oxygen is not replaced as quickly as by coatings, and the carbon dioxide that is produced cannot easily escape through coating, so it builds up inside the produce. Eventually, the fruit and vegetable will undergo partial anaerobic respiration, which uses less oxygen. Less oxygen results in a disruption of the ethylene cycle, which speeds up the ripening process, and a reduction in physiological water loss (McHugh and Senesi, 2000). As a result, the fruits and vegetables have a nearly doubled shelf life while still remaining firm, fresh, and nutrient-dense. The degree to which the internal atmosphere (oxygen and carbon dioxide) are modified as well as the level of reduction in weight loss will depend on the natural barrier on fruit and vegetables, the type and amount of coating (Dhall, 2013). Materials with the ability to form films can be used to create edible coatings. In a solvent, such as water, alcohol, a mixture of the two, or a combination of other solvents, the film materials must be dispersed and dissolved during production. This process allows for the addition of plasticizers, antimicrobials, vitamins, minerals, colours, and flavours (Vaishali et al., 2019). For the specific polymer, pH adjustments and/or solution heating can be used to speed up dispersion. The film solution is then cast and dried to achieve freestanding films at the desired temperature and relative humidity. In addition to dipping, spraying, brushing, and panning, the film solutions could also be applied to food and then dried.

Coating using different safe and biocompatible materials have been successfully explored to improve the shelf stability and bioactivity of different fruits like pears (Sinha et al., 2021), banana (Thakur et al., 2019; Wantat et al., 2021), avocado (Saidi et al., 2021), plum (Li et al., 2021), and strawberry (Liu et al., 2021). Similarly, to prolong the shelf life of banana, several types of coatings such as carrageenan, starch, and chitosan have been studied (Domínguez-Espinosa et al., 2022; Dwivany et al., 2020). The use of *Sonneratia ovata* extract incorporated PVA coating and heterojunction catalyst composite based PVA coating for banana have also been reported (Pham et al., 2022; Xie et al., 2022). The natural-based coatings are safer compared to their chemical counterparts and are reported to maintain better freshness and keep the quality of agricultural produces (Li et al., 2021).

Poly(vinyl alcohol) (PVA) is a biocompatible and biodegradable polymer with outstanding physical, optical, mechanical, and film-forming properties in addition to excellent chemical resistance (Zanela et al., 2018). PVA and its composites have successfully been studied for their potential applications in food packaging systems (Youssef et al., 2019). Considering its non-toxic and safe profile, it has earned the Generally Recognized As Safe (GRAS) status, promising its use for the production of edible films (Keller and Heckman, 2018). The incorporation of bioactive components such as phenolic compounds has substantial potential for applications in food packaging (Andrade et al., 2021). Gallic acid is a water-soluble phenolic compound that has been ascribed with potent antioxidant and antimicrobial properties. The enhancement of the antioxidant properties has been reported in gallic acid-incorporated PVA films (Awad et al., 2017).

Possible scope for further research on antioxidant – based coating of fruits

From the available literature, it is envisaged that the incorporation of gallic acid-rich extract in PVA coatings can be beneficial for delaying the ripening of bananas. The leaf extract of *F. auriculata* is found to be rich in gallic acid and exerts high antioxidant activity (Baite et al., 2021). This shows that the extract could potentially be used as an additive to enhance the shelf life of fresh produces. However, no work has been

reported regarding the use of *F. auriculata* leaf extract for extending the shelf life of fruits. Despite its desirable properties and safety, the application of PVA for the direct edible coating of banana is scant. Thus, there is a potential for the development of antioxidant – incorporated coating for the delayed ripening of perishable produces such as banana and consequently enhancing the shelf life.

1.6.3. Development of antioxidant formulations using plant extract

Herbal extracts have poor flowability and compactability due to their high hygroscopicity, which also affects particle interactions. Additionally, since the typical single dose of herbal extracts has a large volume, the amount of excipient must be kept to a minimum in order to create a herbal tablet that is easy to swallow (Son et al., 2019). Therefore, choosing the right excipient and maximising the amount of excipient are crucial steps in the production of tablets containing herbal extracts. The main factors influencing the continued popularity of herbal tablets are their low cost of production, ease of dosing, and superior storage stability compared to liquid and semi-solid formulations. One of the most advantageous processes for making tablets is direct compression of the active ingredient with adequate excipients (Gallo et al., 2012). For direct compression, a variety of pharmaceutical excipients including a variety of polymers, can be used. These macromolecules include both natural and synthetic ones such as cellulose and poly(vinyl pyrrolidone) or poly(acrylic acid) (Domínguez-Robles et al., 2019). Polymers are particularly helpful in the design of modified release drug delivery systems and have been successfully used in the formulation of solid, liquid, and semi-solid dosage forms. The use of natural polymers for pharmaceutical applications is appealing because they are affordable, easily accessible, non-toxic, capable of chemical modification, potentially biodegradable, and with a few exceptions, also biocompatible (Malafaya et al., 2007; Quan et al., 2019). But for a product to work properly, drugs and excipients must exhibit low hygroscopicity, good flowability, and compactability.

In addition to affecting the material's physical and chemical stability negatively, hygroscopicity plays a significant role in particle-particle interactions and may be a factor in poor powder flowability (Gallo et al., 2012). To guarantee homogeneous and

quick flow, and consequently, uniformity of dose and weight during die-filling, the flowability must be appropriate. For effective tableting, compactability is essential (i.e. the powder must remain in the compact form once the compression force is removed) (Son et al., 2019). Dry plant extracts typically consist of complex, amorphous, and viscous substances. They frequently exhibit hygroscopic and tacky characteristics as well as poor physico-mechanical properties because of their high affinity for water vapour. Therefore, prior to direct compression, the use of suitable excipients and/or the application of suitable processing technologies is required (de Souza et al., 2007). Additionally, since phytomedicine tablets typically contain a high concentration of dry plant extract, the amount of excipients that can be added becomes a crucial consideration when producing tablets of a manageable size.

Possible scope for further research on gallic acid – based antioxidant formulation

In most of the existing literatures, preparation of antioxidant formulation often requires large number of excipients which may increase the cost. The arrangement for development of tablets may require expertise in operation and may have high costs. Therefore, there arises a need for the development of free – flowing formulations using cheap and easily available ingredients and tabletting methods which still exhibits good antioxidant properties.

1.6.4. Extraction of valuable compound from extraction by-product of gallic acid and its application

The efficient conversion of biomass components to biofuel and other value-added products is the subject of extensive research at the moment. Many upcoming issues may be resolved by the valorization of lignocellulosic biomasses. One of the most popular renewable polymers right now are lignins, which have a wide range of uses in industries like biomedicine, cosmetics, energy, food, coatings, and composites (Mujtaba et al., 2022). Their applications in the agro-food industries have resulted from the useful physical, mechanical, antimicrobial, and antioxidant properties of lignin-derived products (Cassoni et al., 2022). In the food industry, lignin can be transformed into

polymers with added properties used for packaging or even used as a functional ingredient in food products. Numerous authors have noted the significant antioxidant properties of lignin; these properties have been linked to the polyphenolic structure and play a significant role in its suitability for use in food and packaging (Kai et al., 2016; Sun et al., 2018). Studies have shown that lignin has antimicrobial properties, especially against common food contaminants (Hambardzumyan et al., 2015). Lignin has many beneficial effects on the physical and mechanical properties of biopolymers, including thermal stability, UV resistance, hydrophobicity, tensile strength, and biodegradability, in addition to its antioxidant and antimicrobial properties (Cassoni et al., 2022). It has become possible to improve the UV barrier resistance of bio-based packaging systems by using biopolymeric (natural and synthetic) materials. Due to the presence of UV-absorbing functional groups like phenolic units, ketone, and chromophores, lignin nanoparticles have recently gained popularity as effective UV barrier materials. When lignin is added to a packaging matrix, it exhibits excellent UV and antioxidant properties because of the presence of these functional groups (Rukmanikrishnan et al., 2020). Manufacturing of active food packaging is just one of the many uses for biopolymers. Such biopolymers' economic value depends on extending shelf life through better packaging that guarantees product quality. In this regard, lignin's antioxidant and antimicrobial properties can be very helpful to prevent or get rid of harmful species. Hence, for development of low – cost packaging system with desirable properties, a workable method for utilising biomass is to take advantage of the sensible use of lignin for PVA composites.

Poly(vinyl alcohol) (PVA) is a biocompatible polymer with excellent film forming as well as mechanical, physical, and optical properties. Hence, it is extensively utilized in food industry as well as biomedical, domestic, and construction sectors. In spite of this, PVA's use in food packaging applications has been constrained by its poor moisture barrier properties and lower mechanical strength than conventional packaging materials. Additionally, PVA is deficient in desirable characteristics for materials used in food packaging, such as antioxidant, antimicrobial and UV barrier properties (Nguyen and Lee, 2022). Several inorganic nanoparticles have been used to create PVA composites

with improved performance. However, because of the filler's poor interfacial compatibility with PVA, some properties such as mechanical behaviour of the composites tend to be negatively affected. Furthermore, by incorporating expensive inorganic nanoparticles, the biodegradability of PVA nanocomposite films is somewhat diminished. For the fabrication of fully biodegradable functional polymeric materials, it is highly desirable to look for green resources like biomass as a substitute to the aforementioned inorganic fillers.

Possible scope for further research on lignin extraction from waste and application

Despite having a wide range of potential uses, the use of lignin is currently still constrained because of its complex and irregular chemical structure. Lignin derived from biomass, such as *Ficus auriculata* leaves, is a suitable candidate for the formation of safe, biodegradable, and beneficial packaging film owing to its strong antioxidant and antimicrobial activity. However, studies on the synthesis and isolation of lignin from such sources is scarce. The hydrophobic nature of lignin can also potentially improve the water barrier properties of hydrophilic PVA films. There is also little research on how lignin incorporation affects the physical and chemical characteristics of PVA films used as packaging. Studies on the synthesis of lignin from waste and its direct application in the food industry is limited. The utilization of lignin incorporated films for food packaging is scant. Therefore, there is a scope for the synthesis of valuable components from extraction water and by-products. The synthesized compounds can be further studied for their potential application such as in the development of composite materials for food packaging.

1.7. Objectives of thesis work

Based on the above state of the art literature review and scope of possible work, the objectives of this thesis work are identified as below:

- Investigation of the ultrasound assisted extraction of gallic acid from *Ficus auriculata* leaves using green solvent

- Preparation and characterization of gallic acid (antioxidant) incorporated poly (vinyl alcohol) coating for delayed ripening of green bananas
- Preparation and evaluation of antioxidant formulations containing gallic acid enriched extract
- Extraction of lignin from waste *Ficus auriculata* leaves and its potential application for bread packaging

1.8. Organization of the thesis

Chapter 1 discusses the background of the problems undertaken in this work i.e. the gap associated with the extraction and utilization of bioactive compounds using green techniques. The objectives of the present work are also highlighted here. **Chapter 2** gives a detailed explanation of the experimentation involved in the extraction of gallic acid from *Ficus auriculata* leaves using green solvent and technique. Investigations were done into the effects of time, temperature, sonication intensity, and solid to solvent ratio on gallic acid extraction. The extraction efficiency of different solvents *viz*., ethanol, methanol and alkaline water compared. The influence of sonication system on extraction of gallic acid was explored. The kinetics of the extraction process was investigated using different models. The extracted gallic acid was purified using different processes. **Chapter 3** gives a complete description of the experimentation involved in the development of gallic acid – PVA coating for preserving bananas. Coating films were characterized for various properties using different techniques. Green banana samples were coated using the prepared solutions of different compositions. The influence of the coating on the physicochemical properties of the fruit was observed. **Chapter 4** describes the preparation and evaluation of antioxidant formulations containing gallic acid-enriched extract and its subsequent tablet formation. Easily available compounds such as starch and different sugars were used as excipients at different proportions. The free-flowing formulations were formed into tablets using a hand-operated simple pellet maker. The formulations and the prepared tablets were evaluated for physical and chemical characteristics. **Chapter 5** presents the recovery of lignin from spent *F. auriculata* leaves obtained after extraction of gallic acid and its

subsequent application in food packaging. The extracted lignin as well as the lignin – incorporated PVA films were characterized using different techniques. The prepared films were evaluated for their performance as a packaging material in inhibiting mold growth during bread storage. The films were also compared with commercially – used bread packaging material during storage under different conditions. **Chapter 6** summarizes the inferences drawn from the different works and provides some suggestions towards future research.

Chapter 2

Investigation of the ultrasound – assisted extraction of gallic acid from *Ficus auriculata* leaves using green solvent

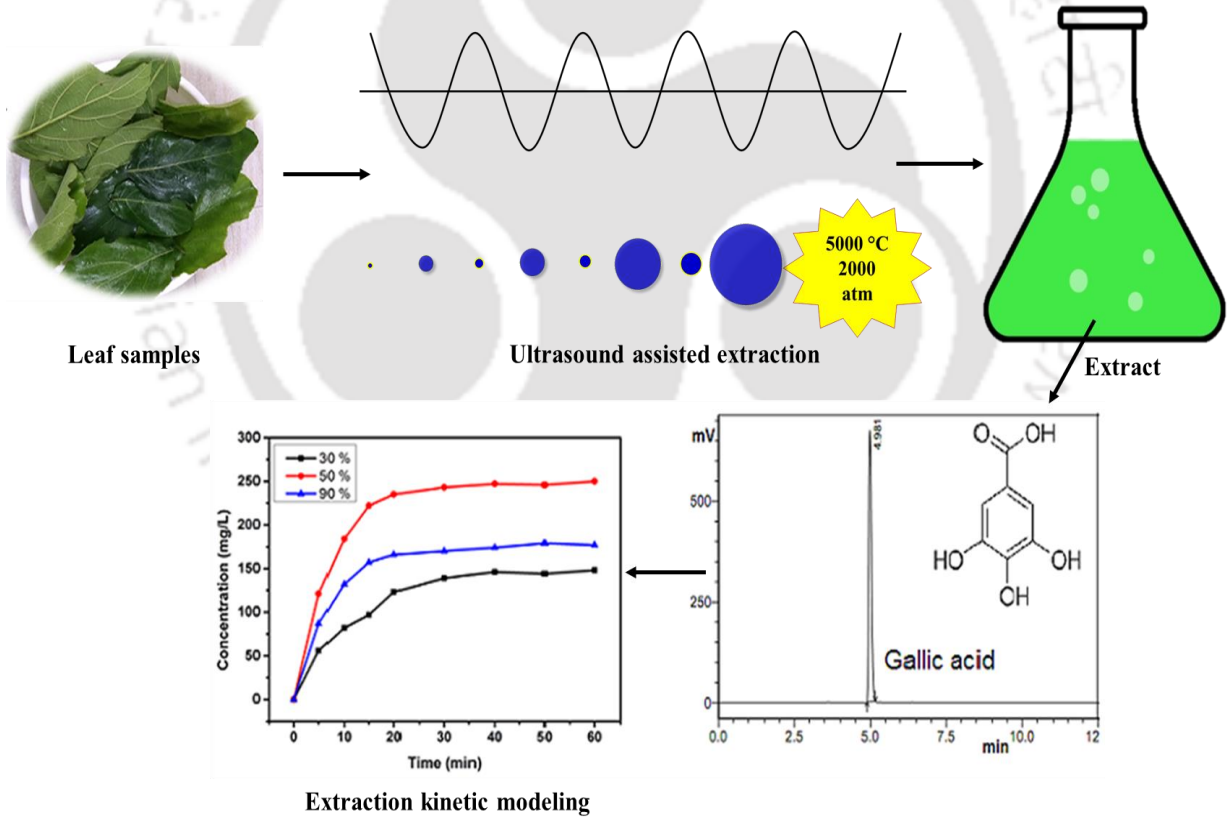

Extraction kinetic modeling

Ultrasound assisted extraction of gallic acid from *Ficus auriculata* leaves

Chapter 2

Investigation of the ultrasound assisted extraction of gallic acid from *Ficus auriculata* leaves using green solvent

This chapter gives a complete description of the experimentation involved and results thereon in the extraction of gallic acid from Ficus auriculata leaves using ultrasound assisted extraction. Various operating parameters like extraction time, temperature, sonication power, solvent to powder ratio and pH of aqueous solvent were optimized to get maximum gallic acid yield in the extract. Different kinetic models were used to investigate the extraction process. Furthermore, purification of the extract was studied using reverse osmosis (RO) and chromatographic techniques to obtain pure gallic acid. The background of this work, details of literature and the scope of work are elaborated in Chapter 1, Section 1.2 and Section 1.6.1, respectively. This work has been scientifically acknowledged in the Food and Bioproducts Processing.

2.1. Materials

2.1.1 Plant materials

The leaves of *F. auriculata* plant were obtained from the campus of Indian Institute of Technology Guwahati, India. The leaves were cleaned with tap water to remove any dirt particles and oven dried (HERAtherm, Thermo Scientific) at 50 °C overnight. The dried leaves were then grinded using a kitchen grinder and sieved through a screen with 600 µm holes. The moisture content of dried sample was 10.84% (wet basis). The ground sample was stored in an airtight container until further use.

2.1.2 Chemicals

The standard gallic acid (Purity ≥98%) was purchased from Sisco Research Laboratories, India. High Performance Liquid Chromatography (HPLC) grade acetonitrile and ortho-phosphoric acid were kindly supplied by Merck, India. The water used in all the experiment was obtained from Millipore Milli-Q® (M/s Millipore, USA) water purification system.

2.2. Extraction process

The *F. auriculata* leaf extract was obtained by mixing the ground sample with aqueous solvent in a sonication bath (Elmasonic, model: P 30H) equipped with variable power level and dual frequency levels (37 kHz and 80 kHz). The pictorial representation of the extraction process is shown in **Fig. 2.1.** A constant frequency of 37 kHz was used for all experiments. The efficiency of extraction was studied and optimized for various extraction parameters *viz*., extraction temperature, treatment time, sonication power level, solid solvent ratio and pH. The optimization was performed based on the concentration of gallic acid extracted in the first stage of extraction. The ranges of various extraction parameters are shown in **Table 2.1**.

Table 2.1 Parameters for optimization for the extraction of gallic acid from *F. auriculata* leaves

Parameter	**Values**
Extraction temperature (°C)	30 – 80
Extraction time (min)	5 – 60
Sonication power (%)	30 – 90
Solid to solvent ratio (g/mL)	1:5 – 1:40
pH	2 – 10

Figure 2.1 Ultrasound – assisted extraction process of gallic acid from *F. auriculata* leaves at 37 kHz

2.2.1 Comparison of different solvents

The extraction of bioactive compounds from any source is highly influenced by the solvent type, polarity and solubility of the compound in that particular solvent. Methanol and ethanol are two of the most commonly used organic solvents during the extraction of polyphenols. Hence, to compare the extraction efficiency of these solvents with water, 50% ethanol and 50% methanol in water and aqueous solvent with optimum pH were used to extract gallic acid under the same condition.

2.2.2 Comparison of the efficiency of sonication bath and probe sonicator for extraction of gallic acid

Water and solid sample at the ratio of 30:1 (mL/g) was taken in two separate beakers and extracted for 15 min each at 50% power level using a sonication bath. The temperature of the bath was maintained at 50 ℃. The extraction was carried out in pulsed and continuous mode. The same water sample ratio was taken and extraction was performed using a probe sonicator (Pro – 650, Labman Scientific Instruments). Briefly, the sample beaker was placed inside the sonication chamber fitted with a temperature sensor. The depth of probe immersed into the sample was adjusted and power level was set to 25%. For the pulsed mode, pulse was set as 5 s on/ 2 s off and extraction time set as 15 min. Continuous mode of extraction was carried out by setting the time as 15 mins of sonication with zero pulse off.

2.3. Analysis of extract

2.3.1 HPLC, UV-Vis, FTIR and LCMS analysis

The extracts obtained were centrifuged at 10000 rpm for 10 min and the supernatants were collected and filtered using Whatman® filter paper (nos. 1 and 42) prior to HPLC analysis. HPLC analysis was performed using HPLC system equipped with refractive index (RI) and UV – Visible detectors (Prominence, Shimadzu). The method used by (Singh et al., 2012) was followed with a modification in terms of solvent composition. The separation was carried out by injecting 20 µL of sample onto a Shimpack C18 column with a dimension of 250 mm × 4.6 mm. The mobile phase consisted of pure acetonitrile (A) and 0.1% ortho-phosphoric acid in water (B). The flow rate was set at 0.8 mL/min with constant composition of 20% A and 80% B, and total run time of 20 mins. The absorption maxima of gallic acid standard was found to be at 270 nm, and measured by UV- Vis spectrophotometer (UV – 2600, Shimadzu). The detection wavelength for HPLC was therefore set at 270 nm. The functional groups present in the extract and standard (≥98% of gallic acid) were determined by Attenuated Total

Reflection – Fourier Transform Infrared Spectroscopy (ATR – FTIR) (IRAffinity-1, M/s Shimadzu, Japan). For each sample, an average of 30 scans were recorded over the range of 4000 – 400 cm^{-1}. To further confirm the presence of gallic acid, Liquid Chromatography Mass Spectrometer (LCMS) (Model: Q-TOF Premier, Waters) was used to analyse the extract. The extract was first dissolved in acetonitrile. About 0.5 µL sample was injected and mass spectrum was obtained in positive ion mode with the following condition: 0.5 s scan time; source temperature 85 °C; desolvation temperature 350 °C; cone voltage of 30 V, capillary voltage of 3.49 kV; ion guide 2.1; sampling cone 52; extraction cone 20; cone gas 50 L/h and desolvation gas 450 L/h. Mass spectrum was recorded in the m/z (mass-to-charge ratio) range of 90 to 260.

2.3.2. Estimation of antioxidant activity (AA) and total phenolic content (TPC)

The antioxidant activity of the extract was estimated using the 2,2-diphenyl-1-picrylhydrazyl (DPPH) method used by (González-Palma et al., 2016) with slight modification. Briefly, 0.5 mL of aqueous extract was mixed with 3 mL of methanol and 0.3 mL of 0.5 mM DPPH solution in methanol. For blank, the DPPH solution was replaced with same volume of methanol. The samples were incubated in dark for 100 min and their absorbance was recorded at 517 nm using a UV – Vis spectrophotometer (UV – 2600, Shimadzu). The percentage antioxidant activity in terms of DPPH inhibition was calculated as

$$AA = \left\{1 - \left(\frac{(Ab_{sample} - Ab_{blank}}{Ab_{control}}\right)\right\} \times 100 \quad (2.1)$$

Where,

Ab_{sample} = Absorbance of sample after 100 min on incubation

Ab_{blank} = Absorbance of blank

$Ab_{control}$ = Absorbance of control (3.5 mL methanol + 0.3 mL DPPH solution) at the moment of preparation

The total phenolic content (TPC) was measured using a typical Folin – Ciocalteu (FC) method adopted by González-Palma et al. (González-Palma et al., 2016) with some modifications. Briefly, 0.50 mL of the diluted sample was added into 2.5 mL of 1:10 diluted Folin–Ciocalteu reagent. After 5 min, 2 mL of saturated sodium carbonate solution (7.5%) were added. The absorbance of the mixture was measured at 765 nm after incubation for 2 h at room temperature. Gallic acid was used as a reference standard, and the results were expressed as milligram gallic acid equivalents (mg GAE)/100 g of sample.

2.3.3. Purification of gallic acid by reverse osmosis (RO) and high-performance liquid chromatography (HPLC)

Purification of the extract was done by reverse osmosis (RO). The application of membranes for various bio-separation processes are reported in our previous work (Dhadge et al., 2019; Emani et al., 2013; Purkait, 2011). In this work, the leaf extract was first vacuum filtered through a Whatman® filter paper (no. 42) having a pore size of 2.5 μm. The filtered sample was then passed through reverse osmosis membrane (Dow Filmtec Plastic) with 75 gallon per day (GPD) capacity in a high reject low pressure RO system. The permeate from the first run was used as feed in the second run and the resulting permeate was again used as the feed for the third run. Samples from feed, reject and permeate from each run were compared for gallic acid content. Purification was also carried out using high performance liquid chromatography (HPLC). In this method, the filtered extract was first injected into the analytical HPLC system. The fraction eluted from the system was then collected for the period of the appearance of gallic acid peak in the chromatogram (4.6 – 5.2 min). The collected fraction was injected further into the HPLC system in order to increase the purity.

2.4. Kinetic modeling of the extraction process

The kinetics of gallic acid extraction was studied to apprehend the relationship between the duration and the concentration of the extract at the condition in which individual

parameters resulted in highest efficiency. Four empirical kinetic models *viz.*, modified Peleg, Power, Parabolic diffusion and unsteady diffusion models (**Table 2.2**) were used and compared to determine the best fit model for the extraction process. The MatLab™ 2015a was used to fit the experimental data of gallic acid concentration. The extraction kinetics were observed at three different sonication powers. The following general assumptions were applied for the models: (i) all the particles are uniform in size (ii) the extractable gallic acid is evenly distributed in the sample matrix and (iii) the solid particles are well mixed with the solvent. Additionally, some model specific assumptions were also applied.

Table 2.2 Various kinetic models for gallic acid extraction

Model	Equation	Constants
Peleg Hyperbolic (Anbalagan et al., 2019)	$f(t) = \frac{t}{(k_1 + k_2 t)}$	k_1 = initial rate (1/min) k_2 = const. related to maximum extraction yield (1/min)
Power Law (Baite and Das, 2018)	$f(t) = k_3 \times t^n$	k_3 = rate constant (min^{-n}) n = diffusional exponent
Parabolic diffusion (Cheung et al., 2013)	$f(t) = k_4 + k_5 \times t^{1/2}$	k_4 = initial yield k_5 = initial yield
Unsteady diffusion (Cheung et al., 2013)	$f(t) = (1 - k_6) \times e^{-k_7 t}$	k_6 = washing coefficient k_7= rate constant

The power law model assumes the extraction as diffusion using a non – swelling device. Both the parabolic and unsteady diffusion models assume two stage extraction, (a) the rapid washing of compounds from the solid surface, and (b) a slower diffusion of solute inside the solid particles (Bucić-Kojić et al., 2007; Rostami and Gharibzahedi, 2017). Peleg model was originally recommended to describe the moisture sorption curve. However, studies have proven that sorption curves and extraction curves are similar in shape. Hence, it has been successfully used for studying extraction kinetics of bioactive compounds from plants (Anbalagan et al., 2019; Baite and Das, 2018; Bucić-Kojić et al., 2007; Cheung et al., 2013; Gerke et al., 2018; Rostami and Gharibzahedi, 2017; Rouhani, 2019; Segovia et al., 2016; Turhan et al., 2002).

2.5. Results and discussion

2.5.1 Confirmation of gallic acid in the extract

The presence of gallic acid in the extract was confirmed by comparing the retention time in HPLC with that of the pure gallic acid as shown in **Fig. 2.2**. Among other components present in the extract, one significant peak has a retention time of 4.9 min, which corresponds to that of gallic acid. This peak has the highest intensity and the highest area under the peak, implying that gallic acid is the major compound present in the *F. auriculata* leaf extract. This is corroborated by the Liquid Chromatography-Mass Spectrometry (LCMS) chromatogram in **Fig. 2.3**, where a peak at m/z value of 171 is observed (Sun et al., 2014).

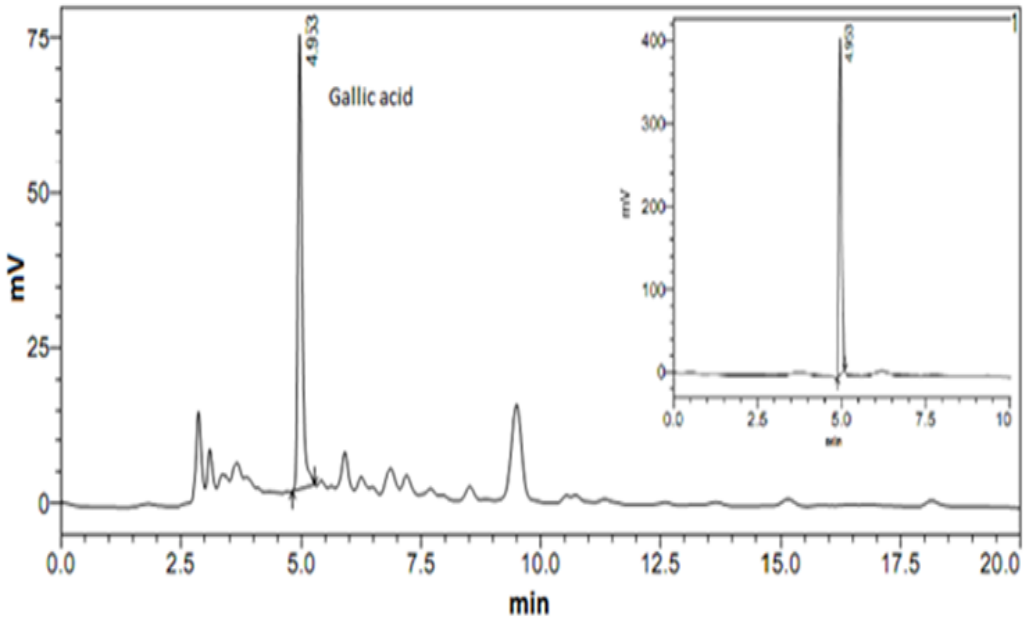

Figure 2.2 HPLC chromatogram of *F. auriculata* leaf extract. Inset: HPLC chromatogram of gallic acid standard

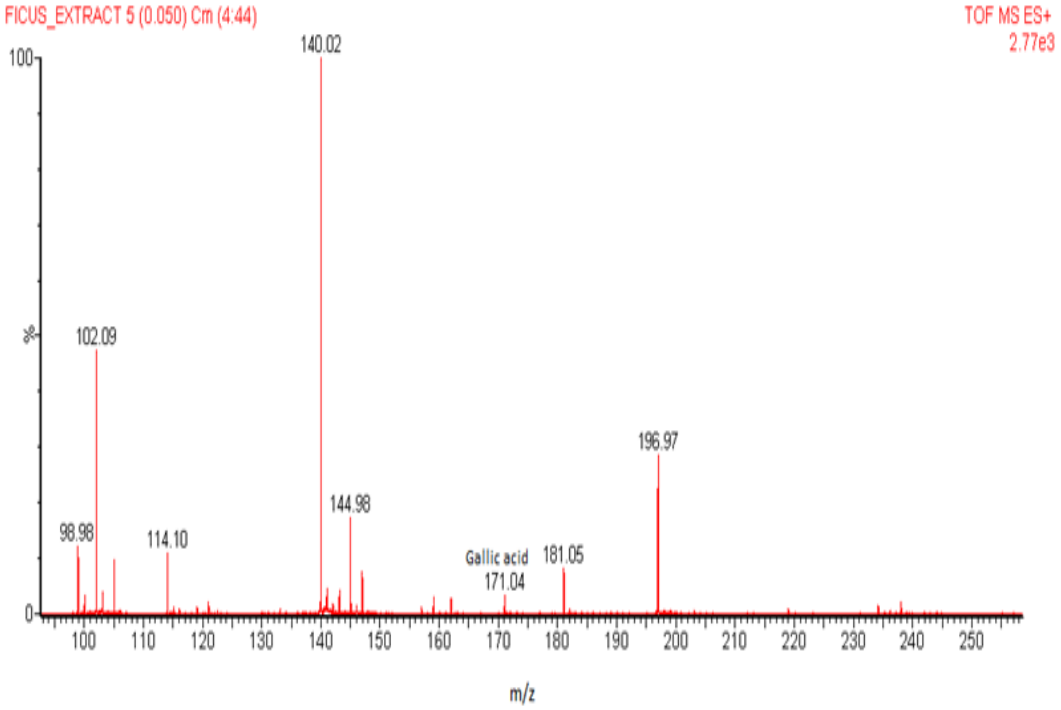

Figure 2.3 LCMS spectra of *F. auriculata* leaf extract

The Fourier Transform Infrared (FTIR) spectra (**Fig. 2.4)** further confirms the presence of gallic acid in the extract, wherein both the extract and standard gallic acid showed similar major peaks at 3301 and 1640 cm^{-1}, corresponding to the O-H and the C=C stretching of the aromatic ring, respectively.

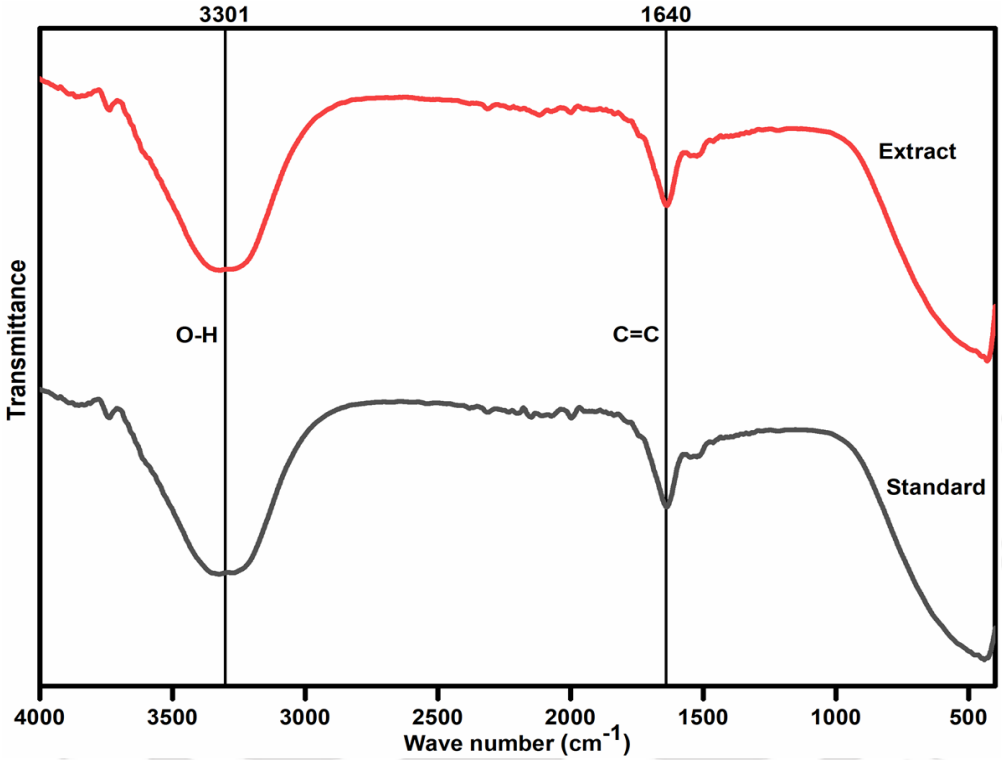

Figure 2.4 FTIR spectra of the *F. auriculata* leaf extract and the standard

2.5.2 Effect of different parameters on gallic acid extraction

2.5.2.1 Variation with time

Extraction of bioactive compounds is affected by operating time as the target components may not be removed efficiently at the beginning from the leaves. To evaluate the effect of time on gallic acid yield, extraction was performed for varying durations, while maintaining 50 °C, pH 7, 20 mL/g solvent solid ratio, and 50% sonication power. The concentration of gallic acid in the extract increased from 121 mg/L at 5 min to 243 mg/L at 30 min. Thereafter, significant change was not found in

the gallic acid concentration and the extraction curve remains almost in a plateau (**Fig. 2.5**). This higher extraction at initial stages was presumably because of the increased mass transfer, which in turn was caused by the violent collapse of the cavitation micro bubbles. This facilitates the release of most of the active components into the water in the first few minutes.

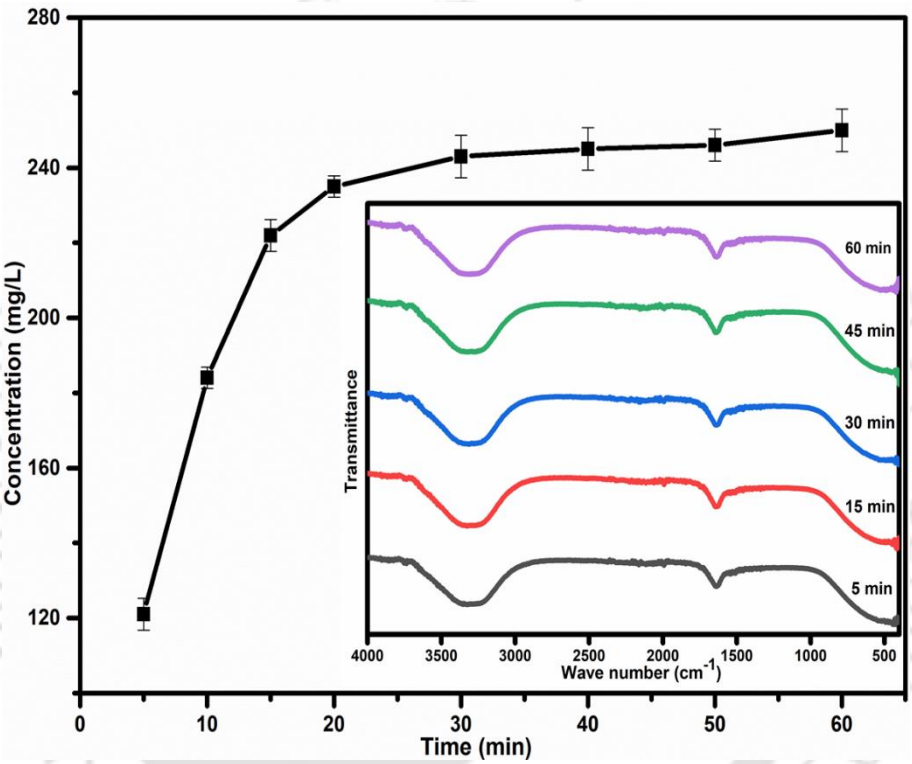

Figure 2.5 Variation in gallic acid concentration with extraction time (Temperature: 50°C; pH: 7; solvent solid ratio: 20 mL/g; sonication power: 50%). Inset: FTIR spectra of extract with variation in time

The insignificant increase in extract concentration after 30 min may be indicative of equilibrium concentration of extraction. Similar observations were made in previous studies during the extraction of plant phytochemicals (Ghafoor et al., 2009; González-Centeno et al., 2014; Rostagno et al., 2003; Vuong et al., 2013) using various organic solvents. The FTIR and UV – Vis spectra of extract at different duration of extraction did not show any significant difference (**Fig. 2.6**). This proves that the gallic acid present in the extract did not undergo any major structural change during extraction

under sonication. Hence, it may be concluded that 4.86 mg of gallic acid can be extracted per gram of *F. auriculata* leaves under aforesaid condition.

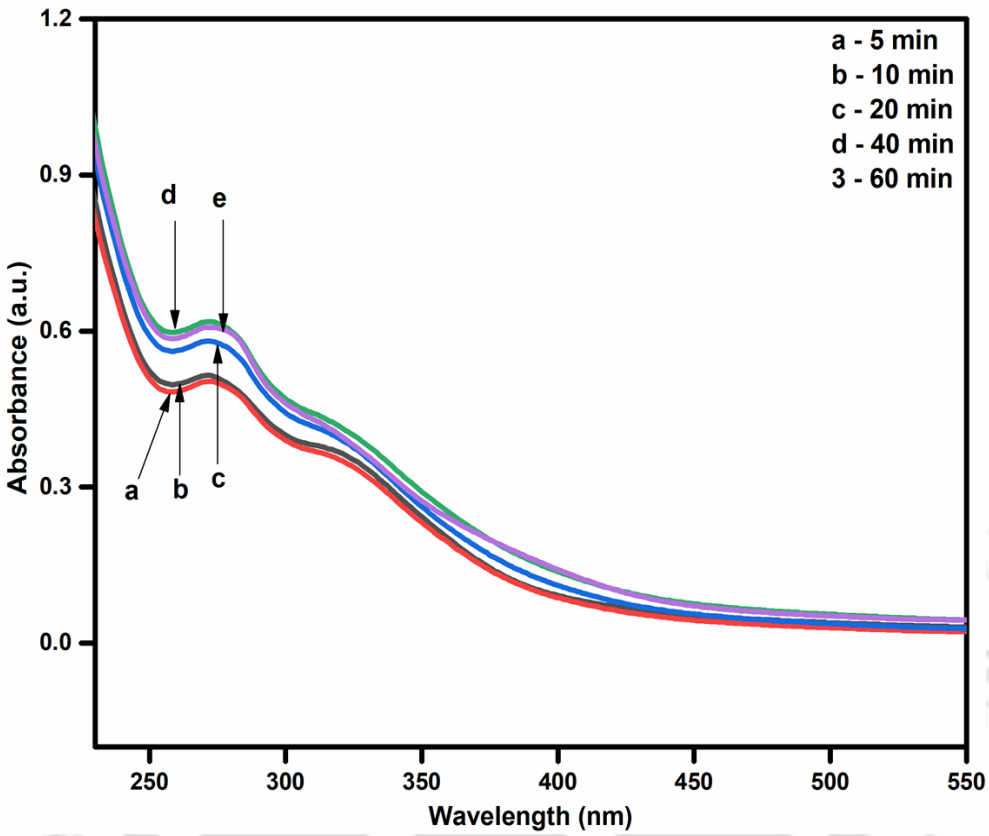

Figure 2.6 UV – Vis spectra of *F. auriculata* leaf extract at different extraction time.

2.5.2.2 Variation with temperature

The efficiency of extraction strongly depends on the temperature, as it affects the solubility of the solute as well as additional thermal effects. The influence of temperature was studied by setting a fixed sonication power of 50%, pH 7 and 20 mL/g solvent solid ratio. At this condition, the extraction was carried out for 15 min at temperatures ranging from 30 ˚C to 80 ˚C. **Fig. 2.7** showed that the concentration of gallic acid in the extract increased up to 235 mg/L when the extraction temperature was raised to 50 °C. This was due to the increase in solubility and mass transfer rate with temperature. However, with the increase in extraction temperature beyond 50 °C, there was continuous reduction in the extent of gallic acid extraction to 106 mg/L at 75 °C.

This was probably due to the initiation of degradation of gallic acid beyond 50 °C. Higher temperature in combination with hydroxyl radicals formation may enhance the oxidation rate, which in turn influences the gallic acid degradation rate (Zhang et al., 2015).

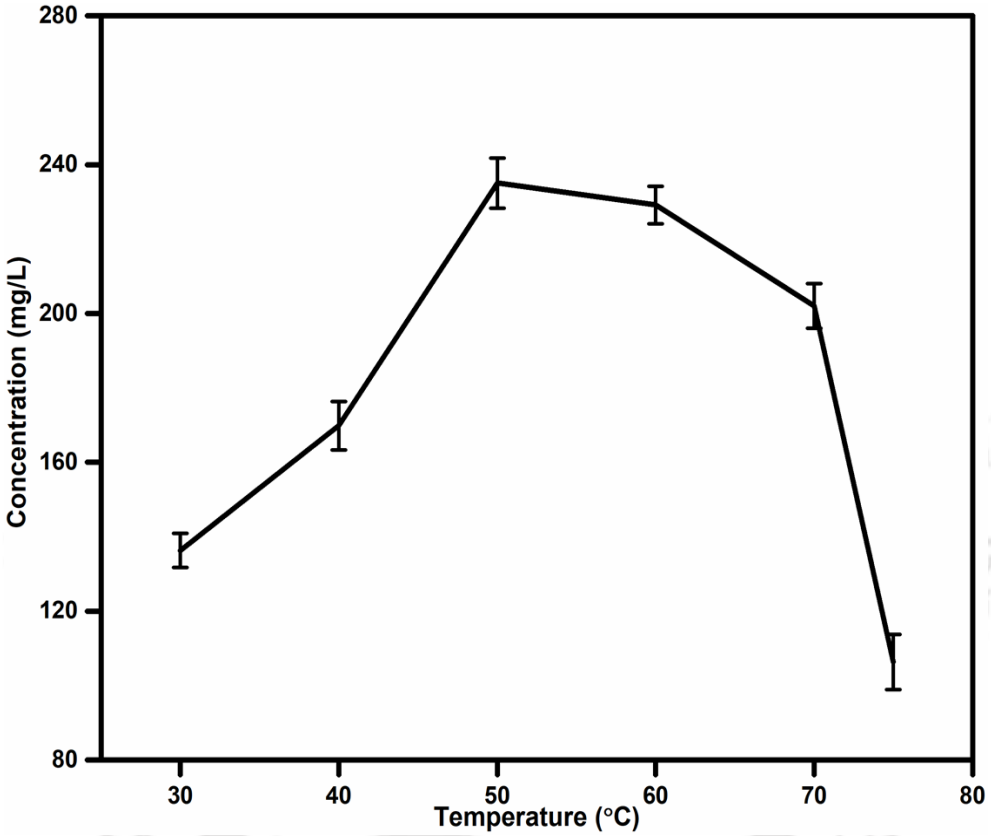

Figure 2.7 Variation in gallic acid concentration with extraction temperature (Time: 15 min; pH: 7; solvent solid ratio: 20 mL/g; sonication power: 50%)

2.5.2.3 Variation with sonication power

The efficiency of ultrasound assisted extraction is attributed to the effects of cavitation, causing the breakage of cell walls, which leads to an enhanced release of target components into the extracting medium. This results in accelerated removal of desired components from the plant matrix. The FESEM images showing the structural change in the sample before and after ultrasonic treatment is illustrated in **Figs. 2.8a** and **2.8b**.

Comparison of the images shows a visible change in the morphology and the opening of the tissue after sonication.

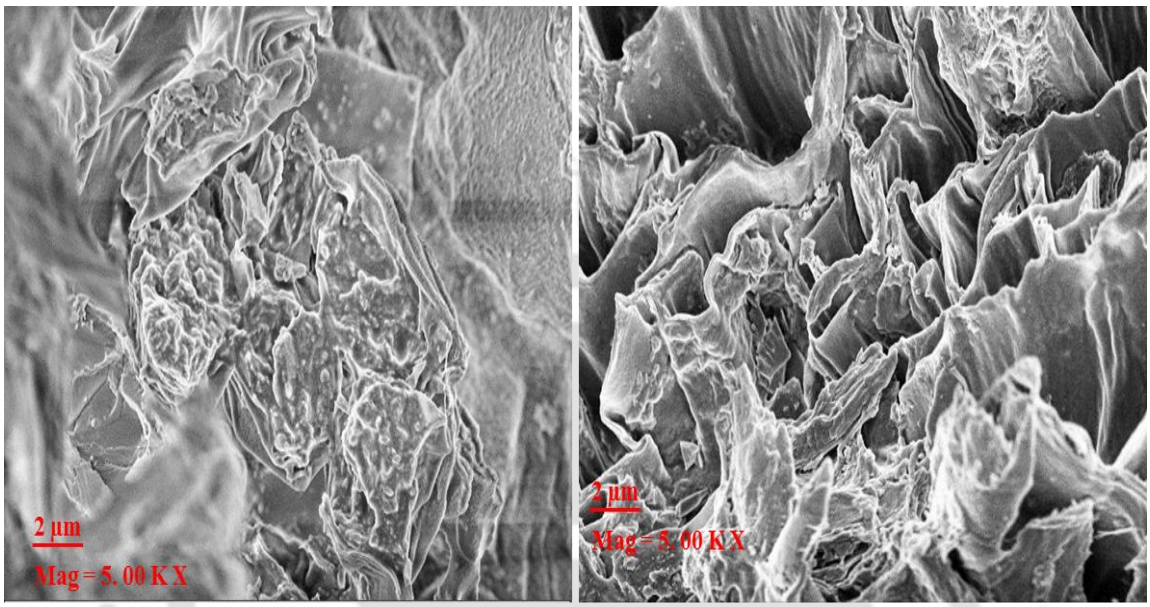

Figure 2.8 FESEM images of (a) unsonicated leaves and (b) sonicated leaves after extraction. Temperature: 50°C; pH: 7; solvent solid ratio: 20 mL/g; sonication power: 50%.

The sonication, therefore, allows better penetration of solvent into the cells, and the microbubbles formed as a result of cavitation further assists the disruption of the cell wall, thereby releasing the active ingredients (Xia et al., 2012). An increase in the mass transfer as a result of structural damage caused by sonication can be inferred. Similar findings were obtained during the ultrasonic treatment of peach samples where sonication positively influenced the cell damage and consequently the extraction process (Altemimi et al., 2016).

Variation of sonication level influences the efficiency of extraction since it affects the cavitation phenomenon. The extraction condition was maintained at 50 ˚C, 20:1 mL/g solvent solid ratio, 15 min extraction time, while sonication power was varied from 30% to 90%. The extracted gallic acid was found to increase with sonication power level

from 83 mg/L at 30% to 224 mg/L at 50%. As in the case of other parameters, it reached the maximum extraction at 50% sonication and decreases thereafter (**Fig. 2.9**). This may be attributed to the increased formation of hydroxyl radicals caused by cavitation upto 50% of sonication power. The generation of higher amount of hydroxyl radicals may promote the oxidation of gallic acid and react with other compounds in the solution beyond the sonication power of 50%, causing an increase in gallic acid exhaustion (Dükkanci and Gündüz, 2006).

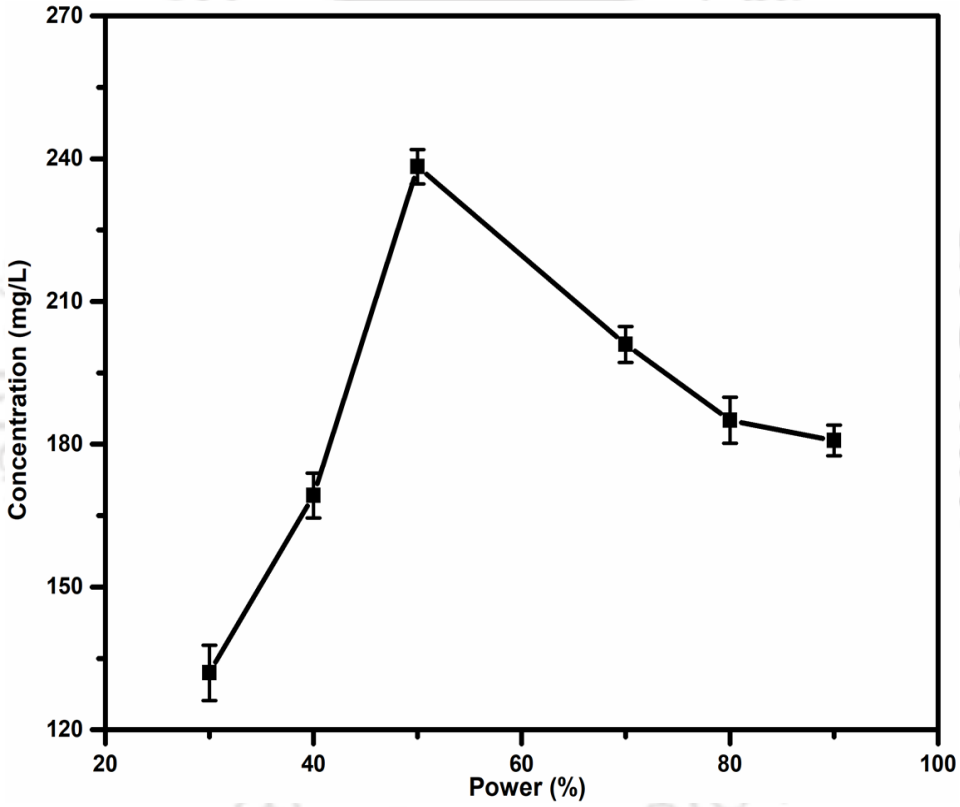

Figure 2.9 Variation in gallic acid concentration with sonication power (Temperature: 50°C; time: 15 min; pH: 7; solvent solid ratio: 20 mL/g)

2.5.2.4 Variation with solvent to powder ratio

Variation in solvent to solid ratio influences the extraction efficiency from plant matrix since the availability of solvent for leaching out the target component is affected. This effect was studied by varying solvent solid ratio from 5:1 to 40:1 mL/g, keeping other

parameters constant at 50 ˚C, 50% power, 15 mins of extraction at neutral pH. **Fig. 2.10** shows the gallic acid content in the extract when the solvent sample ratio is increased from 5:1 to 40:1 (mL/g).

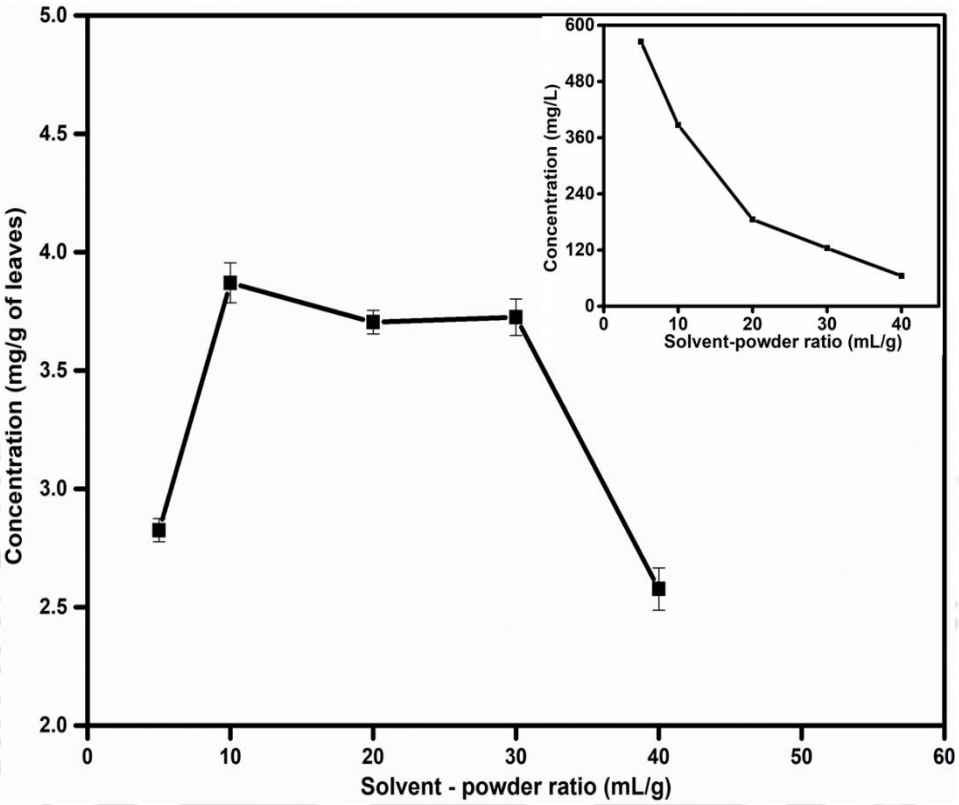

Figure 2.10 Variation in gallic acid concentration with solvent sample ratio (Temperature: 50°C; time: 15 min; pH: 7; sonication power: 50%).

The extracted gallic acid per gram of leaves increased when the solvent with respect to powder was increased from 5:1 to 10:1 mL/g. The initial increase with solvent to powder ratio agrees with the mass transfer principles, which states that concentration gradient between the solid and liquid phases is the driving force for mass transfer. Hence the extraction increased with increase in the solvent to solid ratio (Mokrani and Madani, 2016). However, there was a continuous decrease in extraction on increasing the ratio beyond 10:1 mL/g. This may be due to the limited content of extractable gallic acid, which can be removed with a solvent sample ratio of 10:1 (mL/g). On the

contrary, increasing the amount of solvent per unit mass of sample may lead to the dilution of extractable gallic acid.

2.5.2.5 Variation with pH

The solubility of a solute in aqueous solution is affected by the pH of the solution. The variation in gallic acid extraction with pH of mixture is shown in **Fig. 2.11**.

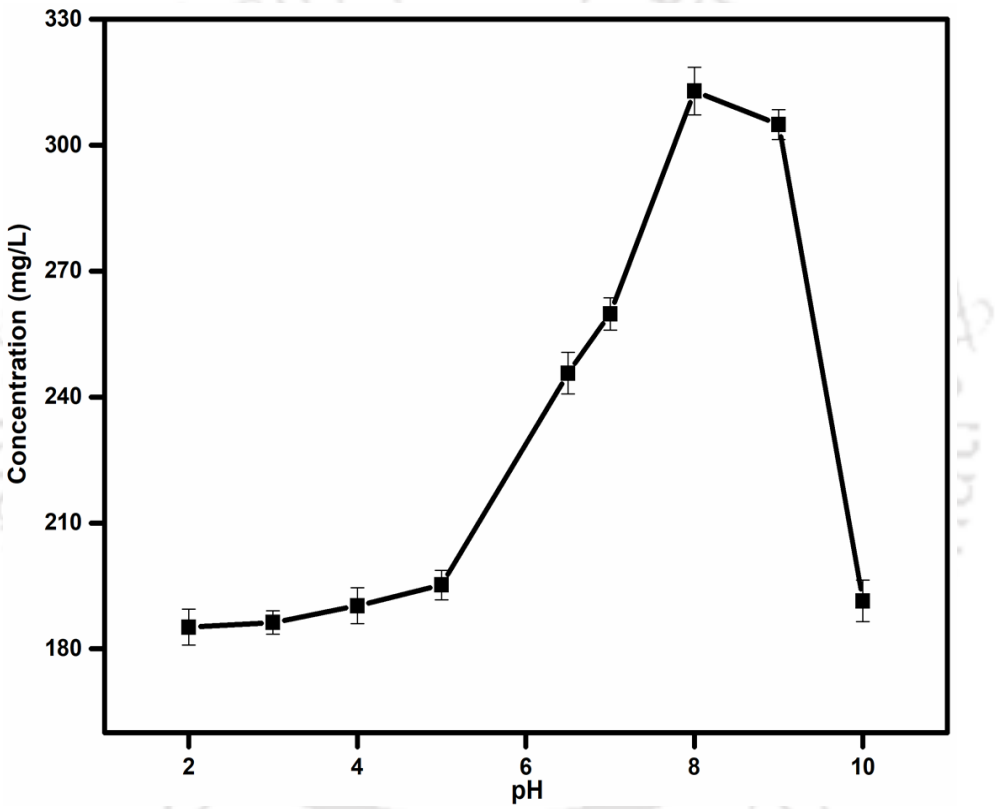

Figure 2.11 Variation in gallic acid concentration with pH (Temperature: 50°C; time: 15 min; solvent solid ratio: 20 mL/g, sonication power: 50%).

It can be seen from the figure that at pH below 5, extraction is low but as the pH increases, it increased from 185.2 mg/L at pH 2 and is highest at pH of 8 where 312.9 mg/L gallic acid was extracted. Subsequently, the extraction drastically decreased after pH of 8 with concentration of 191.4 mg/L at pH 10. The increased extraction at mild alkaline condition may be attributed to the alkaline hydrolysis of the walls, resulting in the release of the bound gallic acid. The carboxyl group of gallic acid are mainly bound

to the hydroxyl group of cell wall components by ester linkage (Shahidi and Yeo, 2016). These ester bonds are resistant towards acidic condition but are labile to mild alkaline condition (Max et al., 2010). The extracted gallic acid is thus found to be maximum at slightly alkaline pH of 8. This agrees with the findings of (Vadivel and Brindha, 2015), where phenolic recoveries were higher at alkaline condition than acidic condition. But as the pH value increases, there is reduction in extraction as gallic acid is found to be unstable at highly alkaline conditions (Friedman and Jürgens, 2000).

2.5.3 Antioxidant activity and total phenolic content

The antioxidant activity of the extract obtained at the condition of maximum gallic acid yield was determined using DPPH method. DPPH assay is an easy and rapid method commonly employed for determination of antioxidant capacity. Using **Eqn. 2.1**, the antioxidant activity of the extract was found to be 91.7%. The TPC was found to be 653.8 mg/100g where gallic acid content was found to be 6.24 mg/g.

2.5.4 Effect of solvent type and sonication system on gallic acid extraction

2.5.4.1 Comparison of different sonication system

It has been observed that the sonication bath had higher efficiency for extraction of gallic acid as compared to the probe sonicator (**Table 2.3**). In the case of probe sonicator, the temperature rises continuously and rapidly during the entire extraction period. In addition, since the sonication source comes in direct contact with the sample, the effects induced by sonication is much more intense. The rapid rise in temperature combined with the hydroxyl radicals produced may cause the oxidation of extracted compounds at the initial stages of extraction. This could lead to degradation of gallic acid. However, in the case of sonication bath, the temperature is maintained at 50 °C where gallic acid remains stable, as mentioned in a preceding section. This results in better retention of the stability of the extracted compounds. Furthermore, probe sonicators possess disadvantages in terms of process reproducibility as well as

repeatability. Hence, sonication bath as a better choice for gallic acid extraction is inferred.

Table 2.3 Variation of gallic acid extraction at different sonication conditions

Sonication equipment	Sonication mode	Amount of gallic acid after 1st extraction stage (mg/L)
Probe sonicator	Pulsed	24.3 ± 3.03
Sonication bath	Pulsed	284.1 ± 8.92
Probe sonicator	Continuous	189.4 ± 6.67
Sonication bath	Continuous	302.3 ± 9.38

2.5.4.2 Comparison of different solvents

The choice of solvent is one of the most important factors as efficiency of extraction is directly affected by the solubility of the target compound in the solvent considered. The extraction potential of three different solvents *viz*., 50% methanol in water, 50% ethanol in water, and alkaline water of pH 8 are shown in **Table 2.4**. 50% methanol showed the highest gallic acid content in extract, followed by alkaline water and 50% ethanol.

Table 2.4 Comparison of 3 different solvents in the extraction of gallic acid at solvent solid ratio of 30:1

Solvent	Gallic acid concentration in the extract (mg/L)
50% Ethanol	183. 7 ± 5.39
50% Methanol	329.5 ± 9.22
Alkaline water (pH 8)	312.92 ± 8.78

This variation in extraction capacity may be due to the difference in solubility of gallic acid in these solvents and also their interaction with the other components present. Although aqueous methanol showed higher efficiency (329.5 mg/L), it poses environmental damage on disposal and also any trace residue in the purified compound may cause toxicity, especially when the end application is in food systems. On the other hand, alkaline water showed comparable result, although slightly lesser (312.92 mg/L). Considering the safety, environment and economic point of view, it may be concluded that water can replace organic solvents by altering its pH based on the compound of interest.

2.5.5 Purification of gallic acid

The purification of gallic acid by reverse osmosis (RO) and high-performance liquid chromatography (HPLC) is shown in **Fig. 2.12**. The retentate stream contained higher concentration of gallic acid than the feed while the permeate contains negligible amount of gallic acid (**Fig. 2.12(a)**). Some other components are also rejected by the RO membrane. The results obtained indicate that RO is not selective towards gallic acid. On the other hand, the concentration of gallic acid in the retentate increased by 35%, as a consequence of some other components permeating through the membrane. RO being environmental-friendly and having ease of operation, may be an effective purification method for gallic acid and can be explored further. The fraction collected from the elute in the HPLC system gave a very distinct gallic acid peak (**Fig. 2.12(b)**) when this was reinjected for analysis.

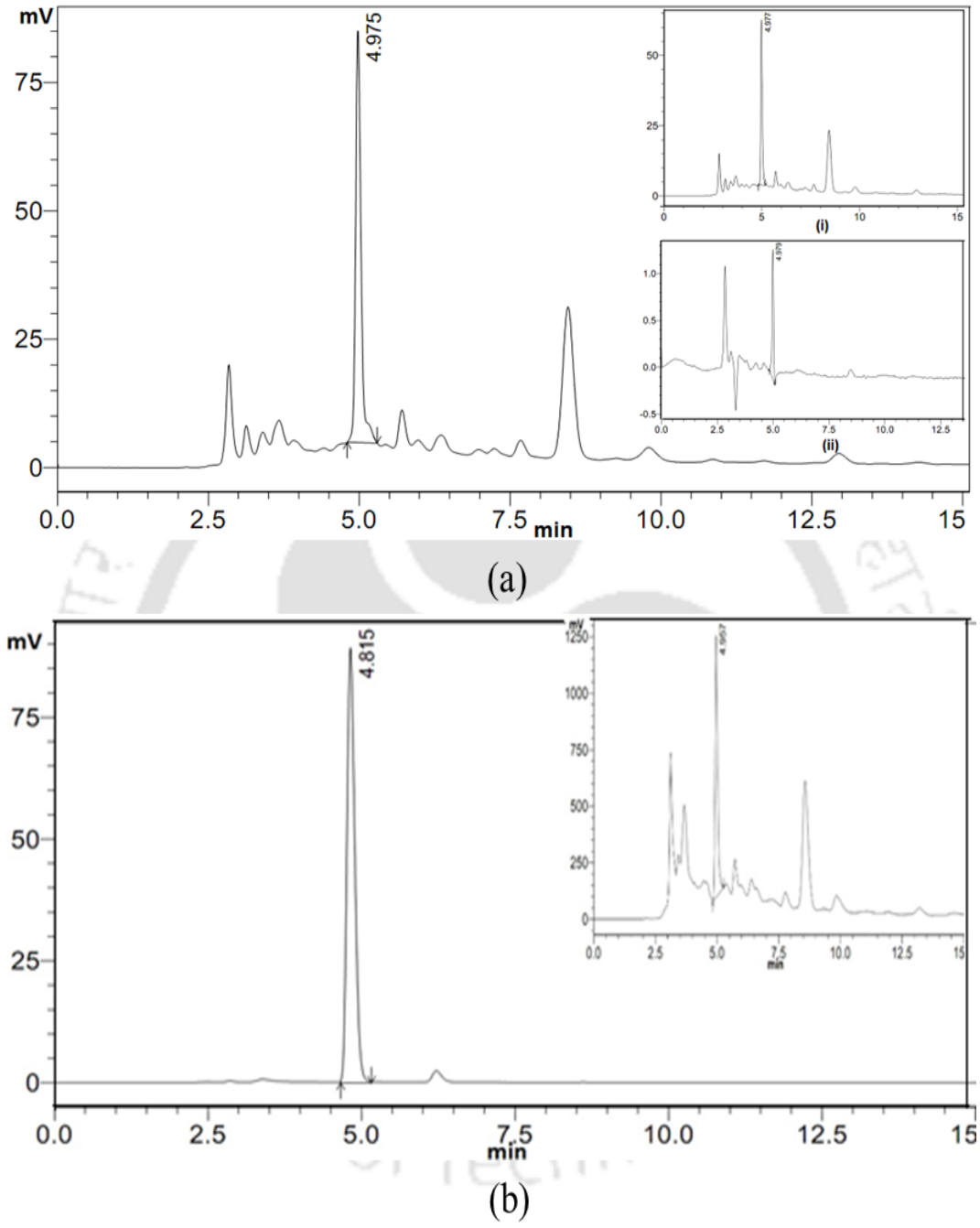

Figure 2.12 (a) HPLC of retentate after purification by RO. Inset: (i) RO feed (ii) RO permeate (b) HPLC of extract after purification of 4.5 – 5.5 min fraction. Inset: before purification by HPLC.

The percentage area coverage in the chromatogram increased significantly to 95% in collected fraction from 17% in feed. This shows that HPLC can be efficiently used for the purification of gallic acid without any prior treatment like adsorption, which increase the overall complexity and cost.

2.5.6 Extraction modeling results

The insight of the extraction of gallic acid from *F. auriculata* leaves was investigated using the Peleg, Power Law, Parabolic diffusion, and unsteady diffusion models at three sonication power levels. The goodness of fit of the models was characterized by the coefficient (R^2) value (**Table 2.5**).

Table 2.5 Model constants for different kinetic models

Model	Equation	Constant term	R^2	Adj. R^2
Peleg	$f(t) = \frac{t}{(k_1 + k_2 t)}$	**30%** k_1= 0.06206 k_2=0.005507	0.99	0.99
		50% k_1= 0.01883 k_2=0.003556	0.99	0.99
		90% k_1= 0.02631 k_2=0.005015	0.99	0.99
Power	$f(t) = k_1 \times t^n$	**30%** k_1 = 39.22 n = 0.3427	0.97	0.96
		50% k_1 = 111.3	0.95	0.94

		n = 0.2141		
		90%	0.95	0.95
		k_1 = 79.12		
		n = 0.2139		
Parabolic diffusion	$f(t) = k_1 + k_2 \times t^{1/2}$	**30%**	0.93	0.92
		k_1= 15.41		
		k_2= 19.73		
		50%	0.80	0.78
		k_1= 57.54		
		k_2= 30.48		
		90%	0.81	0.78
		k_1= 40.89		
		k_2= 21.65		
Unsteady diffusion	$f(t) = (1 - k_1) \times e^{-k_2 t}$	**30%**	0.61	0.56
		k_1=-65.5		
		k_2=- 0.01588		
		50%	0.45	0.37
		k_1= -137.5		
		k_2= -0.01228		
		90%	0.46	0.38
		k_1= -97.24		
		k_2=-0.01234		

Peleg model describes the extraction process as one that follows first order kinetics in the initial stage, where the concentration increases with time and zero order in the later stage, with the concentration approaching a maximum or plateau (Cheung et al., 2013).

This corroborates with our experimental results. The constants k_1 and k_2 relate to the initial extraction rate (B_0) and maximum extraction yield, i.e. equilibrium concentration (C_e) of extracted gallic acid, respectively (Bucić-Kojić et al., 2007). Their relations are expressed as given in **Eqs. (2.2)** and **(2.3)**

$$B_0 = \frac{1}{k_1}; \tag{2.2}$$

$$C_e = \frac{1}{k_2} \tag{2.3}$$

The value of k_1 decreased from 62.06 $\times 10^{-3}$ at 30% to 18.83$\times 10^{-3}$ at 50% and then increased to 26.31$\times 10^{-3}$ at 90%. This shows the highest initial extraction rate at 50%, which agrees with **Fig. 2.9**. Similarly, k_2 was found to be minimum at 50%, indicating maximum concentration at equilibrium. Using **Eqs. (2.2)** and **(2.3)** the initial extraction rate was found to be 53 mg GA/min and predicted equilibrium concentration at 50% was found to be 281 mg/L. It was established that the Peleg model is the best fitted model (>0.99) for all the power levels considered herein during the sonication. **Fig. 2.13** shows the variation in calculated and experimental gallic acid extraction with time using Peleg model. It may be seen from the figure that the extraction increases sharply upto around 15 min and becomes gradual thereafter. This trend may be explained on the basis of principle of mass transfer phenomenon. The faster extraction at the initial stage might be due to the higher gallic acid load in the leaves. Once a major part of gallic acid comes out from the leaves, the extraction rate becomes gradual due to lower gallic acid load.

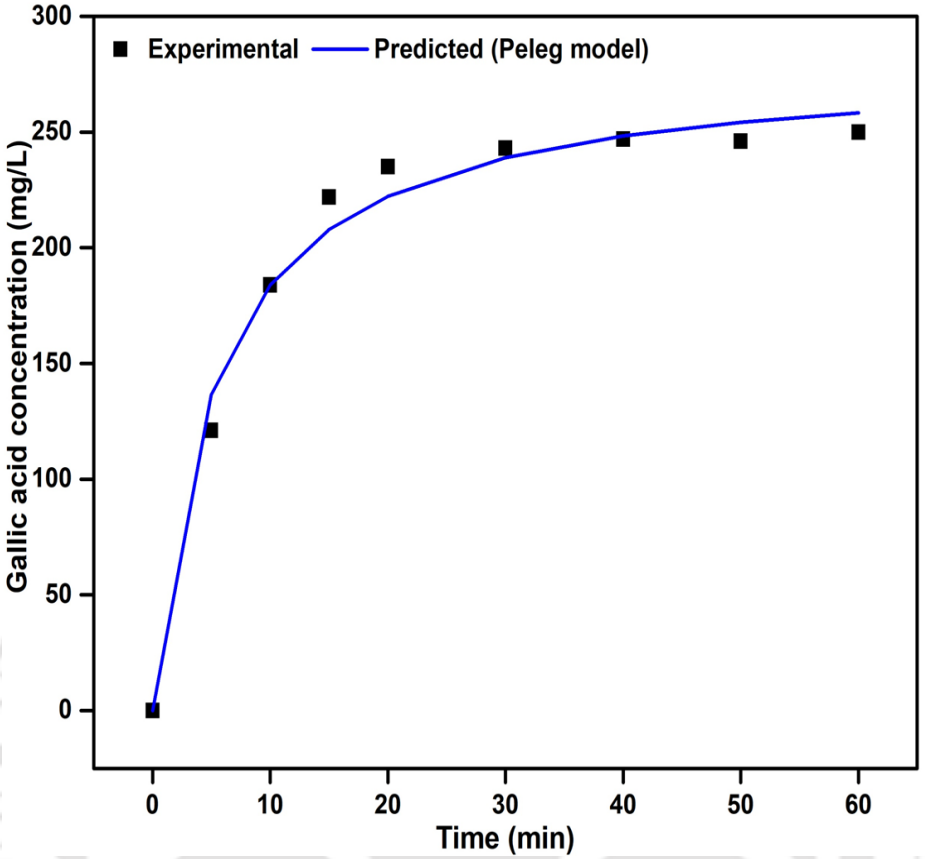

Figure 2.13 Experimental and Peleg model predicted gallic acid concentration at 50% sonication power.

2.6. Summary

This chapter discusses the extraction of gallic acid from *F. auriculata* leaves using ultrasound assisted extraction and the optimization of the process parameters. The influence of time, temperature, sonication level and solid to solvent ratio on gallic acid extraction was investigated. Maximum extraction was obtained after 30 min at 50% sonication level, 1:10 g/mL solid to solvent ratio, 8 pH at 50 °C. Among the various solvents, 50% methanol resulted in highest extraction followed by alkaline water and 50% ethanol. The gallic acid extracted using different solvents were found to be 329.5 mg/L, 312.92 mg/L and 183.7 mg/L for 50% methanol, water at pH 8 and 50% ethanol, respectively. Sonication bath was found to perform better in extracting and retaining extracted gallic acid as compared to probe sonication. The kinetics of the extraction was

studied and Peleg model was found to have the best correlation with highest regression coefficient value (R^2>0.99). The extracted gallic acid was purified using reverse osmosis and HPLC.

Chapter 3

Preparation and characterization of gallic acid (antioxidant) incorporated polyvinyl alcohol coating for delayed ripening of green bananas

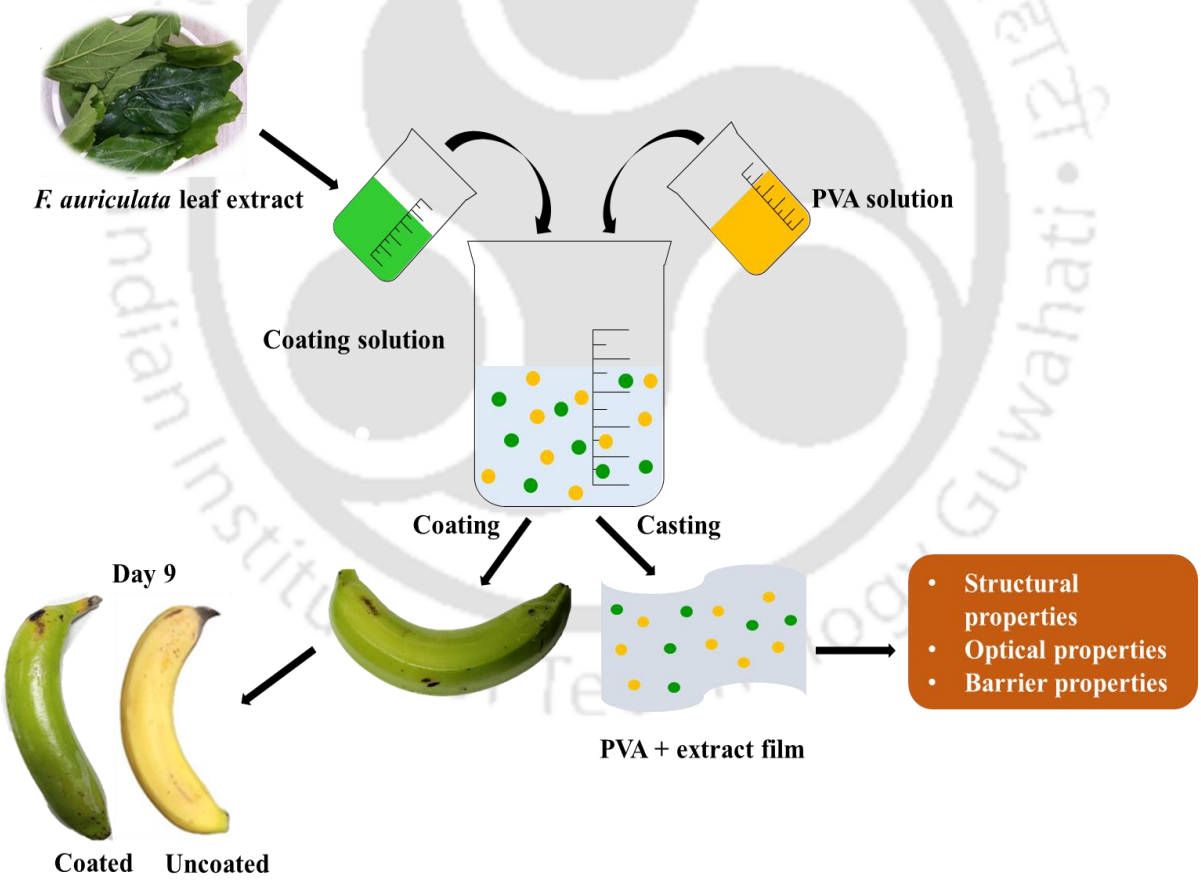

Preparation and application of PVA-gallic acid coating

Chapter 3

Preparation and characterization of gallic acid (antioxidant) incorporated polyvinyl alcohol coating for delayed ripening of green bananas

In this chapter, the detailed experimental method is discussed for the development of PVA-gallic acid coating for enhancing the shelf life of bananas by delaying the ripening process. Gallic acid-rich extract of Ficus auriculata leaves was incorporated as an additive to augment the functional properties of the coating. The coatings were characterized by various characteristics that affect the efficiency of their use as edible coating of bananas. Insights into the effect of different types of coatings on change in physicochemical attributes of bananas during storage were critically analyzed. The background, state of art literature and the scope of this research have been described in Chapter 1, Section 1.3 and Section 1.6.2., respectively. This work has been published in ACS Omega.

3.1. Experimental

3.1.1 Materials

F. auriculata leaves were collected from the IIT Guwahati campus. Poly(vinyl alcohol) (PVA) (M.W. 1,15,000) was obtained from Loba Chemie (Mumbai, India). Sodium hydroxide (NaOH) was obtained from Merck, India. Water from the Millipore Milli-Q purification system was used in all the experiments. Green banana samples were collected from a local market. They were thoroughly washed to remove any adhered dust and dirt particles and air-dried.

3.1.2 Preparation of extract and coating solution

The gallic acid-rich extract from *F. auriculata* leaves was prepared using an optimized protocol from our previous work (Baite et al., 2021). Briefly, leaf powder and slightly alkaline water at pH 8 were mixed at a ratio of 1:10 g/mL. The mixture was subjected to ultrasound-assisted extraction at 50 °C and 50% sonication power for 30 min using a sonication bath (P 30H, Elmasonic). The concentration of gallic acid in the extract from *F. auriculata* leaf was found to be 312.9 mg/L. the antioxidant activity of gallic acid enriched extract was 91.7%. The coating solution was prepared by mechanical mixing of PVA solution and the extract at different concentrations and denoted as PP (pure PVA), PE1 (PVA+1% extract), PE5 (PVA+5% extract) and PE10 (PVA+10% extract) (**Table 3.1**).

Table 3.1 Composition of the coating groups

Name	**PVA%**	**Extract% (with respect to PVA solution)**
Control	---------	----------
Pure PVA (PP)	10	----------
PE – 1 (PE1)	10	1
PE – 5 (PE5)	10	5
PE – 10 (PE10)	10	10

10% PVA solution was first prepared by heating the mixture at 90 °C under stirring for 6 h. Following the complete dissolution, the solution temperature was brought down to 50 °C and the extract of *F. auriculata* leaves was added to the PVA solution on the basis of the total coating solution. The solution was mixed for another 30 min at 50 °C. The

final blend was centrifuged at 10000 rpm for 10 min to remove any undissolved particles or gas bubbles. To allow the characterization of the coating surface, the solution was cast using a casting knife on clean glass plates to obtain films containing different extract concentrations. The films were then dried overnight under ambient condition and dried through assisted airflow in a laminar hood.

3.1.3 Application of coating on banana samples

The green banana samples with intact peel were then coated with the prepared solution by dipping the fruits in the solution for 30 s. The coated samples were separately grouped according to the composition of the coating solution. The bananas were then removed and placed on a metal grid until the solution stopped dripping. The samples were then transferred to a chamber maintained at 25±1 °C where the study continued. Three samples were removed from each group every third day to measure various physicochemical properties until full ripening. The entire process of preparation of film forming solution and its application as a coating for green bananas is shown in **Fig. 3.1.**

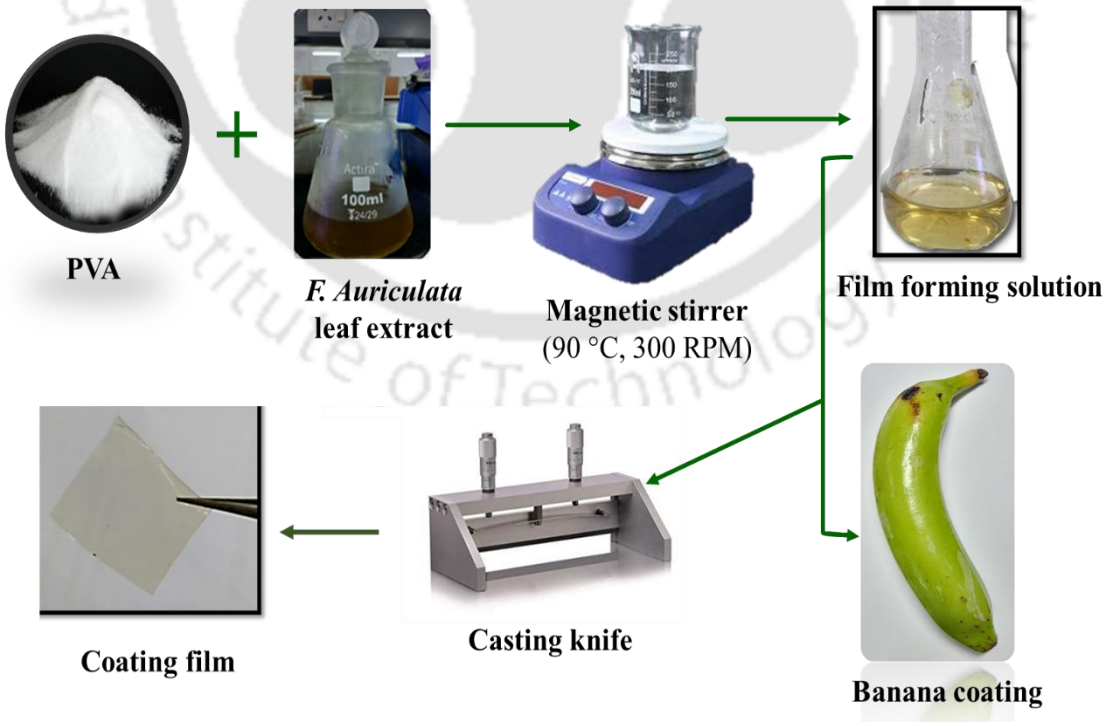

Figure 3.1 Preparation of PVA - based antioxidant coating of green bananas

3.2. Characterization of the coating films

3.2.1 Structural properties

The morphology of the films was visualized using a field emission scanning electron microscope (FESEM) (Zeiss, Sigma). The images of the surface of the films were recorded at 2000–3000 V using Inlens detector. The surface roughness was examined with the help of an atomic force microscope (AFM) (Innova, Bruker). The microscopic images were obtained at a 1 Hz scan rate. The functional groups present on the different films were analyzed using attenuated total reflectance – Fourier transform infrared (ATR – FTIR) spectroscopy (IRAffinity-1, M/s Shimadzu, Japan). The spectra were obtained by scanning the films over a range of 4000 – 400 cm^{-1} wave number with an average of 30 scans per sample. The crystallography of the films was studied with the help of an X-ray diffractometer (Bruker D8 Advance) provided with CuKα radiation, and the diffractogram was recorded in the 2θ range between 5 – 60°. The surface chemistry of the films was further elucidated using X-ray photoelectron spectroscopy (XPS). The spectrometer (ESCALAB Xi+, Thermo-Scientific) was operated in constant analyzer energy (CAE) mode using a monochromatic Al Kα X-ray source with a spherical energy analyzer.

3.2.2 Optical properties

The optical property of the film in terms of opacity was analyzed using the technique adopted by (Cazón et al., 2020) with minor changes. The absorbance of the films at 500 nm were recorded employing a UV – Visible spectrophotometer (UV-2600, Shimadzu, Singapore). The opacity (A/mm) was calculated using **Eqn (3.1)** as below:

$$\text{Opacity} = \frac{Abs_{500}}{x} \tag{3.1}$$

Where,

Abs_{500} = the absorbance at 500 nm (A), and x = film thickness (mm).

3.2.3 Thermal properties

The thermal properties of the films were investigated utilizing a thermogravimetric analyzer (TGA) (TG 209 F1 Libra, Netzsch, Germany). Around 7 mg of films were used for each analysis and the films were subjected to heat treatment by heating from 20 – 800 °C at a rate of 10 °C/min under a nitrogen environment to maintain an inert condition. The graph indicating the change in mass with an increase in temperature was plotted.

3.2.4 Water solubility and water vapour permeability

The water solubility of the films was measured using the protocol adopted by Terzioğlu et al. (Terzioğlu et al., 2021) with minor modification. For this, films of 2×2 cm^2 were cut and dried at 50 °C for 24 h to evaporate any residual moisture. The initial weight of the films (W_1) was noted and they were placed in a 100 mL beaker containing 50 mL of distilled water and allowed to stand for 24 h at ambient temperature. After 24 h, the films were dried again at 50 °C for 24 h to remove the absorbed moisture and the final weight was recorded (W_2). The water solubility of the films was deliberated by using **Eqn (3.2)**.

$$\text{Solubility}(\%) = \frac{W_1 - W_2}{W_1} \times 100 \qquad (3.2)$$

The barrier property measured through water vapour transmission rate and permeability (WVTR and WVP) was determined using the protocol followed by Devi et al. (Devi et al., 2019) with slight modification. Briefly, glass cups half-filled with calcium chloride were covered using the pure and blended films and were placed inside a desiccator. A relative humidity (RH) of 75.2±0.17% was maintained inside the desiccator by using a saturated sodium chloride solution (Othman et al., 2017). The transport of water vapour through the films was obtained by measuring the weight gain of the cups at an interval of 24 h for 7 days and the weight gain was plotted against time. The WVTR was

determined from the slope obtained from the linear regression by dividing the slope by the area of vapour transfer (in m^2). The
(g /h/Pa/m) was estimated using **Eqn (3.3)**.

$$WVP = \frac{WVTR \times x}{P(R_1 - R_2)} \quad (3.3)$$

where P = saturation vapour pressure of water at ambient temperature, R_1 and R_2 = Relative humidity values in the desiccator, and the cup, respectively, and x = thickness of the film (m). [P (R_1 − R_2)] is the driving force for the moisture transfer and is 2376.30 Pa under these conditions.

3.3 Analysis of fruit

3.3.1 Weight loss

Weight loss is brought by moisture loss from the banana samples, which in turn influences the appearance and acceptability of the fruits. The weight of the samples from different sample groups was recorded every day using an analytical weighing balance. The average values of the weight change are presented as below:

$$WL\ (\%) = \frac{W_0 - W_i}{W_0} \times 100 \quad (3.4)$$

Where,
W_0 and W_i are the initial and weight at sampling time, respectively.

3.3.2 Titratable acidity (TA)

For the measurement of TA, the banana pulp is first blended in a mixer grinder to get a homogeneous paste. This was centrifuged at 10000 rpm for 10 min to get a clear juice free from the pulp.

TA was determined using the protocol followed by Hajji et al. (Hajji et al., 2018). Briefly, 1 mL of juice was mixed with 9 mL distilled water and the diluted juice was titrated against 0.1 M NaOH solution to a final pH of 8.1. Three drops of phenolphthalein indicator were added to identify the endpoint. Malic acid is the predominant organic acid present in bananas and hence, calculations for titratable acidity are made based on this acid.

The TA denoted as g of malic acid per 100 g of fruit juice was calculated using **Eqn (3.5)**.

$$TA\ (\%) = \frac{V_{NaOH} \times 0.1 \times 0.067}{V_{sample}} \times 100 \qquad (3.5)$$

Where,

V_{NaOH} = Volume of NaOH used to bring the pH to 8.1

0.1 = Molarity of the NaOH solution

V_{sample} = Volume of the juice taken

0.067 = Conversion factor for malic acid

3.3.3 Total soluble solids (TSS)

TSS is a vital parameter for the determination of the quality of bananas since it indicates the level of sweetness. The TSS of the sample on each collection day was measured by using a portable refractometer (Erma, Japan). 1-2 drops of the homogenized juice were placed on the sampler and the reading was noted and the TSS was presented as °Brix.

3.3.4 Chlorophyll content

The chlorophyll content of the coated and uncoated banana peels was measured in intervals of three days until the completion of the study. For this, 0.1 g of peel free from pulp and fibers were mixed with 80% acetone using a mortar and pestle for 3-5 min. The chlorophyll solution was filtered with Whatman 1 filter paper and the absorbance of

the filtrate was measured with a UV – Vis spectrophotometer (UV-2600, Shimadzu, Singapore). The chlorophyll content of the peels was determined using **Eqns (3.6), (3.7), (3.8),** and **(3.9)** (Thakur et al., 2019).

$$\text{Chlorophyll a} = 12.7 \times A_{663} - 2.995 \times A_{645} \quad (3.6)$$

$$\text{Chlorophyll b} = 22.95 \times A_{645} - 4.67 \times A_{663} \quad (3.7)$$

$$\text{Total chlorophyll (mg L}^{-1}) = \text{Chlorophyll a} + \text{Chlorophyll b} \quad (3.8)$$

$$\text{Total chlorophyll (mg g}^{-1}) = \frac{\text{Total chlorophyll (mg L}^{-1}) \times 25\text{mL}}{\text{Sample weight} \times 1000} \quad (3.9)$$

3.3.5 Ion leakage

The leakage of the electrolytes from the banana peels represented by the membrane stability index (MSI) was measured using the protocol followed by (Thakur et al., 2019) with a slight alteration. Briefly, three grams of sliced banana peel free from the pulp were taken in a 50 mL beaker that contains 30 mL of deionized water. The mixture of peel and water was kept covered at room temperature and stirred at 150 rpm for 4 h. The conductivity of the solution (k_1) was measured at the end of 4 h using a conductivity meter (CON 2700, Eutech Instruments). Then, the beaker was held in a water bath at 100 °C for 30 min to facilitate the release of the electrolytes. Then, the mixture was cooled to room temperature followed by the conductivity measurement (k_2). The MSI was determined using the following relation,

$$\text{Ion leakage (\%)} = \frac{k_1}{k_2} \quad (3.10)$$

3.3.6 Statistical analysis

The results were presented as mean ± SD obtained from three replicates. The one-way analysis of variance (ANOVA) and Tukey's test was performed to determine the statistical difference between different study groups for each sampling day. The test was

carried out using OriginPro 9 and the results were considered to be significant at $p < 0.05$.

3.4 Results and discussion

3.4.1 Structural and functional analysis of films

3.4.1.1 FESEM analysis

It is evident from the FESEM images (**Fig. 3.2**) that the film prepared by PP results in a uniform and homogenous surface with no significant defect.

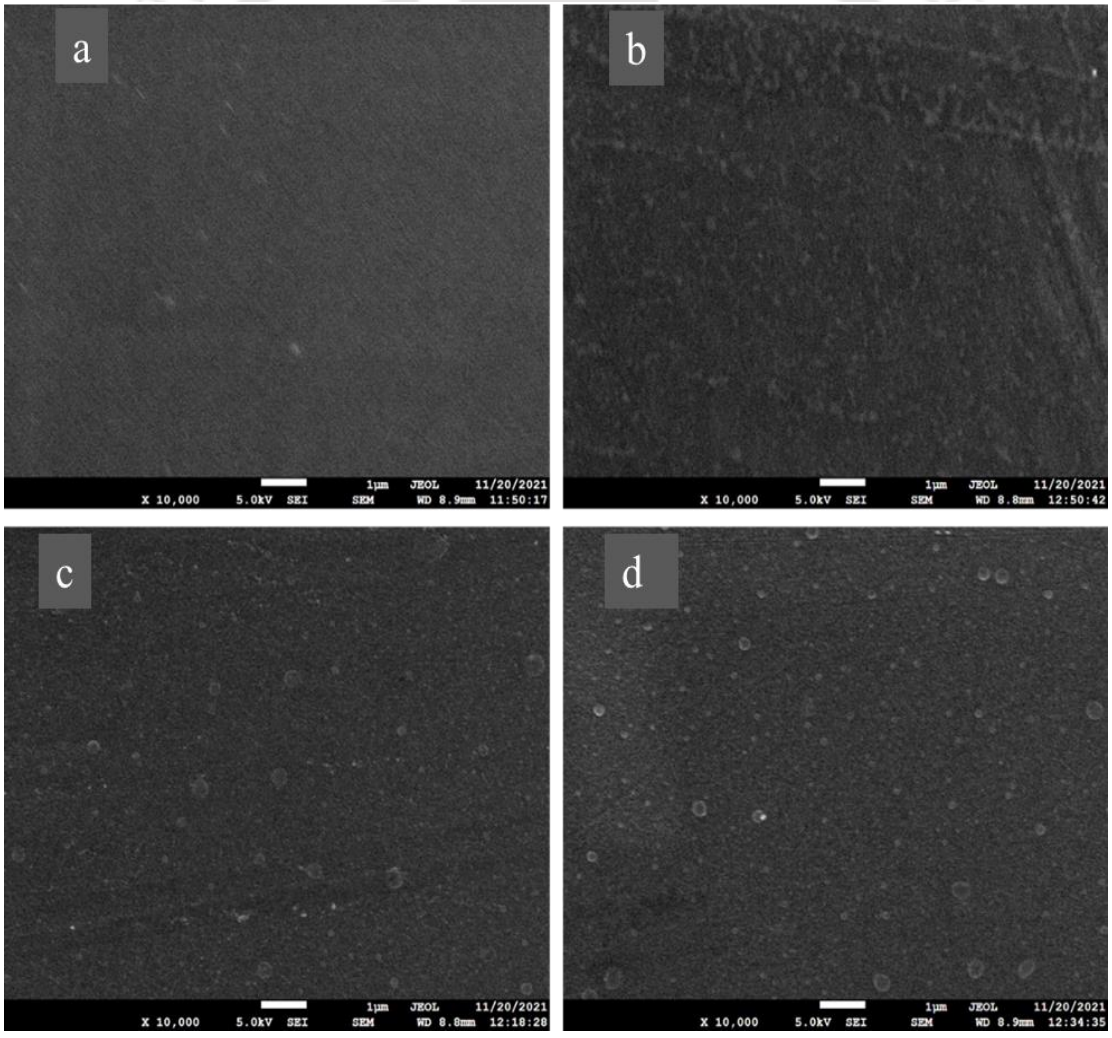

Figure 3.2. FESEM images of films (a) PP (b) PE1 (c) PE5 (d) PE10

This signifies the good film-forming property of the polymer during casting. The addition of the leaf extract affected the homogeneity of the polymer solution at all concentrations. However, the extract seems to be well dispersed in the solution owing to the good hydrophilicity of the phytochemicals present in the extract. Increasing the concentration of the extract enhances the formation of porous-like structures that spread throughout the surface resulting in a rough surface. This may be ascribed to the rearrangement of the water-soluble components like gallic acid during the evaporation of water during the film preparation (Luzi et al., 2019).

3.4.1.2 AFM analysis

It was observed from AFM images (**Fig. 3.3**) that the addition of extract increased the surface roughness consistent with the concentration.

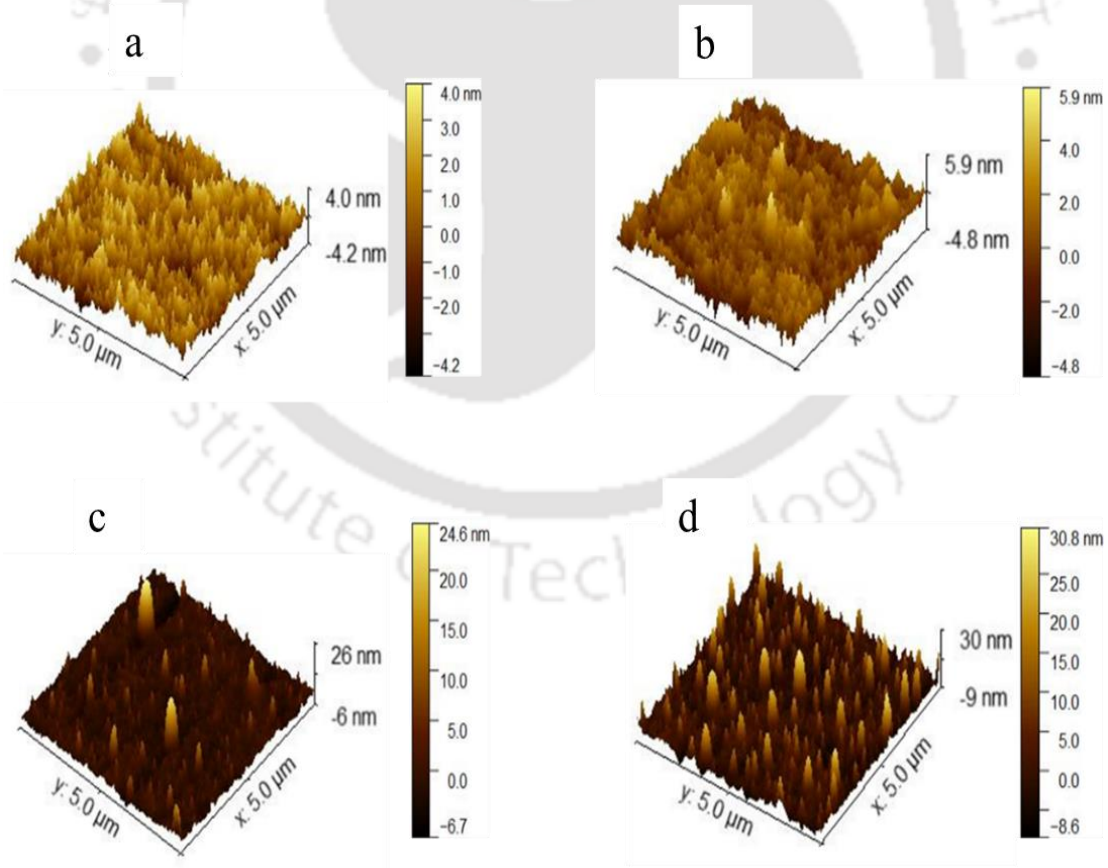

Figure 3.3. AFM images of films (a) PP (b) PE1 (c) PE5 (d) PE10

At a lower concentration of 1% (PE1), the average roughness increased just slightly to 1.286 nm from 1.073 nm of the PP film. This indicates a uniform mixing of the extract components with the polymer matrix at the molecular level in low concentrations. However, as the extract increased from 5% (PE5) and 10% (PE10), the average surface roughness increased to 2.475 nm and 4.535 nm, respectively. This is presumably due to the dispersion and aggregation of the compounds present in the extract leading to an increased roughness (Kasai et al., 2018). In addition, the evaporation of water from the non-homogenous regions may lead to increased surface roughness. The findings corroborate the FESEM results.

3.4.1.3 FTIR analysis

The functional groups responsible for the chemical interactions in the films determined through FTIR (**Fig. 3.4)** show a peak at 3265 cm^{-1}, which is allotted to the O-H stretching of the alcohol and carboxylic acid. However, this peak shift slightly towards the left with a marginal increase in the width with the addition of the extract. This may be elucidated by the establishment of hydrogen bonds subsequent to the interaction between the hydroxyl groups of PVA and the phenolics such as gallic acid that are present in the extract (Chenwei et al., 2018). The peaks at 2924 cm^{-1} and 1710 cm^{-1} may correspond to the C-H stretching as well as C=O stretching of gallic acid ester, respectively (Chenwei et al., 2018). The peaks at 1420 cm^{-1}, 1080 $cm^{-1,}$ and 840 cm^{-1} can be attributed to C-H vibration, C-O stretching, and C=C bending, respectively (Suganthi et al., 2020; Yu et al., 2015).

3.4.1.4 XRD analysis

The diffractogram of the films obtained from the XRD analysis (**Fig. 3.5)** shows the crystal structure. The peaks at 2θ = 19.28°, 26.38°, and 44.4° are characteristic of PVA and correspond to the crystal planes of (101), (200), and (102), respectively (Tang et al., 2015). The peak position corresponding to (101) plane is attributed to the hydrogen bonding resulting from the molecular chains within or between PVA.

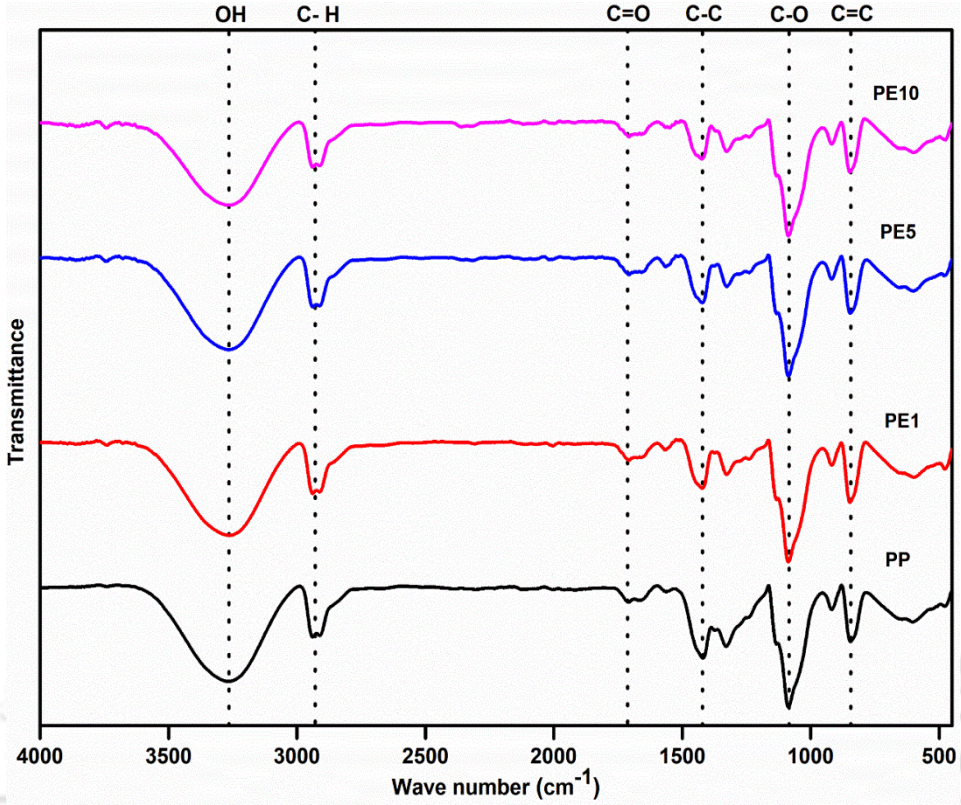

Figure 3.4 FTIR spectra of the coating films (PP: Pure PVA; PE1: PVA+1% extract; PE5: PVA+5% extract; PE10: PVA+10% extract)

The addition of extract did not cause any shift in peak position or any new peak, indicating that the crystal structure remains unaffected. There is an intensification of the peak with the addition of the extract. This may be explicated by the hydrogen bonding between PVA and the constituents of the extract that improves the ordering arrangement of PVA molecules (Guan et al., 2016). The position of the PP peaks remains unchanged in all the blend films extract which indicates that there was no significant change in the lattice distance resulting from the blend (Xiong et al., 2020).

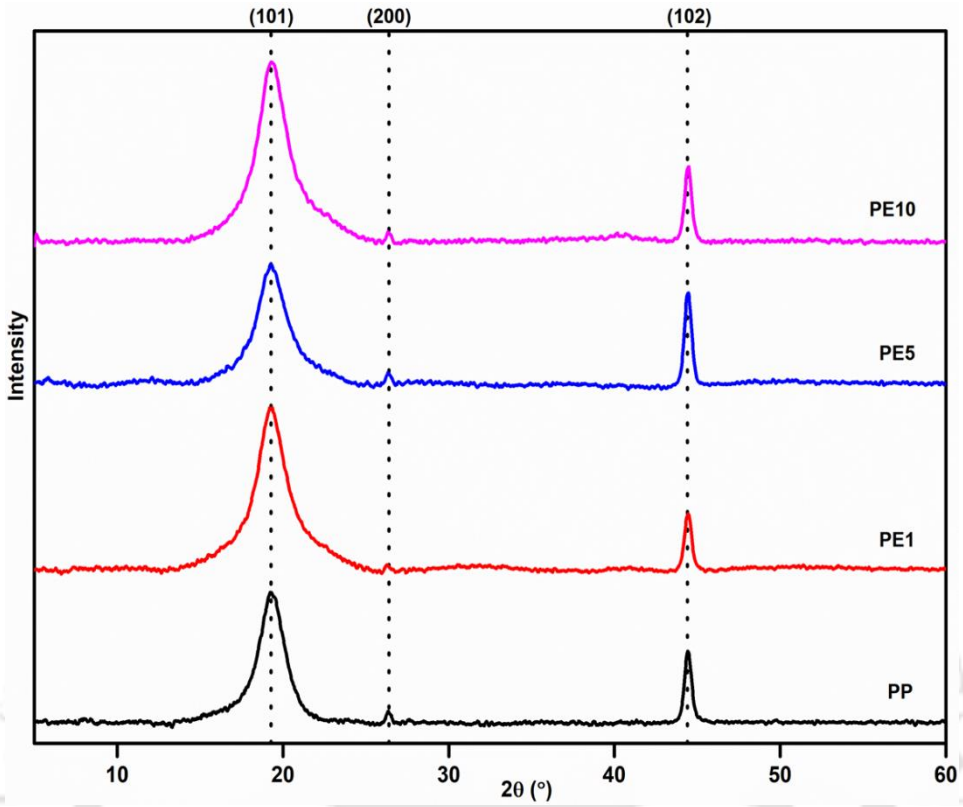

Figure 3.5 XRD diffractogram of coating films. (PP: Pure PVA; PE1: PVA+1% extract; PE5: PVA+5% extract; PE10: PVA+10% extract)

3.4.1.5 XPS analysis

XPS was used to further comprehend the surface chemistry of the pure and extract incorporated PVA films (**Fig. 3.6**). The deconvoluted C1s spectra depicted four major surface components corresponding to binding energies of 284.5 eV, 284.9 eV, 286.09 eV, and 288.8 eV that can be attributed to C-C, C=C, C-O, and O-C=O, respectively (Das, Mandal, & Gumma, 2020). The binding energies shift positively with the increasing concentration of the extract, which might be due to the modification of the PVA surface. This could be ascribed to the strong interaction between the increasing concentration of extract and PVA (Saxena & De, 2021). The addition of extract resulted in a change in carbon-oxygen ratios as observed from the survey plots (**Fig. 3.7**). The atomic percentage of carbon increased from 62.3% in PP to 62.6%, 65.4%, and 71% in

PE1, PE5, and PE10, respectively (**Table 3.2**). This may be attributed to the increase in carbon moieties present in the constituents of the extract.

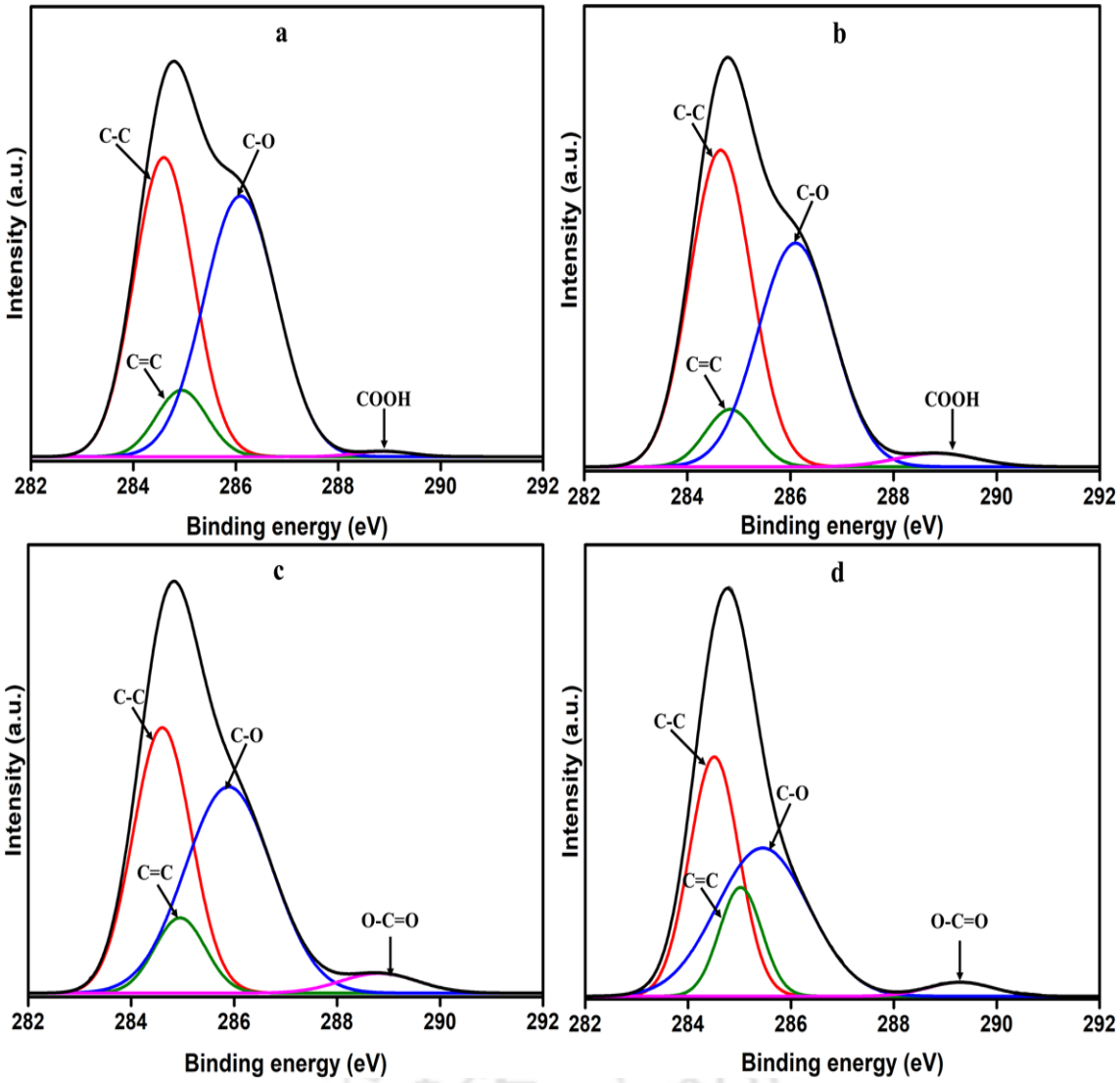

Figure 3.6 XPS spectra of (a) PP (b) PE1 (c)PE5 and (d)PE10

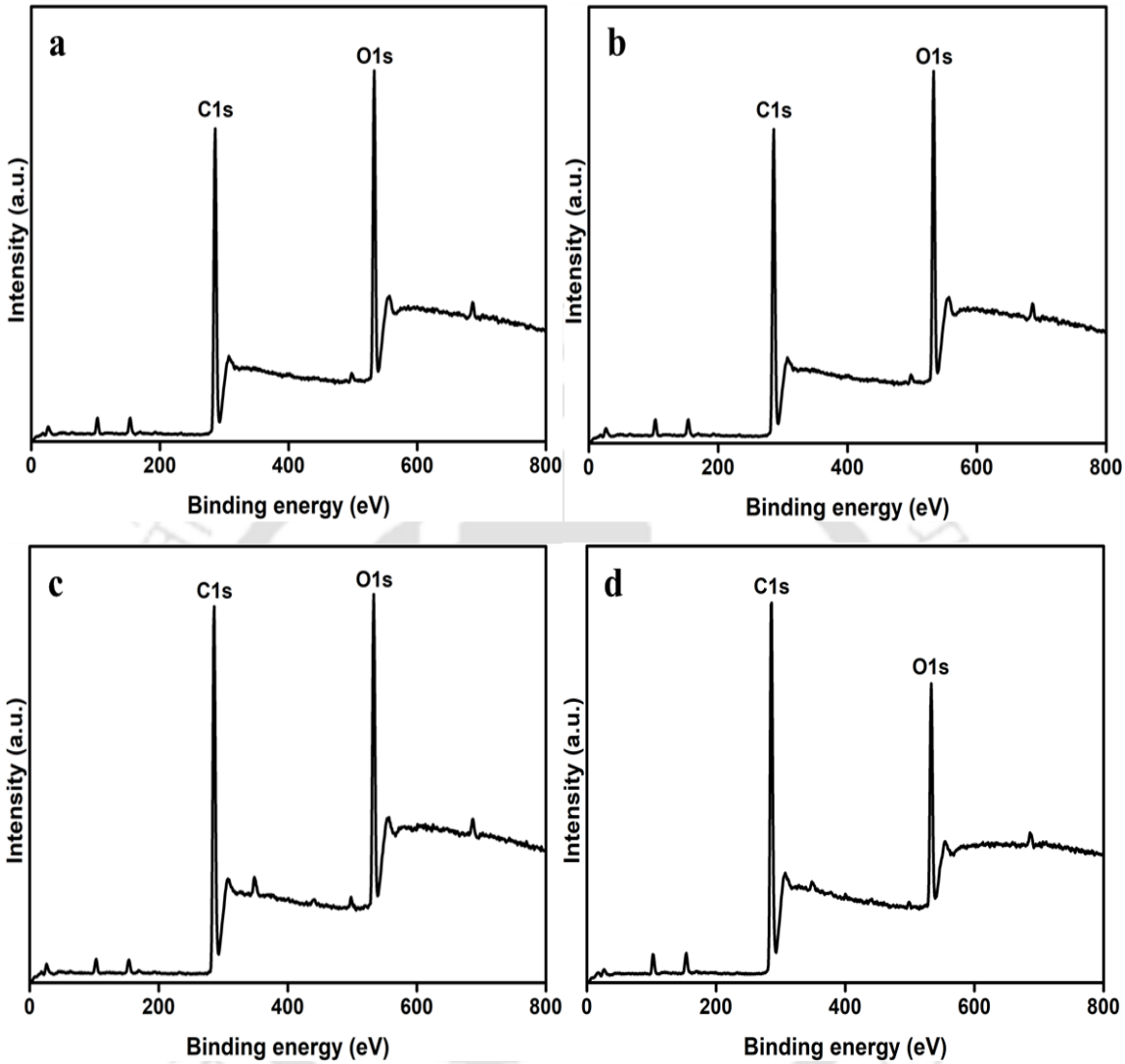

Figure 3.7 Survey spectra of (a) PP, (b) PE1, (c) PE5 and (d) PE10

Table 3.2 Atomic percentages of carbon and oxygen from XPS

Sample	**Atomic percentage**	
	Carbon (%)	**Oxygen (%)**
PP	62.27	37.73
PE1	62.62	37.38

PE5	65.43	34.57
PE10	71.01	28.99

3.4.2 Optical and thermal analysis of films

3.4.2.1 Opacity of films

The transparency and opacity of coating films is an important parameter as it allows the visual observation of the foods being treated at any instance. The films obtained from all the treatment groups resulted in low opacity indicating excellent transparency (**Fig. 3.8**).

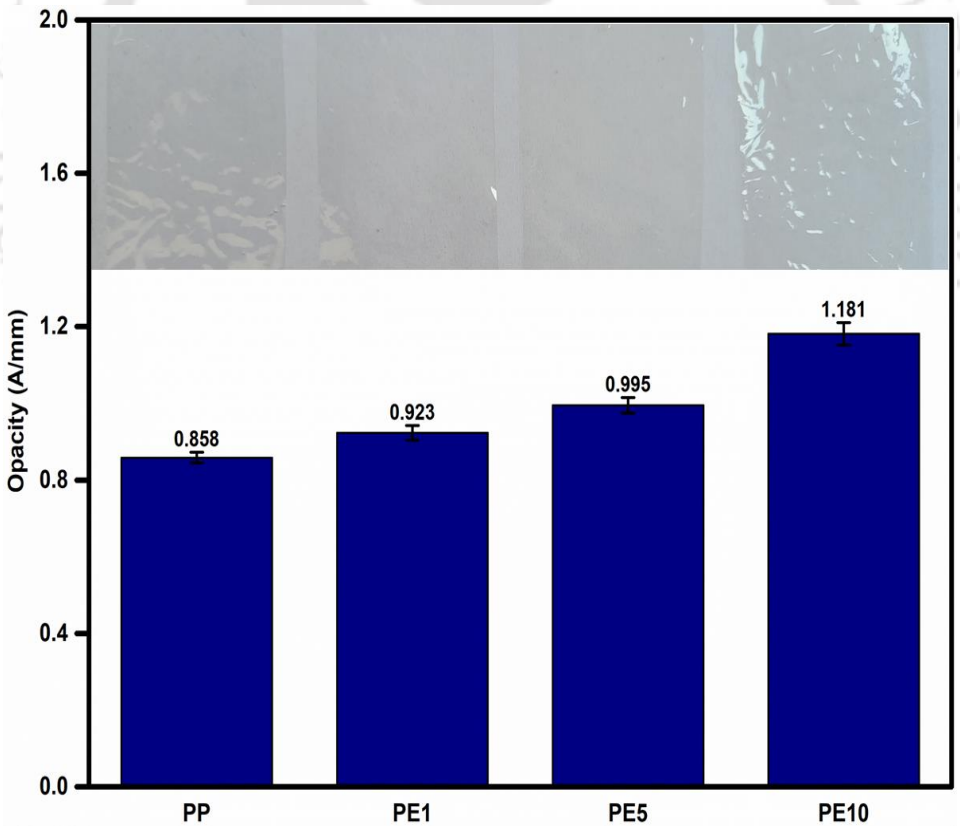

Figure 3.8 Opacity of the films (PP: Pure PVA; PE1: PVA+1% extract; PE5: PVA+5% extract; PE10: PVA+10% extract). Values are mean ± SD obtained from three replications.

The addition of extracts caused a slight rise in the opacity of the films with 0.86 ± 0.014 for PP and 0.92 ± 0.019, 0.99 ± 0.020, and 1.18 ± 0.029 Abs/mm for PE1, PE5, and PE10, respectively. Despite this, the final films resulted in good transparency as can be seen from the images taken with a white background.

3.4.2.2 Thermal analysis of films

The thermogravimetric analyzer was used to observe the thermal property of the PVA-based films under inert conditions (**Fig. 3.9).**

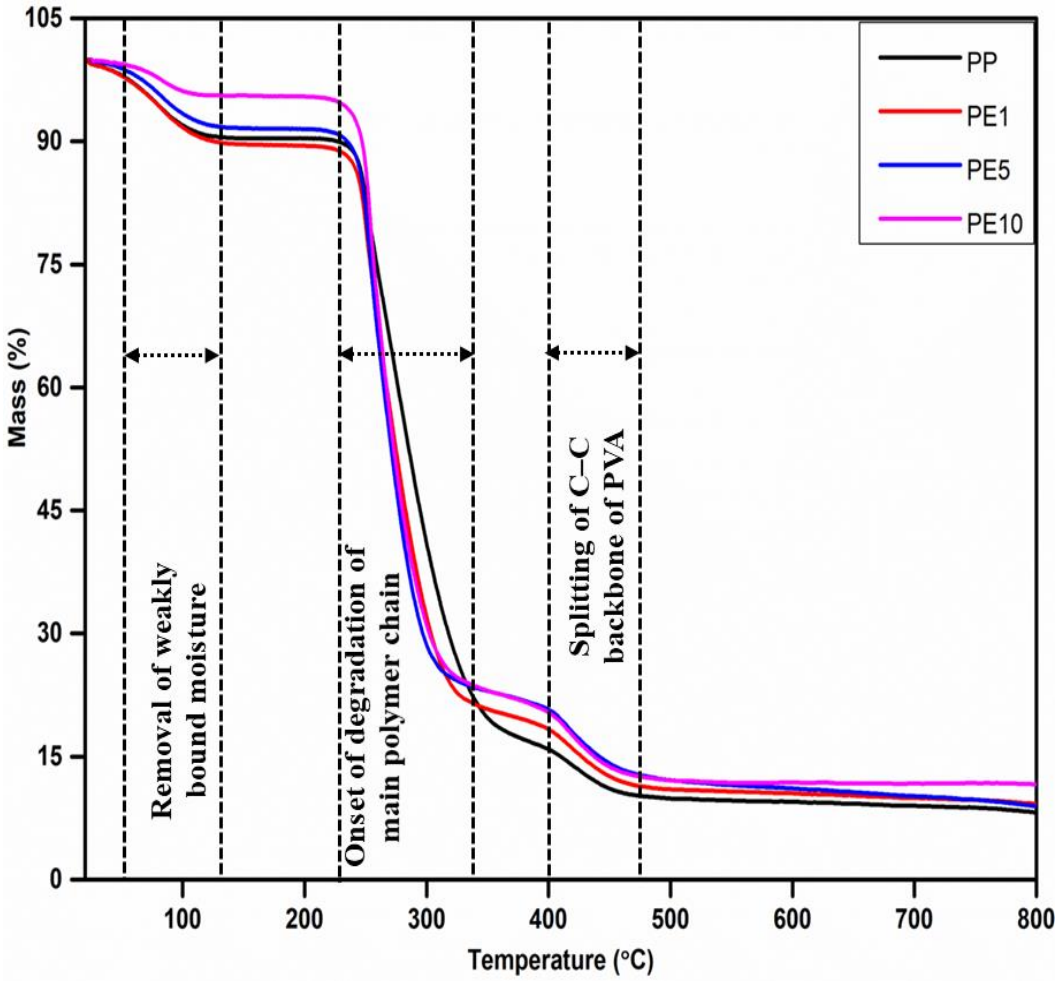

Figure 3.9 TGA curve of films (PP: Pure PVA; PE1: PVA+1% extract; PE5: PVA+5% extract; PE10: PVA+10% extract)

The first degradation was observed in the range of 60 – 120 °C, which may be attributed to the removal of weakly bound surface moisture. This is followed by a sharp degradation (230 – 345 °C) which corresponds to the starting of the degradation of the main polymer chain. The final degradation stage (400 to 460 °C) represents the splitting of the C-C backbone of PVA. The initial decomposition temperature in the second degradation stage as well as the residual mass is slightly higher in the case of extract-incorporated films. This may be caused by the formation of hydrogen and covalent bonds between PVA and the polyphenols present in the extract, resulting in a delay in the decomposition of main polymer chains (Liao et al., 2022).

3.4.3 Water barrier properties of films

The WS and WVP of the films are important parameters in determining the exchange of moisture between the sample and the environment that affects the quality of a commodity. The WVP of PP film was lesser than the films incorporated with extract at all concentrations (**Table 3.3**). The WVP was the least for PP (1.99×10^{-7} g. Pa^{-1} $h^{-1}m^{-1}$) while that of PE1, PE5, PE10 were 2.28, 2.31, and 2.35 $\times 10^{-7}$ g. Pa^{-1} $h^{-1}m^{-1}$, respectively. This can be attributed to an increase in void volume as a result of the destruction of the compact film network brought about by the aggregation of the constituents of the extract (J. Liu et al., 2021). This can consequently influence the channel of water vapour through the films (Liao et al., 2022). The WS of the films increased from 33.19 ± 1.48% for PP to 37.59 ± 1.88%, 40.25 ± 1.33%, and 46.49 ± 2.39% for PE1, PE5, and PE10, respectively. The increase in solubility with the increasing concentration of extract may be caused by the interaction between the hydrophilic groups of the phytochemicals present in the films with water molecules. This, in turn, allows the film network to bind more intensely with water and thereby improves the hydrophilicity of the blend (J. Liu et al., 2021). These findings are supported by the microscopic images of the films (**Fig. 3.2)**.

Table 3.3 WS and WVP of coating films (PP: Pure PVA; PE1: PVA+1% extract; PE5: PVA+5% extract; PE10: PVA+10% extract).

Film	WVP ($\times 10^7$ g. Pa^{-1} $h^{-1}m^{-1}$)	WS (%)
PP	1.99 ± 0.72^a	33.19 ± 1.48^c
PE1	2.28 ± 0.08^a	37.59 ± 1.88^b
PE5	2.31 ± 0.17^a	40.25 ± 1.33^b
PE10	2.35 ± 0.33^a	46.49 ± 2.39^a

The values are mean ± SD obtained from three replicates. Means sharing the same letters within columns are not significantly different.

3.4.4 Physico-chemical analysis of banana

3.4.4.1 FESEM analysis of peels

The assessment of the various physicochemical properties allows us to track the ripening of bananas during the storage period. The FESEM image of uncoated peel show a significantly higher roughness than the coated one (**Fig. 3.10**). On the other hand, the peel coated with polymer solution retains its structural integrity much more than the control. It can be concluded from this that the treatment improves the stability of the banana peels, which helps in delaying the ripening and consequently enhances the storage life.

The change in physicochemical properties of bananas in terms of weight loss, TSS, and TA during storage is presented in the subsequent sections.

3.4.4.2 Weight loss during storage

The quality and value of fresh produce during post-harvest storage can be greatly influenced by the loss of moisture resulting in weight reduction. The surface coating of these produces with an edible film can minimize water loss thereby enhancing shelf life (Cosme Silva et al., 2017). The trend of the reduction in weight of banana fruits during the storage period was measured every day (**Fig. 3.11).** The percentage of weight loss was identical for all the sample groups up to the first three days. This may be influenced by water evaporation from the film surface, resulting in a decrease in weight. The visible change was observed starting from the fourth day when the weight loss was visibly higher in the uncoated group than in any coated fruits.

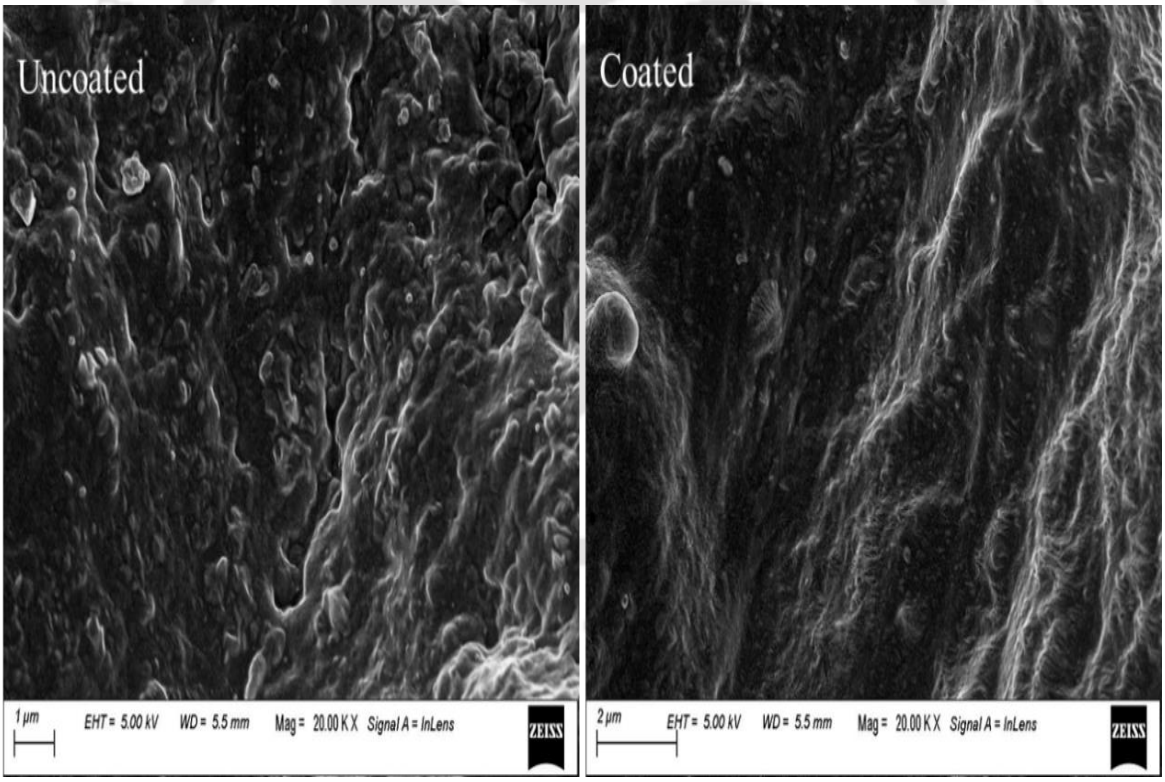

Figure 3.10 FESEM images of control and coated banana peels on day 9

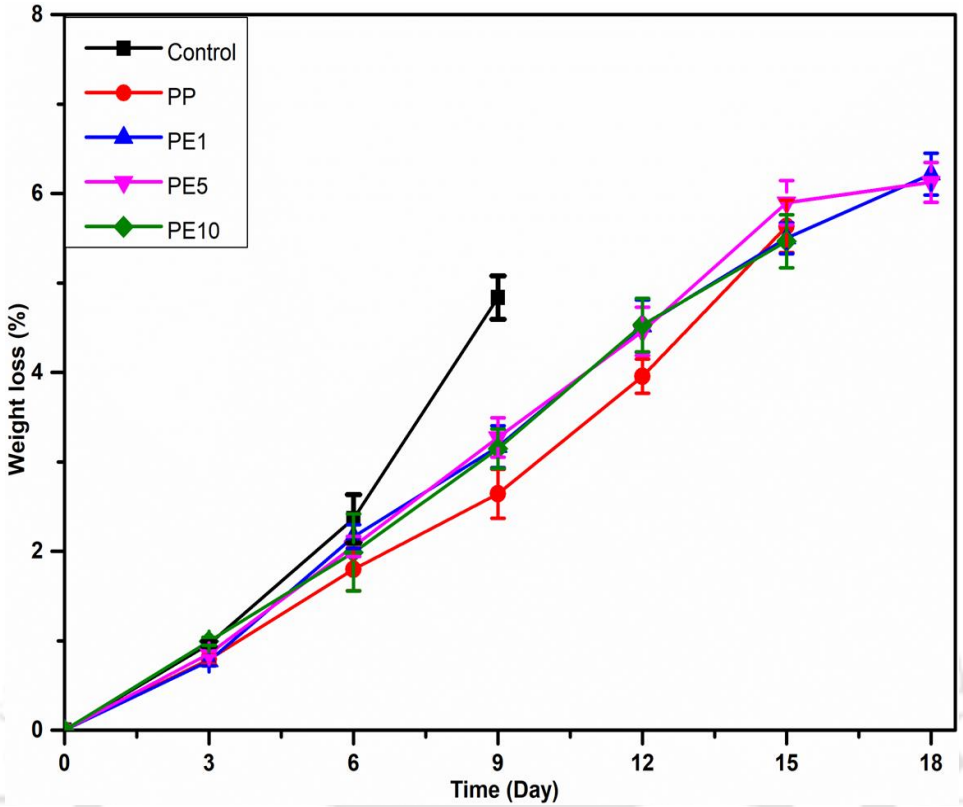

Figure 3.11 Weight loss from fruits during storage. The values are mean ± SD obtained from three replications.

The weight loss continued during the study period, where the control fruit experienced weight loss of 4.84 ± 0.24% on day 9, while that of PP, PE1 PE5, and PE10 was 2.64 ± 0.27%, 3.17 ± 0.23%, 3.27 ± 0.22%, and 3.15 ± 0.2%, respectively. The reduced weight loss in coated samples indicate that the semi-permeable PVA based coating could effectively reduce the moisture loss and mass transfer from the sample surface (Nawab, Alam, & Hasnain, 2017). Among the coated samples, the weight loss was higher in the samples with extract incorporated coatings, as compared to PP. This may be could be attributed to the increased WVP as explained in **Section 3.4.3**.

The control reached maximum stage marketability owing to the full ripeness on the 9th day and hence, it was not analyzed further. The coated fruits, however, showed a slower ripening and were analyzed till day 18. The slower ripening and weight loss from the coated fruits indicate the effectiveness of the semi-permeable film in mass transfer

reduction (Thakur et al., 2019). The weight loss in the fruit coated with the PP solution was lesser than the ones containing extract at all concentrations. This may be explained by the disturbance of film integrity caused by the aggregation of the extract constituents, allowing moisture to pass through more freely as explained in the preceding section.

3.4.4.3 Change in titratable acidity during storage

The TA of all the sample groups showed a declining trend throughout the storage period (**Fig. 3.12**).

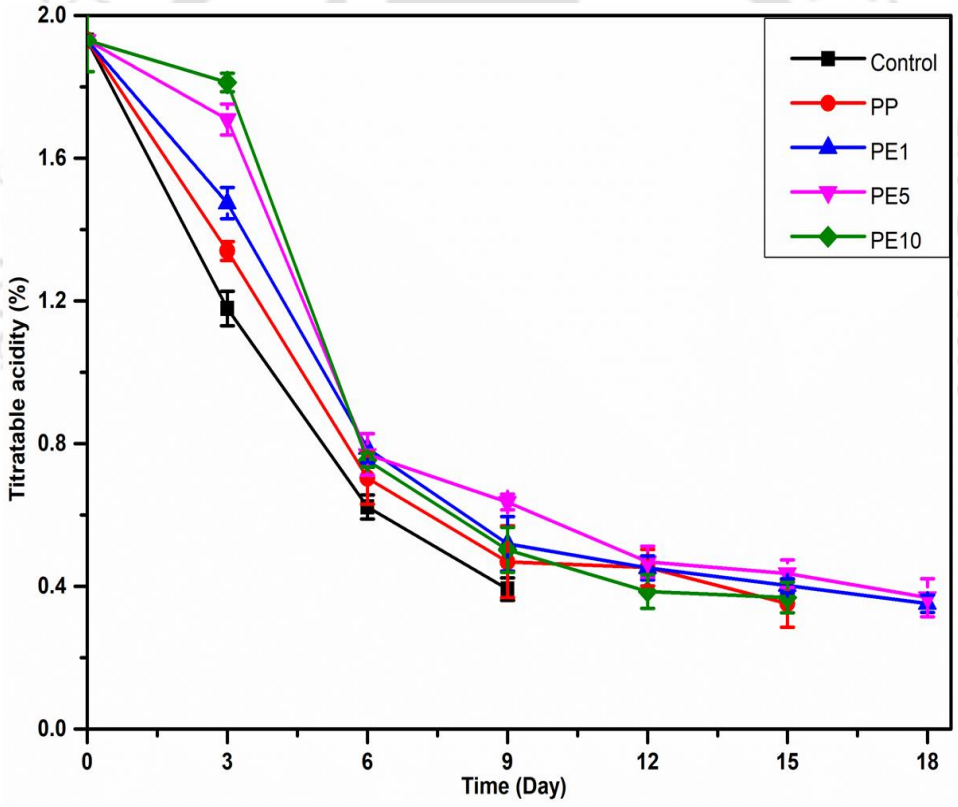

Figure 3.12 Variation in TA of fruits during storage. The values are mean ± SD obtained from three replications.

The reduction in TA of bananas during storage is greatly influenced by the metabolic activities occurring continuously. Organic acids are utilized during metabolic processes like respiration and result in a decreased acidity of the fruit with time (Hossain, Rana,

Kimura, & Roslan, 2014). This reduction can thus be correlated with the various changes in a banana during ripening and storage. In addition, organic acids are converted into sugars during ripening, resulting in the declination of TA (Rooban, Shanmugam, Venkatesan & Tamilmani, 2016). The slower declination in the TA of coated samples can be ascribed to the inhibition of respiration rate caused by the reduced O_2 transfer through the barrier film (Gol & Ramana Rao, 2011).

3.4.4.4 Change in total soluble solids during storage

The TSS of all the samples increased throughout the storage period. The change is more pronounced in the control samples where the TSS increased from 3 °Bx on day 0 to 5 ± 0.23 °Bx, 14.2 ± 0.35 °Bx, and 21 ± 0.29 °Bx on days 3, 6, and 9, respectively (**Fig. 3.13**). The control fruit attained maturity on day 9 while the TSS remained 15.2±0.35%, 5±0.12%, 6±0.29%, and 5.2±0.17% for PP, PE1, PE5and PE10, respectively. PP reached a maximum TSS of 21.8±0.69 °Bx on day 15, while PE10 attained a maximum value of 21±0.35 °Bx on the same day. Similarly, both PE1 and PE5 attained maximum acceptable ripening on day 18 with TSS of 20.8±0.46 and 21±0.58 °Bx, respectively. This increase in TSS in all sample groups can be attributed to the hydrolysis of starch and pectic substances present in the pulp into soluble sugars (Dave, Ramana Rao, & Nandane, 2017).

3.4.4.5 Change in ion leakage and chlorophyll content during storage

The change in ion leakage from fruit peels allows us to assess the viability of fruit peels as it indicates the integrity and stability of membranes (Cosme Silva et al., 2017). Banana peel from all study groups lost integrity with ripening, resulting in 85.61±2.33% ion leakage on day 9 for the uncoated group while that of PP was 56.36±2.95% and that of PE1, PE5, and PE10 remained below 30% (**Table 3.4**). The higher membrane stability in the coated fruits and more so in the groups containing the extract can be credited to the preservation of the peels' cell wall. This may be accredited to the high antioxidant activity of compounds like gallic acid present in the extract (Sun, Wang, Kadouh, & Zhou, 2014). The findings indicated that the increase in ion leakage was

considerably slowed down in the coated banana peels that allow the fruits to be stored for a longer period (Ahmed & Palta, 2016; Thakur et al., 2019).

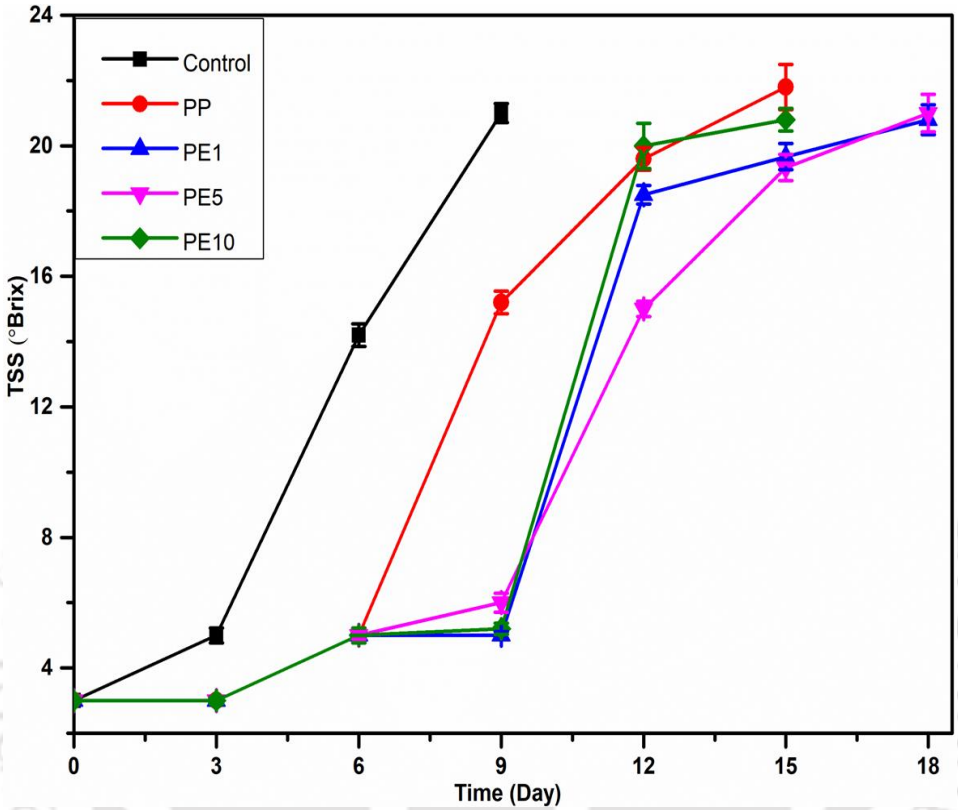

Figure 3.13 Change in TSS of fruits during storage. The values are mean ± SD obtained from three replications.

The measurement of the total chlorophyll (**Table 3.4**) showed a higher content in the treated bananas whereas the untreated ones retained a lesser concentration of the pigment. The better preservation of green pigment in the coated bananas may be ascribed to the modification of the fruit atmosphere by the coating which slowed down and delayed the ripening. Additionally, the antioxidative action of phenolic compounds like gallic acid may delay the oxidation and consequent degradation of chlorophylls. The findings of the current study agree with previous works by (Gol & Ramana Rao, 2011) where coating significantly affected the photosynthesis of pigments in bananas.

Table 3.4 Change in ion leakage and chlorophyll content of peels during storage at 25±1 °C

Treatment\ Day	**0**	**3**	**6**	**9**	**12**	**15**	**18**
Ion leakage (%)							
Control	15.15 ± 1.18^{a}	28.58 ± 3.40^{acd}	53.57 ± 2.82^{a}	85.61 ± 2.33^{a}	NA	NA	NA
PP	15.15 ± 1.18^{a}	14.70 ± 2.32^{b}	21.43 ± 1.42^{b}	56.36 ± 2.95^{b}	61.88 ± 3.03^{a}	85.09 ± 2.15^{a}	NA
PE1	15.15 ± 1.18^{a}	19.34 ± 1.71^{bc}	27.92 ± 4.08^{b}	20.81 ± 2.61^{cd}	49.14 ± 3.44^{b}	82.78 ± 3.00^{a}	85.14 ± 2.36^{a}
PE5	15.15 ± 1.18^{a}	21.13 ± 1.76^{bc}	32.48 ± 1.43^{b}	23.16 ± 2.37^{d}	52.95 ± 1.68^{ab}	82.80 ± 2.76^{a}	86.09 ± 2.28^{a}
PE10	15.15 ± 1.18^{a}	24.46 ± 1.80^{bd}	25.19 ± 2.84^{b}	26.50 ± 2.57^{d}	57.22 ± 2.15^{ab}	91.23 ± 1.78^{a}	NA
Total chlorophyll (mg/g)							
Control	0.20 ± 0.01^{a}	0.17 ± 0.01^{c}	0.16 ± 0.01^{b}	0.05 ± 0.01^{c}	NA	NA	NA
PP	0.20 ± 0.01^{a}	0.24 ± 0.00^{b}	0.23 ± 0.01^{c}	0.08 ± 0.01^{b}	0.06 ± 0.00^{b}	0.04 ± 0.01^{ac}	NA

PE1	0.20 ± 0.01[a]	0.20 ± 0.01[d]	0.18 ± 0.00[b]	0.17 ± 0.01[a]	0.10 ± 0.01[a]	0.07 ± 0.01[a]	0.05 ± 0.01[a]
PE5	0.20 ± 0.01[a]	0.26 ± 0.01[ab]	0.21 ± 0.01[ac]	0.19 ± 0.01[a]	0.08 ± 0.01[a]	0.05 ± 0.01[ad]	0.04 ± 0.01[a]
PE10	0.20 ± 0.01[a]	0.27 ± 0.00[a]	0.20 ± 0.01[a]	0.20 ± 0.01[a]	0.08 ± 0.01[a]	0.03 ± 0.01[bcd]	NA

The values are means ± standard deviation for three replicates. Means sharing the same letters within columns are not significantly different. NA = Not analyzed.

The rate of change of various physicochemical properties is lower in the coated samples as compared to the uncoated ones, where the coatings with extract showed better retention of quality for a longer period. The bioactive compounds present in the extract are secondary metabolites synthesized by plants as a defense mechanism against biotic and abiotic stresses (Saidi et al., 2021). These compounds are efficient antioxidant and antimicrobial agents that have been associated with delaying and decreasing fruit decay (Patel et al., 2020). In addition, certain phenolic compounds are reported to inhibit or delay the biosynthesis of ethylene, the modulator of fruit ripening (Leslie and Romani, 1988). In addition, some phenolic compounds are reported to reduce the presence of enzymes such as catalase, which play an important role in fruit senescence and ripening (Barua et al., 2015; López et al., 2010). Previous studies have hypothesized that antioxidant enzymes such as superoxide dismutase, catalase, and peroxidase play an important role in both senescence and fruit ripening. This has been attributed to the association between ripening-related gene expression and oxidative stress response(López et al., 2010). This could eventually result in a delay in ripening the coatings with extract incorporated. The progression of ripening of the study groups of bananas can be visualized from the digital images as shown in **Table 3.5**. There was an apparent difference in the shelf-life of the treated and untreated groups. These images prove that the coating of banana peels' surface improves the shelf life of bananas, as explained in the preceding and subsequent sections.

Table 3.5 Coated and uncoated bananas during storage at 25±1 °C.

Group/Day	Control	PP	PE1	PE5	PE10
0	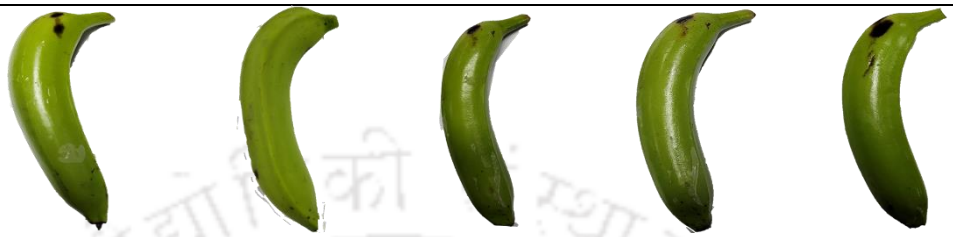				
3					
6					
9					
12	X				

15	X				
18	X	X			X

X indicates that the sample group has attained full maturity and is not analyzed further.

3.5 Summary

This chapter emphasizes on the incorporation of gallic acid rich leaf extract of *Ficus auriculata* rich extract as an additive in polyvinyl alcohol (PVA) coating to delay the ripening of green bananas. The films exhibited low opacity signifying excellent transparency. The weight loss was higher in the uncoated group than in any coated fruits. The change in physicochemical properties was slower in all the coated samples, as compared to the uncoated ones. The coated samples showed better retention and consequently slower degradation of chlorophyll. The fruits without any treatment attained complete maturity on the 9th day while the fruits coated with pure PVA as well as 10% extract incorporated PVA remained acceptable till day 15, while the ones with 1% and 5% of extract reached full ripeness on day 18.

Chapter 4

Preparation and evaluation of antioxidant formulations containing gallic acid enriched extract

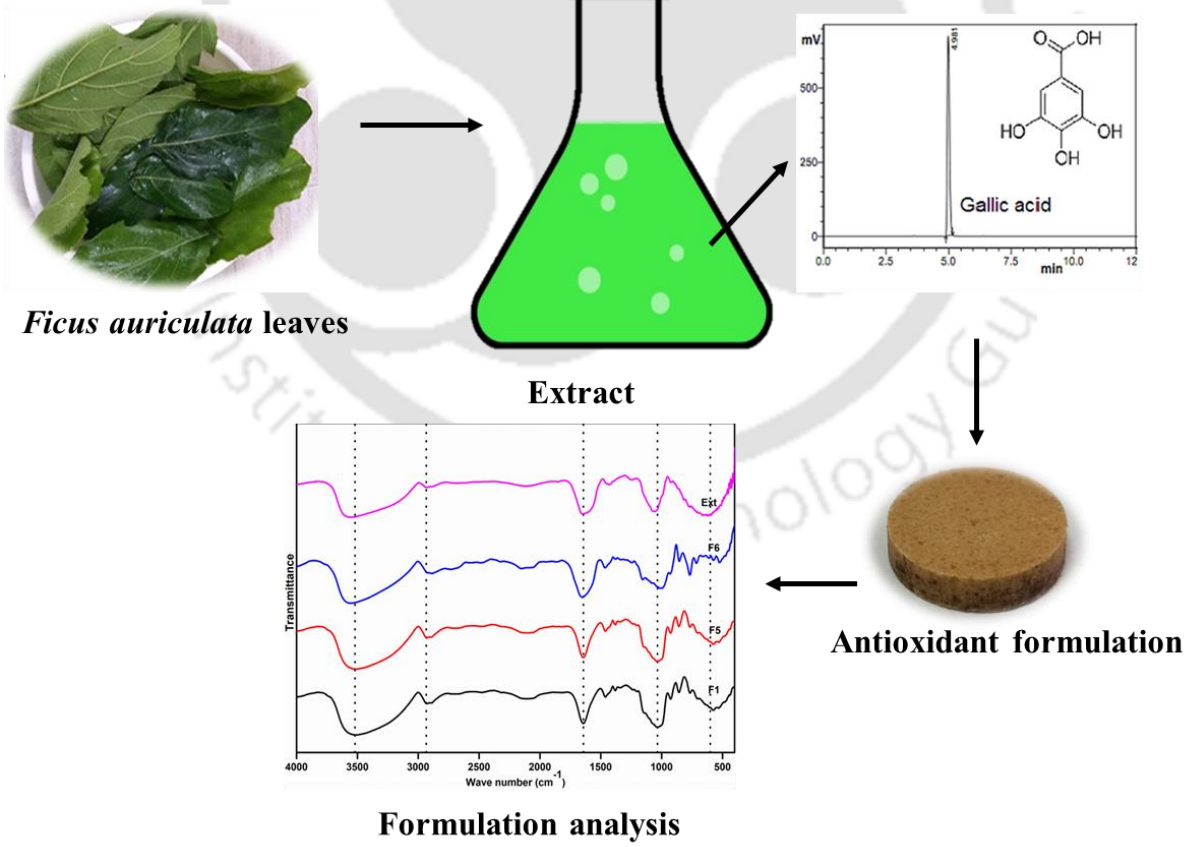

Development of antioxidant formulations based on *Ficus auriculata* leaves extract

Chapter 4

Preparation and evaluation of antioxidant formulations containing gallic acid enriched extract

In this chapter, the detailed method of formulation and development of quick disintegrating chewable antioxidant tablets with gallic acid rich extract as the active pharmaceutical ingredient (API) has been discussed. Common and easily available carbohydrates were used as the excipients to produce the tablets to reduce the required chemicals and overall cost. The quantity of the excipients was maintained to minimize the probable undesirable effects caused by their in large amounts. The background of this work, recent literature and the scope for this work have been discussed in Chapter 1, Section 1.4 and Section 1.6.3, respectively.

4.1. Experimental

4.1.1 Materials

Leaves of *F. auriculata* was collected from the campus of Indian Institute of Technology Guwahati, India. Starch, glucose and sucrose were supplied by Merck, India. Sorbitol powder was purchased from Himedia. Millipore water obtained from Milli-Q® (M/s Millipore, USA) purification system was used throughout the experiment.

4.1.2 Leaf extract preparation

The leaf extract to be used for the formulation was obtained by following the procedure used in our prior work (Baite et al., 2021). Briefly, dried leaf powder and slightly alkaline water (pH 8) at the ratio of 1:10 g/mL was subjected to extraction in a sonication bath at 50 °C and 50% sonication level for 30 min. The extract was centrifuged, filtered and further analyzed for subsequent uses. The extract was analyzed using high performance liquid chromatography (HPLC) to quantify the gallic acid content.

4.2 Analysis of extract

4.2.1 Solid residue (SR) determination

The SR of the extract was determined by first removing majority of the solvent under vacuum by using rotavapor. The concentrated mass was further dried in a hot air oven at 50 °C until there is no mass change. The SR was calculated using the following relation

$$SR\ (\%) = \frac{W_i}{W_f} \times 100 \qquad (4.1)$$

Where, W_i and W_f are the weights of the extract before and after drying, respectively.

4.2.2 Total phenolic content and antioxidant activity

The total phenolic content and antioxidant activity of the extract to be used for the preparation of antioxidant formulations were measured with a typical Folin – Ciocalteu (FC) method adopted by Mondal and Purkait (Mondal & Purkait, 2017) and 2,2-diphenyl-1-picrylhydrazyl (DPPH) method adopted by Baite et al. (Baite et al., 2021), respectively. The analyses were carried out using the procedure reported in a previous section (**Section 2.3.2**).

4.3 Preparation and characterization of formulation

The antioxidant formulation with gallic acid – rich extract of *F. auriculata* as the active pharmaceutical ingredient (API) was prepared as shown **Table 4.1** and **Fig. 4.1**. The formulation studies were carried out with use of components such as starch, sucrose, glucose, sorbitol, flavour, and colour at various concentrations.

Table 4.1 Composition of the different formulations

Formulation	Extract (%)	Starch (%)	Sucrose (%)	Glucose (%)	Sorbitol (%)	Colour (%)

1	30	60	4	2.5	3	0.5
2	30	20	45	2	2.5	0.5
3	20	30	25	12.5	12	0.5
4	40	5	5.5	45	4	0.5
5	10	55	12	12.5	10	0.5
6	50	50				

In the formulation 1 (F1), starch was used as the major ingredient to act as the bulking agent as well as a binder and mixed with the leaf extract. This was further mixed with glucose and sucrose for sweetness, sorbitol for cooling effect and food grade colour (Orange red) for aesthetic purposes. Formulation 2 (F2) was prepared by using sucrose as the major ingredient which was carried out with the aim of minimizing the number of ingredients used. In the case of formulation 3 (F3), all the ingredients were taken at almost similar proportions without giving more priority to a single component. The formulation 4 (F4) was prepared by using glucose as the major ingredient and keeping the percentage of other else low, except for the extract. The percentage of extract was minimized and starch maximized in formulation 5 (F5), while keeping the other ingredients in par with the previous preparations. Formulation 6 (F6) was prepared with only starch and extract consisting of half each of the preparation. The mixture obtained from each formulation were dried in oven at 50 °C to remove all moisture and was stored in a glass dessicator until further analysis and subsequent uses.

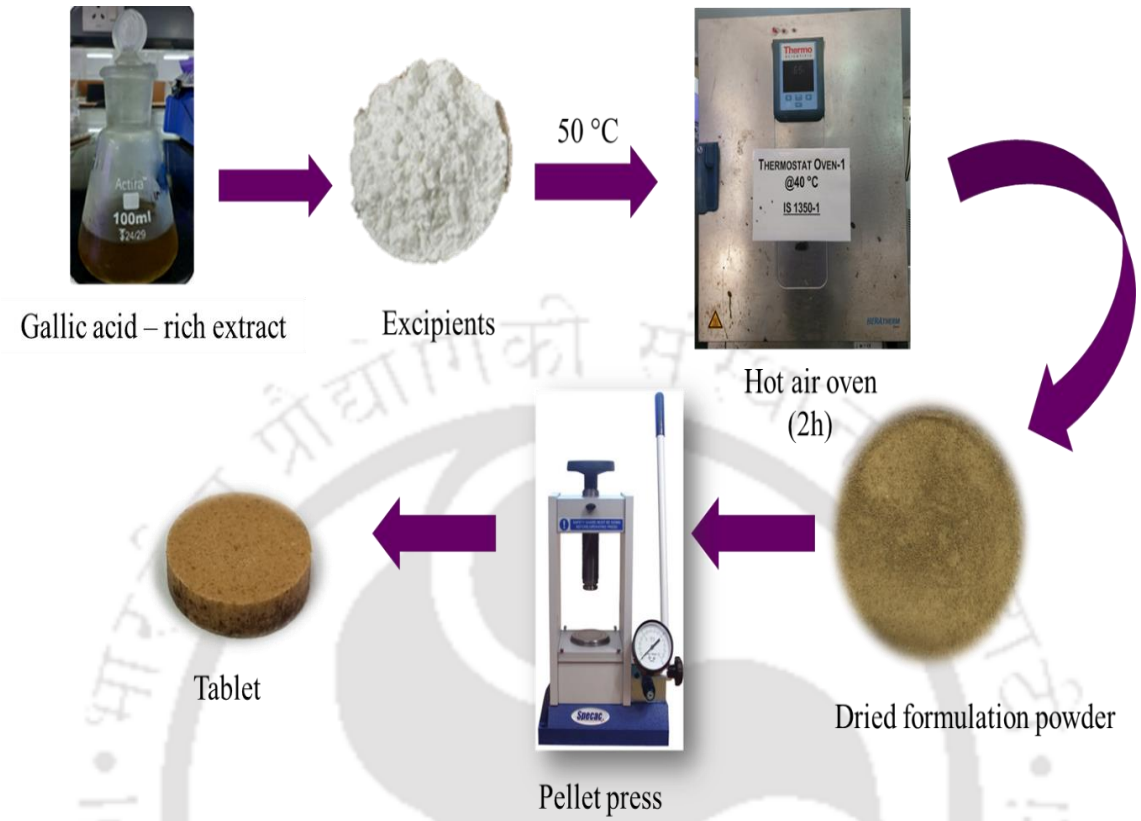

Figure 4.1 Preparation of antioxidant formulations and tablets

4.3.1 Flow properties

The flow properties of the granules obtained from different formulations such as angle of repose, Carr's index and Hausner's ratio were determined by Pharmacopoieal techniques adopted by (Archer et al., 2020).

4.3.1.1 Bulk and tapped density

1 g of granules were poured into a 10 mL measuring cylinder using a funnel. The cylinder was tapped twice to remove the granules adhered to the wall. This was noted as the initial volume (V_0). The cylinder was then tapped 50 times from approximately 2.5 cm height on a wooden table to get a constant volume and the final volume was noted (V_f). The bulk density (D_B) and tapped density (D_T) were calculated using the following relation:

$$D_B = \frac{m}{V_0} \quad (4.3)$$

$$D_T = \frac{m}{V_T} \quad (4.4)$$

Where,

m is the mass of the sample = 1 g

$$\text{Hausner's ratio} = \frac{D_T}{D_B} \quad (4.5)$$

$$\text{Carr's index} = \left(\frac{D_T - D_B}{D_T}\right) \times 100 \quad (4.6)$$

4.3.1.2 Angle of repose

The angle of repose of the granules was determined by using the fixed height method (Osei-Asare et al., 2021). Briefly, granules from each formulation were allowed to flow through a glass funnel fixed at around 2 cm between the base and the tip of the funnel. The resulting height (h) and the radius (r) of the cone formed as a result of the free flow of the granules were noted. The angle of repose (θ) was calculated using the relation

$$\theta = \tan^{-1}\frac{h}{r} \quad (4.7)$$

The experiment was performed in triplicates and the average value was reported.

4.3.2 Functional and morphological studies

The compatibility between the active ingredient and the excipients was studied by comparing the FTIR spectra of the extract and the granules. The samples were mixed with dried potassium bromide (KBr) salt and pressed into thin pellets. The pellets were scanned within the range of 4000 – 400 cm^{-1} wave number with an average of 30 scans using an Attenuated Total Reflection – FTIR (IRAffinity-1, M/s Shimadzu, Japan). The IR spectra of the extract were superimposed with those of different formulations to confirm the presence of the principal peaks from the extract in those of formulations.

4.3.3 Bioactive properties

The antioxidant activity of the extract was estimated using the 2,2-diphenyl-1-picrylhydrazyl (DPPH) method used by González-Palma et al. (González-Palma et al., 2016) with slight modification. First, the bioactive compounds in the formulation granules were extracted with methanol. Then, 0.5 mL of extract was mixed with 3 mL of methanol and 0.3 mL of 0.5 mM DPPH solution in methanol. For blank, the DPPH solution was replaced with same volume of methanol. The samples were incubated in dark for 100 min and their absorbance was recorded at 517 nm using a UV – Vis spectrophotometer. The percentage antioxidant activity in terms of DPPH inhibition is calculated as

$$AA\ (\%) = \left\{1 - \frac{(Ab_{sample} - Ab_{blank})}{Ab_{control}}\right\} \times 100 \quad (4.8)$$

Where,

Ab_{sample} = Absorbance of sample after 100 min on incubation

Ab_{blank} = Absorbance of blank

$Ab_{control}$ = Absorbance of control (3.5 mL methanol + 0.3 mL DPPH solution) at the moment of preparation

4.3.4 Formulation and evaluation of tablets

The herbal tablets containing *F. auriculata* leaf extract were prepared using direct compression method. Briefly, 500 mg of powder formulation were measured and this was formed into tablets using a pellet maker. The granules were pressed at 2 tonne force and was kept on hold for 10 sec until the final tablet was formed. The resulting tablets were kept inside an airtight glass dessicator until further analyses.

4.3.4.1 Disintegration test

The disintegration test was conducted using a modified tester. The tablets were retained in the meshed holder that is suspended inside a 500 ml beaker containing distilled water. The beaker was placed atop a magnetic stirrer maintained at 37±1 °C and 120 RPM. The time taken for disintegration of the tablet until the point of no hard – core residue was recorded. The samples were analyzed in triplicates and their average values determined.

4.3.4.2 Stability study

The stability of antioxidant formulations were studied under different conditions. The pH of the medium was maintained at 2.5 and 8.5 to mimic the environment of stomach and intestine, respectively. 250 mg of formulation granules were taken in 25 ml of solvents maintained in the aforementioned conditions and maintained in room temperature with mild mechanical agitation at 120 rpm. Samples were collected at 0, 0.5, 1, 2, 3, and 4 h, and were and were analysed using UV and FTIR. The changes in the spectra were observed.

4.3.4.3 Cell viability study

The cytotoxicity of the formulation granules was determined by measurement of cell viability using MTT assay. Around 5×10^3 THP–1 monocytes cells were seeded in 96 well plates and incubated for 24 h in complete media. Later, cells were treated with different concentrations of sample for 24 or 48 h. The cells were then treated with 20 µL of 3-(4,5-dimethylthiazol-2-yl)-2,5-diphenyltetrazolium bromide (MTT) and further incubated for 3.5 h. The media was removed carefully and 150 µL of MTT dissolving solution (11% SDS solution in isopropanol and 0.2 M HCl at 1:1) was added followed by shaking for 10 min. the absorbance was measured at 580 nm using a UV – Vis spectrophotometer (Multiscan Go, Thermo Scientific).

4.4 Results and discussion

4.4.1 Analysis of the extract

The *F. auriculata* leaf extract was analyzed to determine its efficacy to be used as an API in antioxidant tablets. The SR and gallic acid content of the extract was found to be 4.06% and 6.24 mg/g dry matter, respectively. The TPC and AA of the extract were found to be 653.8 mg GAE/ 100 g and 91.7%, respectively.

4.4.2 Preparation of formulations

The formulations resulting from different compositions has been shown in **Fig. 4.2**. It was observed that the formulations F1, F5 and F6 were able to disintegrate as free flowing powders while F2, F3 and F4 were not. This might be attributed to higher contents of the water soluble and hygroscopic sugar components used during the formulation. These components form a sticky mass after mixing with the water from the extract which cannot be separated even after drying. Because of this, the formulations F2, F3 and F4 were deemed unfit for tabletting and further studies were conducted with F1, F5 and F6.

Figure 4.2 Different formulations after drying

4.4.3 Morphological and functional study

4.4.3.1 FESEM analysis

The morphology of the tablet formulations F1, F5 and F6 were studied using a field emission scanning electron microscope (FESEM) (Zeiss, Germany, Sigma) (**Fig. 4.3**). Among the three formulations, the particles of F5 were found to be adjoined with one another while that of F1 and F6 were more freely separated.

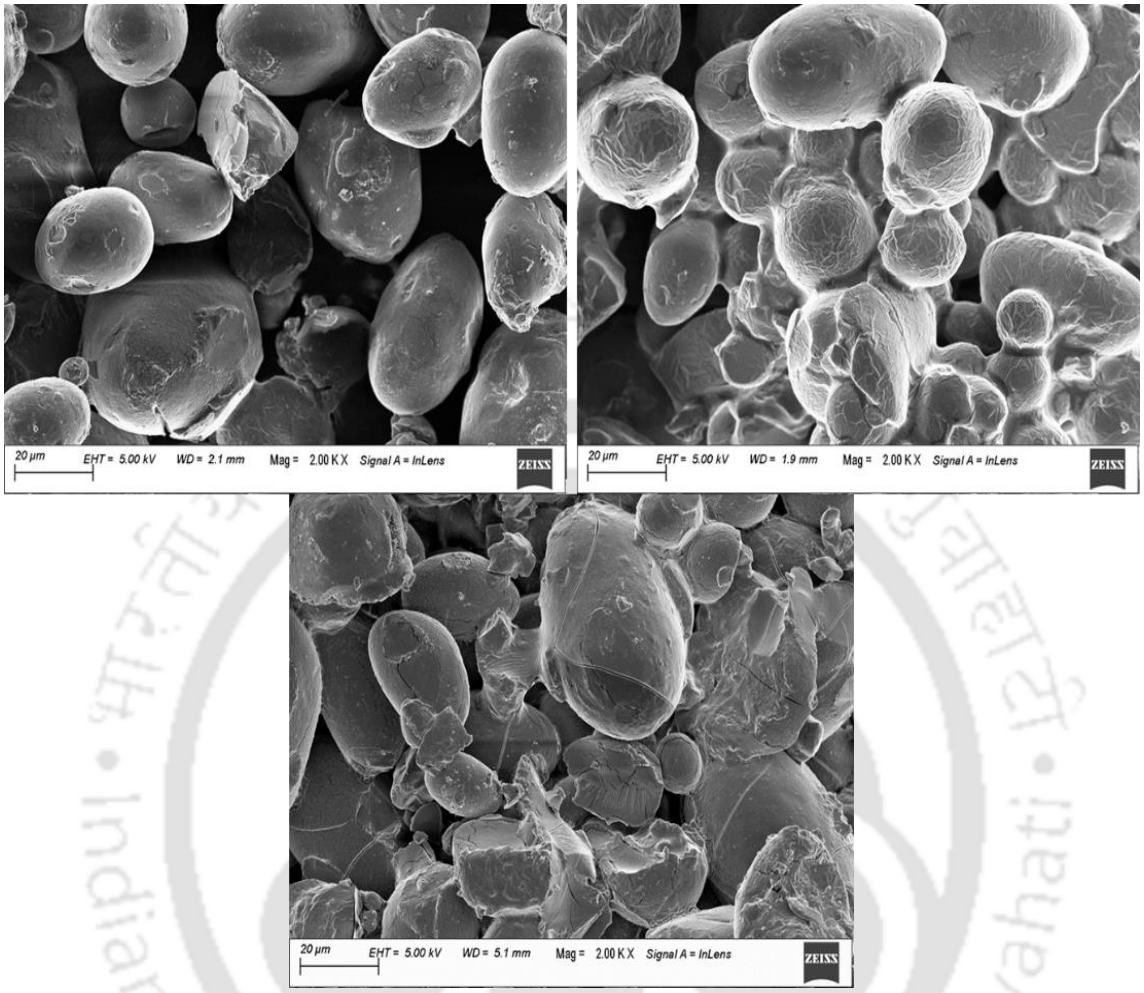

Figure 4.3 FESEM images of formulations F1, F5 and F6

This might be caused by the relatively higher content of hygroscopic sugar components that bind the particles together when they come in contact with atmospheric moisture.

4.4.3.2 FTIR analysis

The FT-IR spectra of the formulations and the extract exhibited absorption in the range of 3283.39 cm^{-1} to 416.04 cm^{-1} (**Fig. 4.4**). The spectrum exhibited a broad band at 3514 cm^{-1} (O–H Stretch) assigned to alcohol and hydroxyl group. A long, sharp peak at 1640 cm^{-1} is attributed to amines (N–H bending)(Archer et al., 2020). This peak becomes sharper in case of formulations indicating an interaction between the excipients and the extract. The peak observed at 1060.93 cm^{-1} also indicates the presence of amines (C–N

stretch). There is no significant shifting, disappearance or emergence of new peaks, indicating a good compatibility between the excipients and the extract.

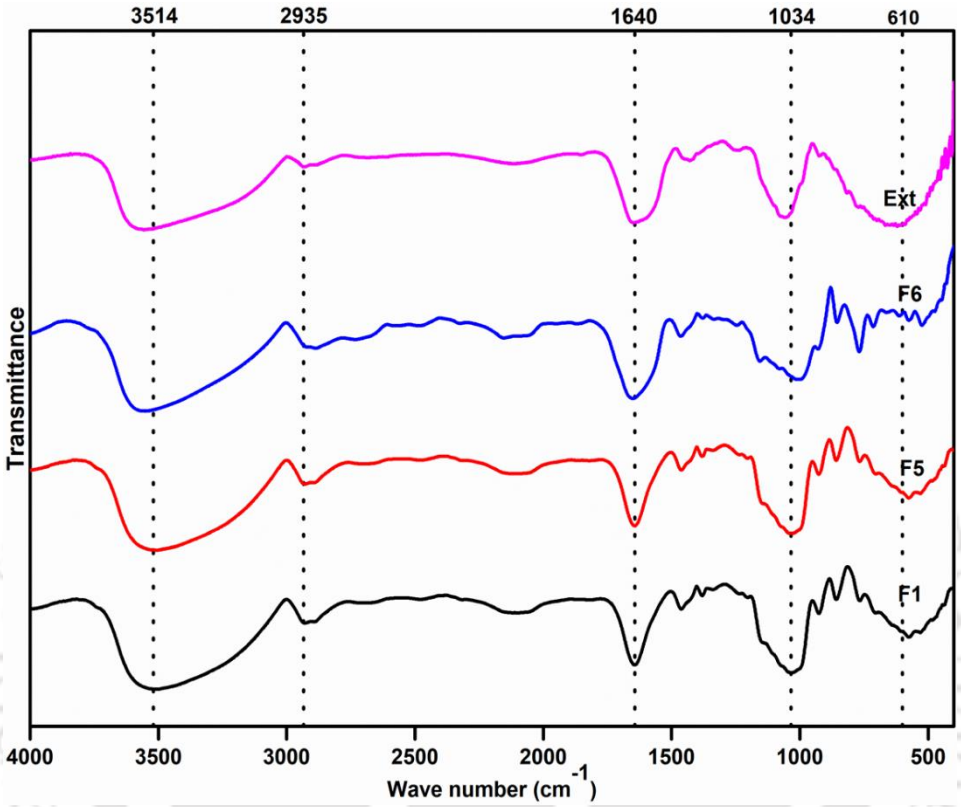

Figure 4.4 FTIR spectra of formulations and extract

4.4.4 Flow properties

The flow properties of the formulated F1, F5 and F6 granules were investigated to avoid problems of irregular flow and flow obstruction during tabletting. The results as reported in **Table 4.2** shows that while F1and F6 granules have good flow property, while F5 has fair flow. This means that, F1 and F2 granules would flow better than F5 powder during tabletting. In addition, they would not require vibration, agitation or any mechanical aid to flow during their manufacture. From **Table 4.2**, it can be seen that all the formulations resulted in properties that allow proper tabletting.

Table 4.2 Flow properties of formulations

Formulation	Bulk density (g/mL)	Tapped density (g/mL)	Hausner's ratio	Carr's index (%)	Angle of repose (°)	Flow
F1	0.72 ± 0.01	0.85 ± 0.01	1.16 ± 0.04	14.04 ± 2.92	31.13 ± 4.62	Good
F5	0.32 ± 0.14	0.37 ± 0.13	1.19 ± 0.11	16.08 ± 8.01	40.02 ± 9.05	Fair
F6	0.69 ± 0.02	0.80 ± 0.00	1.18 ± 0.00	15.82 ± 2.92	33.74 ± 2.98	Good

4.4.5 Disintegration study

One important quality control test for tablets is the disintegration test that determines if formulated tablets break up within a specified time when placed in an immersion medium. In order for the active ingredient in formulated tablets to go into solution for subsequent absorption to occur, the tablet must first disintegrate. The results as shown in **Table 4.3** conformed to Pharmacopoeia standards which stipulates a maximum of 30 min disintegration of tablets into a soft core (Archer et al., 2020). F5 tablet recorded the lowest disintegration time of 12.79 min. The thickness of the resulting tablets was in the range of 2.89 to 3.04 cm.

Table 4.3 Tablets from F1, F5 and F6

Formulation	Tablet	Thickness (mm)	Disintegration time (min)	AA (%)

F1		3.04 ± 0.06	13.105 ± 2.8	83.78
F5		2.91 ± 0.12	12.795 ± 0.4	33.51
F6		2.89 ± 0.02	14.375± 1.6	78.92

4.4.6 Stability study

4.4.6.1 FTIR and UV analysis at pH 2.5 and 8

The overall bioavailability process includes gastrointestinal digestion, absorption, and metabolism. Thus, in the gastrointestinal tract polyphenols may be released from the matrix, modified under the influence of digestive enzymes, as well as a result of pH changes (Podsędek, Redzynia, Klewicka, & Koziołkiewicz, 2014). The digestive stability of different food components can be assessed by in vitro digestion method. The UV spectra of the formulation at pH 2.5 remained unchanged up to 2h, after which it starts shifting towards the lower wavelength (**Fig. 4.5**). The peak at 225 nm might correspond to the presence of gallic acid in free form. The hypsochromic effect of UV absorbance spectra may be indicative of changes in the conjugation or formation of complexes between gallic acid and other phenolic compounds present in the extract with

the carbohydrates (Pinho et al., 2015). The FTIR spectra, however, remained identical for all the samples indicating no additional change in functional groups at lower pH.

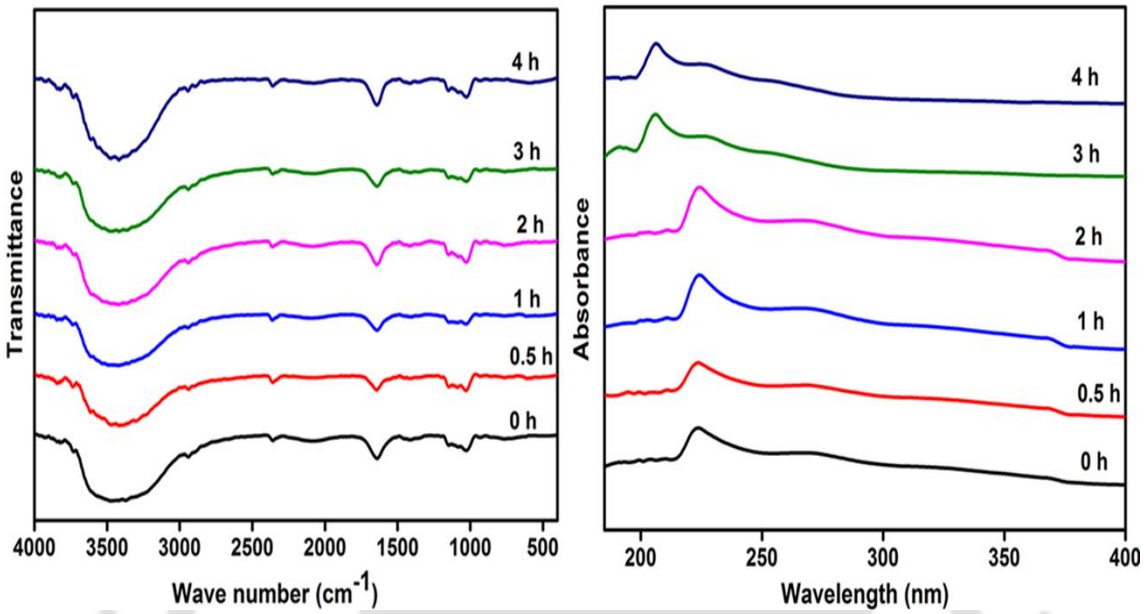

Figure 4.5 FTIR and UV spectra of formulation at pH 2.5

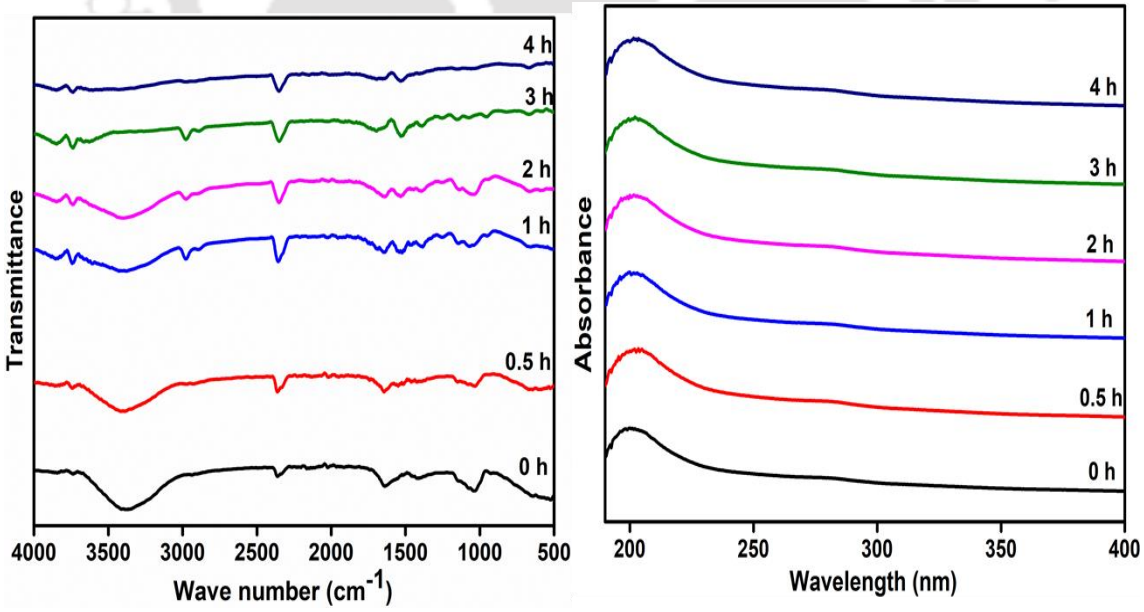

Figure 4.6 FTIR and UV spectra of formulation at pH 8.5

The FTIR spectra of the formulations at alkaline environment shows a reduction in the peak intensities of various functional groups with increasing time (**Fig. 4.6**). This may be attributed to a possible degradation of the compound at alkaline condition. Gallic acid has been found to be unstable at high pH as reported in our previous work (Baite et al., 2021). Hence, this might have contributed to the observed change in functional groups of the formulations.

4.4.7 Cell viability study

The treatment of THP-1 monocyte cells which were differentiated to macrophage with different concentrations was used for the toxicity analysis (**Fig. 4.7**). The study exhibited reduction of cell viability with increasing concentration of the extracts. The extract with concentration up to 500 µg/mL did not show any significant toxicity. From the linear equation, the IC50 was calculated and found to be 20.14 µg/mL.

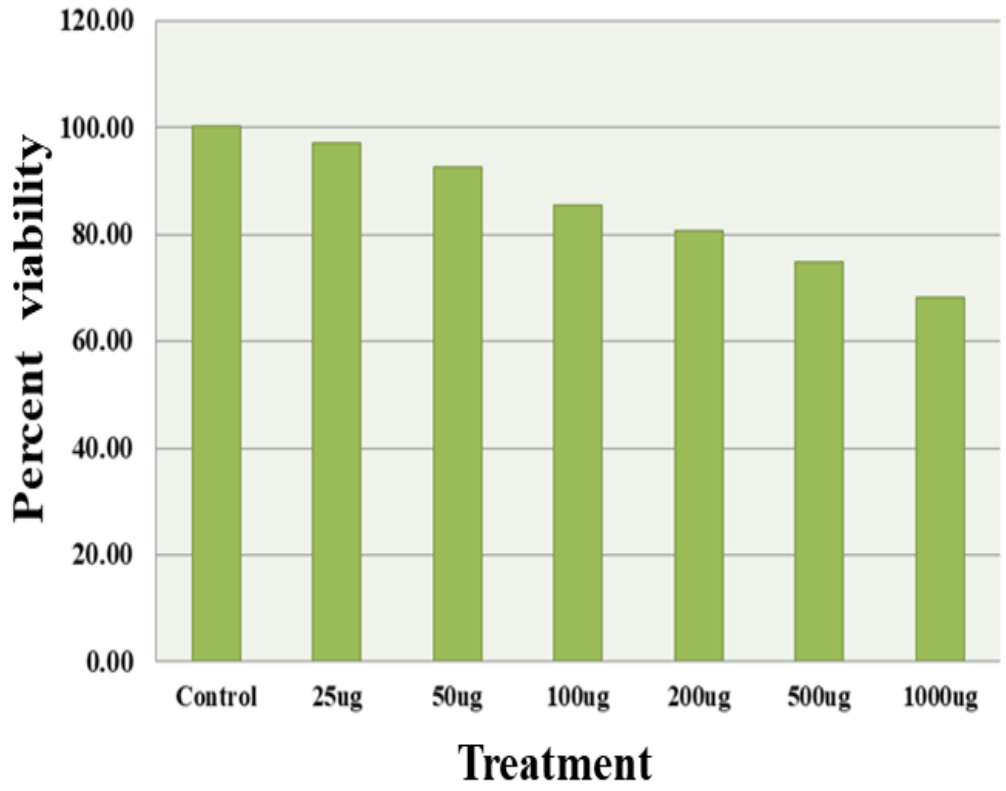

Figure 4.7 Cell viability after treatment with formulation

4.5 Summary

This chapter deals with the preparation of antioxidant formulations using gallic acid – rich extract as the active pharmaceutical ingredient. Common and easily available compounds such as starch and different sugars were used as excipients at different proportions. The free-flowing formulations were formed into tablets using a hand-operated simple pellet maker. The tablets were found to have good antioxidant activity as well as low disintegration time. The active ingredient was found to have good compatibility with the excipients. The tablets were found to be stable under acidic and alkaline conditions upto desirable period.

Chapter 5

Extraction of lignin from waste *Ficus auriculata* leaves and its potential application for bread packaging

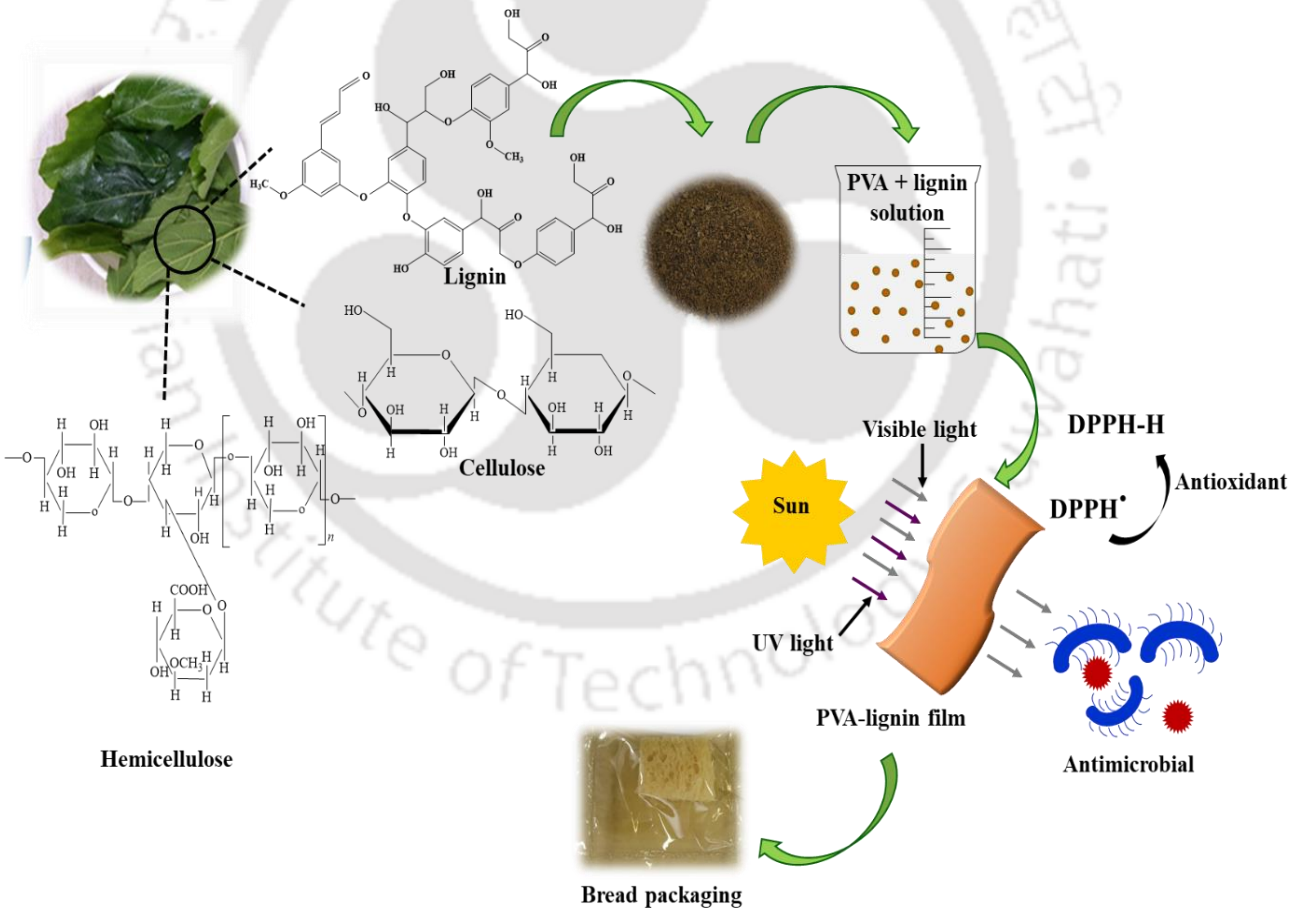

Extraction of lignin from waste leaves and its application in bread packaging

Chapter 5

Extraction of lignin from waste *Ficus auriculata* leaves and its potential application for bread packaging

In this chapter, the detailed experimental method of the extraction of lignin from F. auriculata leaves after extraction of gallic acid is discussed. Lignin was extracted using the waste leaves of Ficus auriculata after the extraction of bioactive compounds and incorporated into PVA. The influence of lignin addition on the characteristics of PVA-based films were thoroughly examined. Additionally, the prepared films were assessed for their potential use as packaging material for bread samples. The background, state of art literature and scope of this work is reported in Chapter 1, Section 1.5 and Section 1.6.4, respectively. This work has been scientifically acknowledged by publication in the International Journal of Biological Macromolecules.

5.1. Experimental

5.1.1 Materials

Poly(vinyl alcohol) (M.W. 1,15,000), sodium hydroxide (NaOH), and nitric acid (HNO_3) were supplied by Merck, India. Millipore water used in all the experiments and was collected from the Milli-Q system. Waste leaves from gallic acid extraction were washed, dried and collected after each extraction.

5.1.2 Analysis of *F. auriculata* leaves

The carbon, hydrogen, and nitrogen content of *F. auriculata* leaves was measured using a CHNS elemental analyzer (EA3000, Eurovector). A simplified method adopted by Mansor et al.(Mansor et al., 2019) was used for the determination of the major components of the *F. auriculata* leaves. Briefly, 1 g (A) dry biomass was mixed with 60

mL acetone, heated at 90 °C for 2 h and dried at 105°C till the weight remained unchanged (B). 1g of acetone-treated biomass (B) was then treated with 150 mL NaOH solution (0.5 mol/L) at 80 °C and kept for 3 h. This was followed by cleaning the treated biomass with deionized water to eliminate the sodium ions until neutral pH was reached which was confirmed using litmus paper. Then, the sample was dried in a hot air oven at 105°C upto a point of constant weight (C). 1g of acetone-treated biomass (B) was mixed with 30 mL of 98% sulphuric acid at ambient conditions for 24h followed by heating at 100°C for 1 h and washed using millipore water. Finally, the sample was dried at 105°C using a hot air oven up to a constant weight (D). The main components of the leaf were then calculated using the following eqns-

Extractives (g) = A – B (5.1)

Hemicelluloses (g) = B – C (5.2)

Lignin (g) = D (5.3)

Where, (A – B) + (B – C) + D + E = 1 g and E = amount of cellulose (g) (5.4)

Table 5.1 shows the composition of used *F. auriculata* leaves.

Table 5.1 Composition of waste *F. auriculata* leaves

Component	**Content (%)**
Carbon	39.36
Hydrogen	5.96
Nitrogen	2.62
Extractives	10.49
Lignin	16.05
Hemicellulose	27.92
Cellulose	45.54

5.1.3 Extraction of lignin from waste leaves

The leaves were collected after extraction of gallic acid, washed to remove any soluble solutes, and dried in a hot air oven. A 1:10 g/mL solid-liquid ratio was used to mix the dried leaves and 3% NaOH solution. The mixture of NaOH and waste leaves was placed in a hydrothermal treatment reactor and kept for 60 min at 121 °C and 15 psi. The resulting solution was filtered and the dark filtrate was collected. By adding HNO_3 dropwise up until a pH of about 2-3, at which point a brown slurry appears, the alkaline filtrate was neutralised. The resulting slurry was then centrifuged (Sigma 3 – 30K, Germany) at 8000 rpm for 10 min. Then the precipitate was washed with tepid water for removing any extra salts and sugars. The cleaned brown-colored solid was kept in an oven to obtain a dried mass of the lignin-enriched fraction (Haldar and Purkait, 2020).

5.1.4 Preparation of lignin incorporated PVA films

Based on the solubility, lignin was dissolved in NaOH solution having final pH of 11. The neat and lignin- incorporated PVA films were produced by mechanically mixing lignin with PVA solution at different concentrations (**Table 5.2**).

Table 5.2 Nomenclature and composition of the films

Name	PVA (%)	Lignin (%)
PP	100	0
PL1	1	99
PL3	3	97
PL5	5	95

The film forming solutions (FFS) were prepared by stirring PVA and PVA-lignin in water at 90 °C and 350 rpm for 6 h. The concentration of the solution was maintained at 10% w/v for every FFS. Following the full dissolution of the polymers, the FFS was

centrifuged for 10 min at 1000 rpm for removal of any particle or gas bubbles. Then the FFS was cast on clean glass plates which was dried overnight under ambient and then under vacuum at 50 °C for 15 h. Lastly, the dried films were characterized for various properties. The process flow chart of extraction of lignin from waste and its incorporation of PVA films is presented in **Fig. 5.1.**

Figure 5.1 Extraction of lignin from waste *F. auriculata* leaves and preparation of PVA - lignin blend films

5.2 Characterization of lignin and lignin-PVA films

5.2.1 Purity of extracted lignin

The sugars, acid insoluble lignin (AIL) and acid soluble lignin (ASL) present in the extracted lignin were analysed using a modified protocol (Dávila et al., 2017). First, lignin was subjected to acid hydrolysis by mixing with 72% H_2SO_4 and maintained at room

temperature for 1 h. The treated lignin was then subjected to a next hydrolysis step by diluting the H_2SO_4 solution down to 12%. The mixture was kept at 121 °C for 1 h, ensued by cooling and filtering the solution. The undissolved solid was denoted as AIL and the ASL was analyzed using UV spectrophotometry and high-performance liquid chromatography (HPLC) (Prominence, Shimadzu, Singapore) for monosaccharides and disaccharides. To determine the ASL, the filtrate was first diluted with 1M H_2SO_4 to bring the absorbance within 0.1-1.0 using a UV – Vis Spectrophotometer (UV-2600, Shimadzu). The ASL was quantified by recording the absorbance of the solution at 205 nm and using the equation below:

$$\text{ASL} = \frac{\text{Abs}_{205} \times \text{DF} \times \text{V}_\text{F}}{\varepsilon \times \text{D}_\text{Mi}} \quad (5.5)$$

Where,

Abs_{205}= Absorbance of the filtrate at 205 nm, DF = dilution factor, VF = Filtrate volume obtained after acid hydrolysis, ε = Extinction coefficient (110 L cm/g for lignin), D_{Mi} = Initial sample mass taken for acid hydrolysis. The concentration of monosaccharides and/or disaccharides present in the acid soluble fraction was determined using HPLC equipped with RI detector. The flow rate of the mobile phase (0.01M H_2SO_4) was kept at 0.6 mL/min. High purity sugars from Himedia were used for calibration.

5.2.2 Structural properties

A field emission scanning electron microscope (FESEM) (Sigma 300, Zeiss) was used to analyze the morphology of the extracted lignin and the neat and lignin-incorporated PVA films. An Inlens detector was used to capture the electron images of the samples. The surface roughness of the films was analyzed by scanning the samples at 1 Hz scan rate with the help of an atomic force microscopy (AFM) (Innova, Bruker). The functional groups on the surface of the lignin particles and films was determined through Fourier transform infrared (FTIR) spectroscopy. The lignin extracted particles and the prepared films were scanned between 4000 – 400 cm^{-1} wavenumber and the spectra were obtained using an attenuated total reflection - FTIR spectrometer (IRAffinity-1, Shimadzu, Japan).

The crystal structure of lignin and the films was observed with an X-ray diffractometer (Smartlab, Rigaku Technologies, Japan) furnished with CuKα radiation. The diffractogram was obtained in the 2θ range of 5 – 70°. The chemical structure of the extracted lignin was studied with the help of proton nuclear magnetic resonance (^{1}H NMR). The spectrum was obtained using a 600MHz NMR Spectrometer (AVANCE III HD, Bruker) where around 2 mg sample was dissolved in 0.5 mL of DMSO – d6 was analyzed. The ultraviolet (UV) absorption by the lignin and the films was analysed by means of a UV spectrophotometer (UV-2600, Shimadzu). The samples were scanned between 200 nm to 400 nm to observe the absorption of UV for lignin and to check the blockage of UV light for the film samples.

5.2.3 Optical properties

The optical property of the pure PVA and lignin-incorporated PVA films with respect to opacity was studied via a procedure implemented in our prior work (Baite et al., 2022) and as described in a previous section (**Section 3.2.2**).

5.2.4 Thermal analysis

A thermogravimetric analyzer (TGA) (STA449F3A00, Netzsch) was employed to determine the thermal properties of the neat and lignin – incorporated PVA films. A heating rate of 10 °C/min was maintained during the analysis where the temperature was kept between 20 – 800 °C and inert condition maintained using nitrogen gas. The change in mass of the samples with respect to increasing temperature was plotted.

5.2.5 Antioxidant property of the films

The DDPH (2,2-diphenyl-1-picrylhydrazyl) assay was employed to measure the antioxidant activity of the neat and lignin – incorporated PVA films (Baite et al., 2021). Briefly, 0.3 mL of DPPH solution in methanol (0.5 mM) was mixed with 50 mg of films and 3 mL of methanol. To serve as the blank for each sample, the DPPH solution was

replaced with 0.3 mL methanol. The antioxidant activity was then measured following the protocol presented in **Section 2.3.2**.

5.2.6 Mechanical properties

The tensile strength and elongation at break of the film samples were analyzed under ambient conditions by means of a 5 kN Electro mechanical universal testing machine (Z005TNProline, ZwickRoell) to study the mechanical properties. The crosshead speed was kept at 5 mm/ min. The specimens had a dimension of 10 mm width and 50 mm length. A digital micrometre having precision up to 0.001 mm was used to measure the thickness of the film samples and averages from ten different points were considered. The films were kept inside an airtight dessicator at room temperature before the measurements.

5.2.7 Water barrier properties

The water solubility (WS) of the pure and lignin – incorporated PVA films was quantified using a modified protocol based on our previous study (Baite et al., 2022). For this, squares of 2×2 cm^2 were cut out from the films and dried at 50 °C for 24 h to dry out any moisture and weighed (W_1). The films were immersed in a 100 mL beaker containing 50 mL of distilled water kept for 24 h at room temperature. Then, the samples were transferred to a vacuum oven maintained at 50 °C and kept for 24 h for removal of the absorbed moisture and the samples were weighed after drying (W_2). The WS was calculated by using **Eqn (5.6)**.

$$\text{WS}\ (\%) = \frac{W_1 - W_2}{W_1} \times 100 \qquad (5.6)$$

The water vapour transmission rate (WVTR) and water vapour permeability (WVP) was determined using a modified procedure (Baite et al., 2022). Calcium chloride salt was used to fill half of glass cups which were then covered with the prepared films and placed inside a dessicator maintained at 75.2 ± 0.17% RH using saturated sodium chloride solution. The moisture transfer across the film samples was determined by recording the change in cup weight at one day intervals for seven days and the resulting weight change

was plotted with respect to time. The slope from the linear regression divided by the transfer area (in m^2) indicated the WVTR. The WVP of the films was calculated using **Eqn (5.7)**.

$$\text{WVP} = \frac{WVTR \times x}{P(R_1 - R_2)} \ \frac{\text{g.m}}{\text{h.pa}} \qquad (5.7)$$

where P: saturation vapour pressure of water at room temperature; R_1: RH inside desiccator, R_2: RH inside the cup; x: film thickness (m), and [P ($R_1 - R_2$)]: driving force for the transport of moisture = 2376.30 Pa at the aforementioned conditions.

5.2.8 Antifogging test

The antifog property relates to the material's ability to prevent the collection of minute water droplets on the inside of the film. Changes in humidity and temperature directly influence the formation of fog. Condensation of water vapour inside the package occurs when the temperature of the film surface drops below the dew point. The antifogging property of the films was tested using an established protocol (Min et al., 2020). Briefly, one side of clean glass slides were half coated with the film forming solution while the other half remain uncoated. The slides were then dried in a vacuum oven at 50 °C. The coated and dried slides placed on top of a beaker containing hot water. The appearance of the glass slides within 5s was recorded. The antifogging property of the films was also assessed using a different modified protocol (Hu et al., 2018). The glass slides which are half coated with the FFS was placed in a freezer maintained at – 23 °C for 2h. After 2h, the slides were brought back to ambient conditions and the antifogging activity was observed by placing the slides over a background.

5.2.9 Leaching behaviour of films

Leaching test was conducted to quantify the amount of the components that can be leached out of the films using a modified protocol (Vu and Won, 2013). Briefly, 1×2 cm^2 films were immersed in three different food stimulants i.e., water, 3% acetic acid, and 10% ethanol solution (Arvanitoyannis and Kotsanopoulos, 2014). The lignin leaching

was quantified by collecting the samples at measuring the absorbance of the solutions at 280 nm at 1 h, 6 h, 12 h and 24 h. To determine the initial amount of lignin loaded on the films, the samples were placed in alkaline water of pH 12 and stirred at 500 rpm for 4 h and their absorbance recorded at 280 nm. The leaching behaviour was defined as the ratio of lignin leached into a food stimulant at a given time to the initial amount of lignin loaded.

5.3 Performance evaluation of the films for bread storage

Bread baked without any added preservatives was procured from a local baker. The commercial package (Repose Foods Pvt Ltd, Guwahati) used for packaging bread was obtained from the market. The mold growth inhibition by the films was assessed by packaging the samples through direct contact with the films. Bread samples were sliced into pieces of 2×2 cm^2, packed with the prepared films and sealed with a heat sealer. To compare the performance of the prepared films, similar bread samples were also packed with commercial packaging films. The initial moisture content of the bread sample was 43.9 ± 0.28% wb. After sealing, the packed samples were stored at 25 °C and 64% RH and the mold growth during storage was observed. To study the influence of temperature on the performance of the films in bread packaging, bread samples were stored in incubators maintained at 30 °C and 35 °C. The RH was kept constant and the mold growth was observed every day.

5.4 Results and discussion

5.4.1 Characterization of lignin

5.4.1.1 Purity and antioxidant activity

The purity of the extracted lignin was determined with respect to the ASL and sugars present. Using **Eqn (5.5)**, the ASL was found to be 4.20±1.61%. Based on the HPLC analysis, glucose was the only sugar detected and its concentration was very low at

0.07±0.01%. Thus, the purity of lignin was found to be 95.73%. The antioxidant activity of the extracted lignin was found to be 83.54%.

5.4.1.2 FETEM analysis

The digital image and the structure of the extracted lignin particles are shown in **Fig. 5.2**. The lignin particles were obtained as brownish granules (**Fig. 5.2(a)**). The FETEM image (**Fig. 5.2(b)**) shows that lignin particles are spherical-like in shape and have a size around 25 – 40 nm. The SAED image for the lignin sample shows a characteristic halo ring pattern, indicating the amorphous nature of the particles (**Fig. 5.2(c)**).

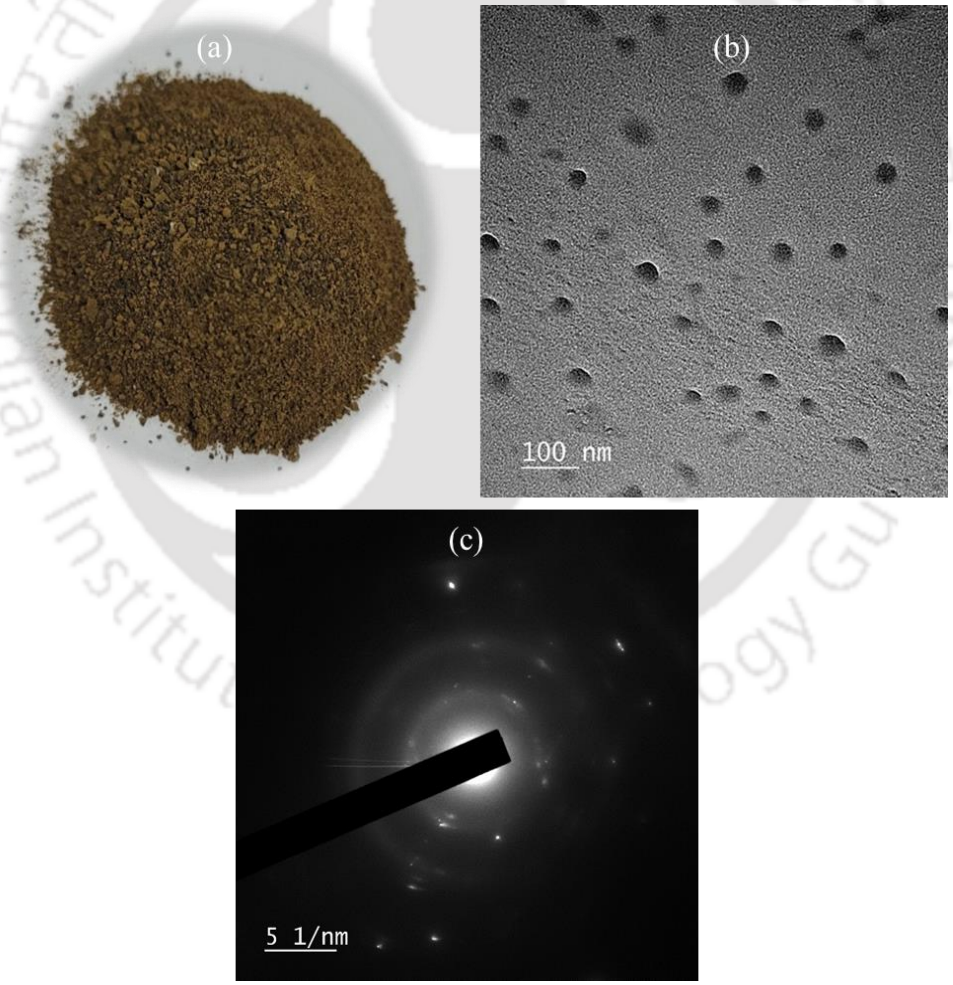

Figure 5.2 (a) Digital image (b) FETEM image and (c) SAED pattern of the extracted lignin

5.4.1.3 ^{1}H NMR analysis

The chemical structure of lignin was elucidated using ^{1}H NMR spectrometry and the corresponding spectra is shown in **Fig. 5.3**. Protons from the carboxylic group are identified by the small signals located at 11.75-12.25 ppm. Phenolic groups with carbonyl groups conjugated with the aromatic ring might be responsible for the small signals between 8 – 9 ppm (Li and Lundquist, 1994). Syringyl (S) and guaiacyl (G) units contain aromatic and vinyl protons in between 6.3–7.6 ppm.

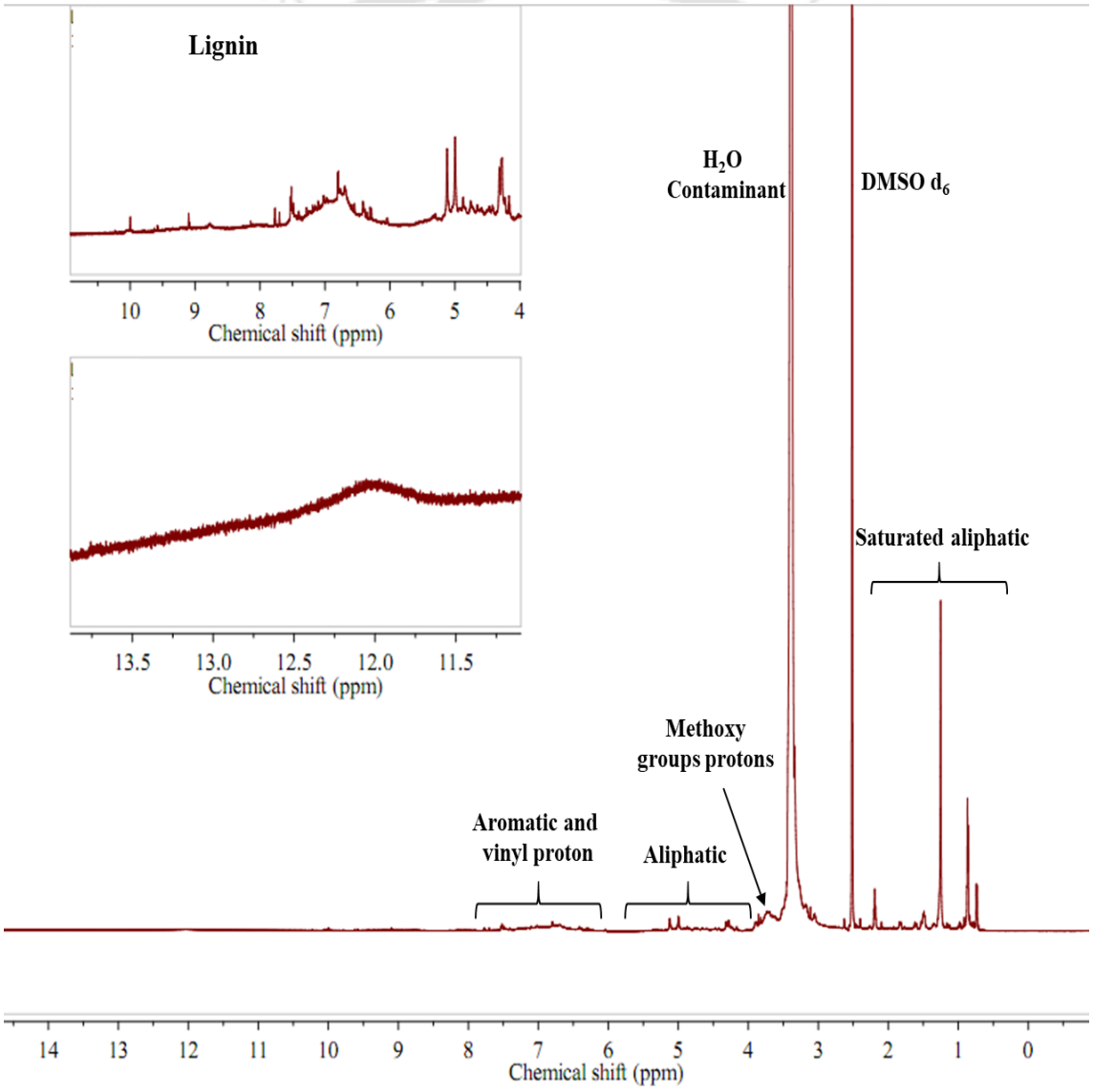

Figure 5.3 ^{1}H NMR spectra of the extracted lignin

In lignin spectrum, few faint signals have been noted that could be a result of the lignin's complex structural makeup. The range encompasses the minor peaks of aliphatic protons (4.2–5.3 ppm). At about 3.65 ppm, a strong signal for the methoxyl proton, that relates to the ratio of the G and S units. This agrees with the findings of Korbag and Mohamed on the study of PVA-lignin composites using commercial lignin (Korbag and Mohamed Saleh, 2016a). At 3.39 ppm and 2.52 ppm, respectively, there are two strong signals that are associated with the water contamination and the solvent DMSO-d6, respectively. The presence of a water contaminant signal is probably caused by moisture absorption by DMSO-d6 while handling and improper drying of lignin. Protons in saturated aliphatics are responsible for peaks in the range of 2.3-1.2 ppm.

5.4.1.4 UV analysis

The lignin particles exhibited UV absorption maxima at wavelength of around 280 nm (**Fig. 5.4**). This is typical of lignin and is attributed to the aromatic rings or the phenolics in lignin (Abdelaziz and Hulteberg, 2017).

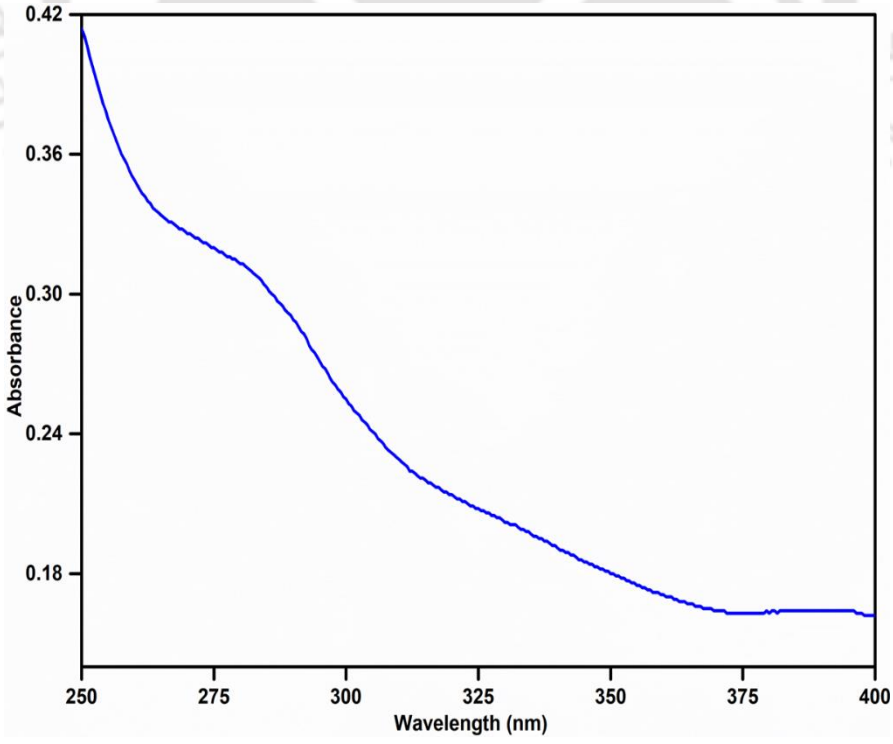

Figure 5.4 UV spectrum of the extracted lignin

5.4.1.5 FTIR analysis

The FTIR transmittance spectra of lignin (**Fig. 5.5)** shows a wide peak at 3536 cm^{-1} that is allotted to OH vibration. The peak at 2928 cm^{-1} might be caused by the stretching vibration of C-H bond of the methylene groups, whereas the peak at 2849 cm^{-1} could be assigned to symmetric stretch for CH_3 of methoxyl group (Nandanwar et al., 2016). The transmittance at 1672 cm^{-1} resulted from the C=O stretching of the carboxylic groups while the one at 1540 cm^{-1} may be allotted to the aromatic skeletal vibration (Horikawa et al., 2019). The peak at 1450 cm^{-1} matches the methyl groups C–H bonding and the one at 1235 cm^{-1} is caused by C-O stretching. The peaks at 1156 cm^{-1} and 1028 cm^{-1} could be associated with the OH bonding of alcohol groups (Gomide et al., 2020).

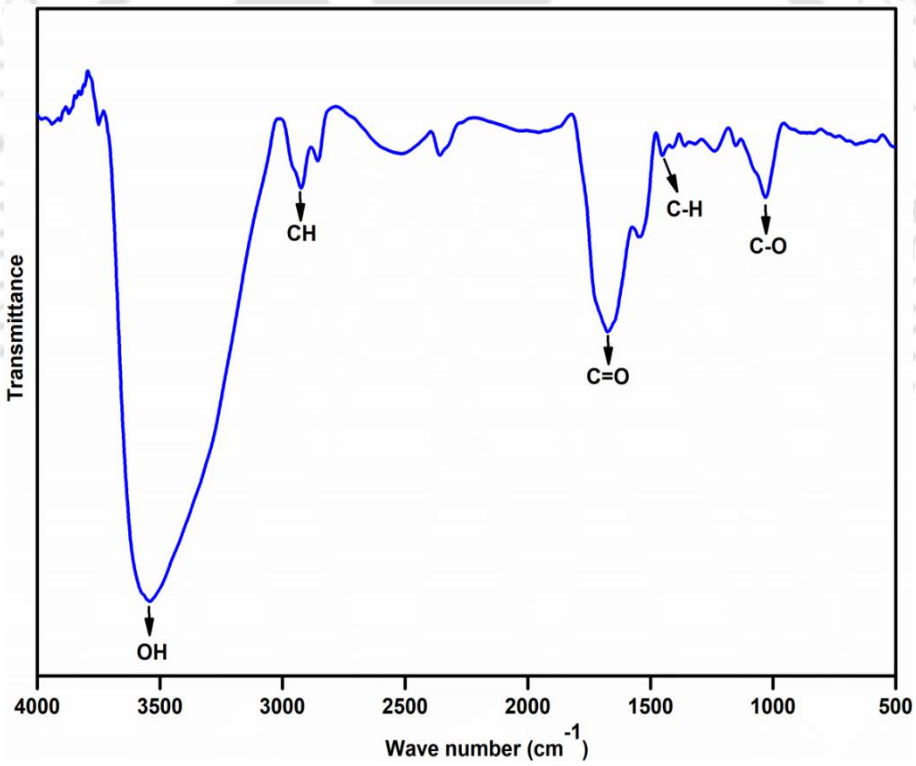

Figure 5.5 FTIR spectrum of lignin

5.4.1.6 XRD analysis

The X-ray diffractogram of lignin is given in **Fig. 5.6**. The lignin particles presented a highest 2θ value at 21.4° while Gomide et al. (Gomide et al., 2020) reported the maximum

peak at 2θ of 20.26°. This variation might be due to the difference in chemical structures, isolation technique and the source of lignin. The X- ray diffractogram of lignin exhibited a broad peak, confirming the amorphous nature of the particles and corroborates with the SAED pattern (**Fig. 5.2(c)**).

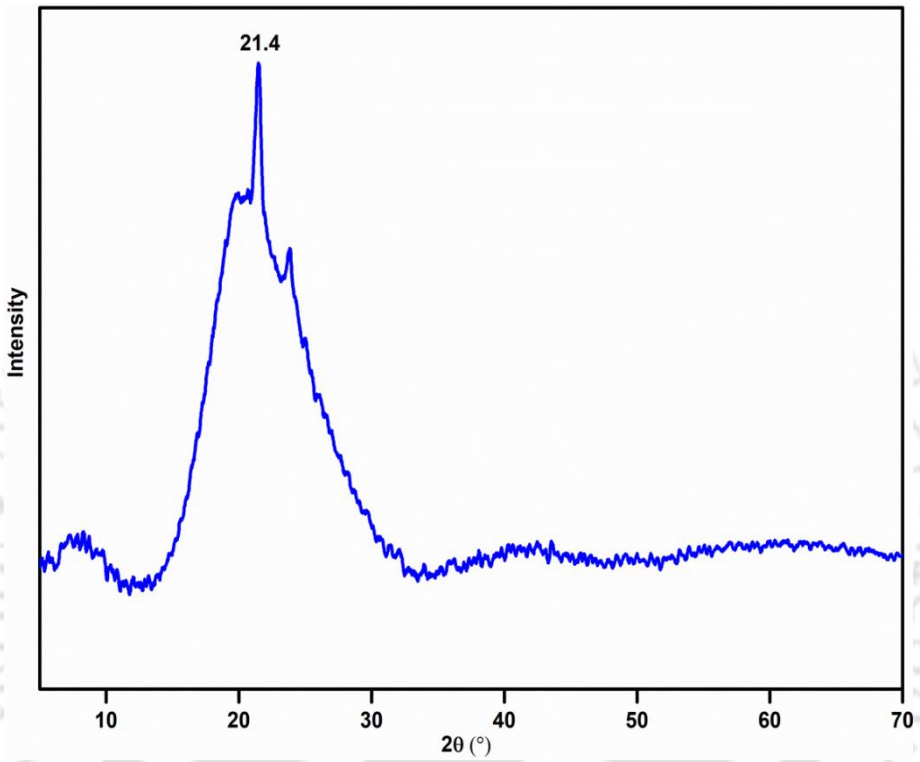

Figure 5.6 XRD diffractogram of lignin

5.4.2 Characterization of films

The digital images of the films against a background is presented in **Fig. 5.7(a)**. The incorporation of lignin caused a visible coloring of PVA films owing to the brown appearance of lignin particles. However, the visibility of the background is not significantly affected by the colour change. The opacity of PP was very less (0.34 A/mm) and increased slightly with increase in lignin concentration (**Fig. 5.7(b)**). Although there is slight increase in opacity with lignin incorporation, the films remained fairly transparent as seen from the preceding observation.

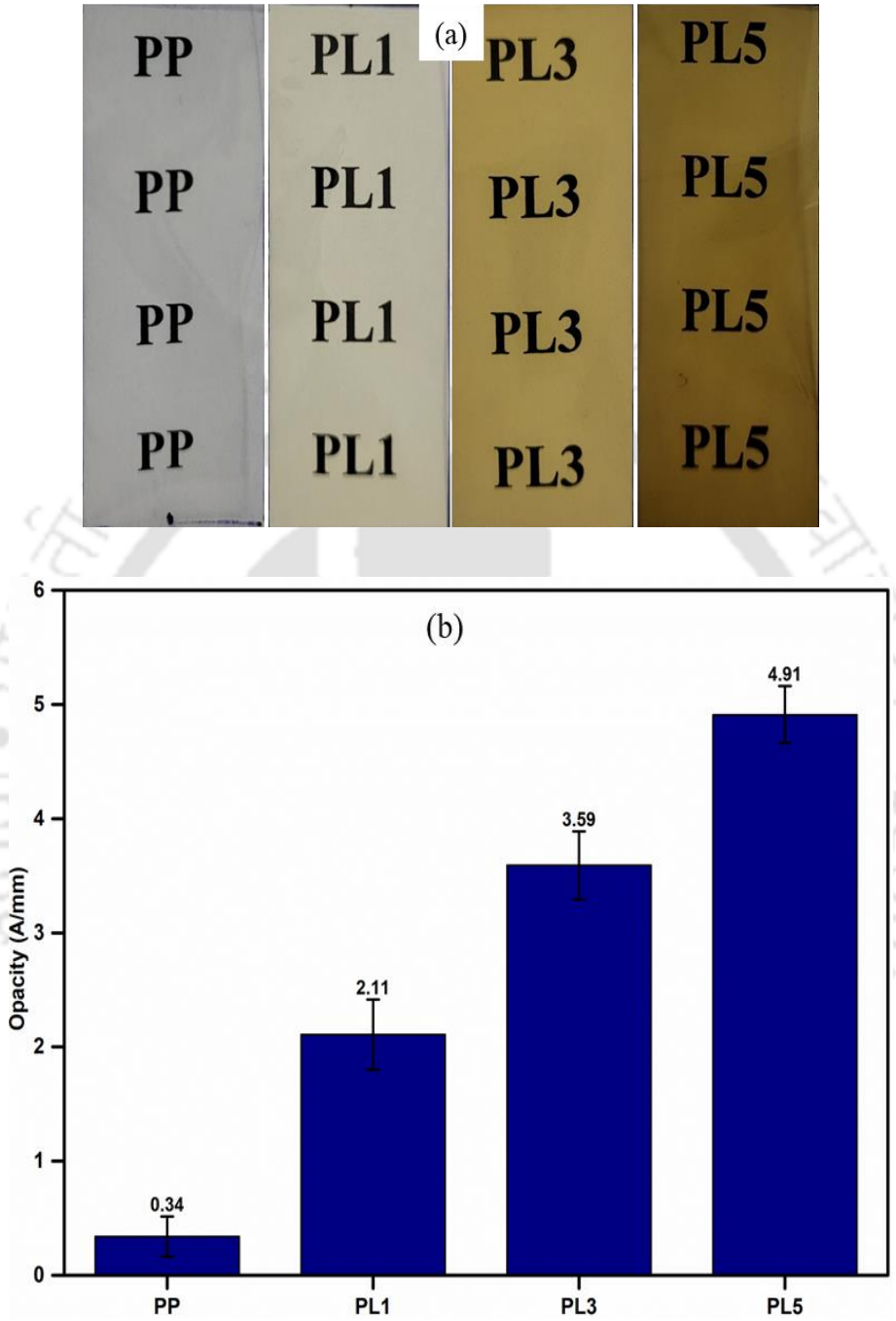

Figure 5.7 (a) Digital images and (b) Opacity of films. (PP: Pure PVA film; PL1: PVA+1% lignin; PL3: PVA+3% lignin; PL5: PVA+5% lignin).

5.4.2.1 FTIR analysis

The OH groups present on the lignin particles and PVA matrix have a strong affinity for interacting with one another. The FTIR spectra of the neat and lignin incorporated PVA films is presented in **Fig. 5.8**.

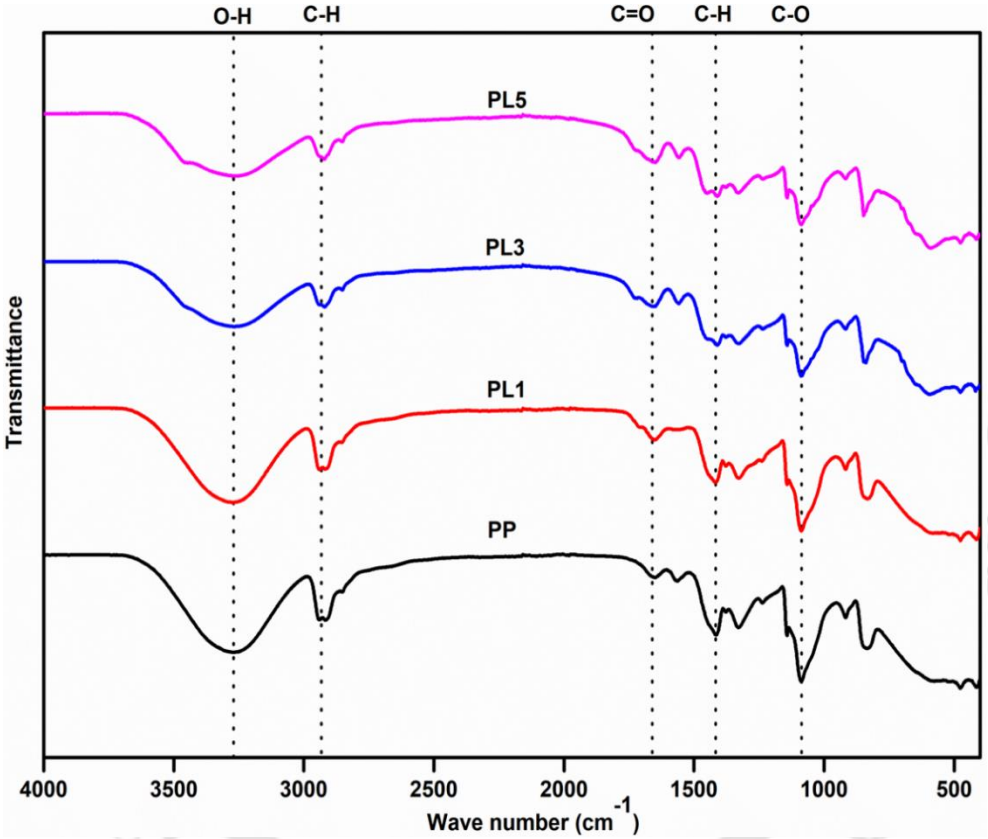

Figure 5.8 FTIR spectra of films. (PP: Pure PVA film; PL1: PVA+1% lignin; PL3: PVA+3% lignin; PL5: PVA+5% lignin).

The peak around 3300 cm^{-1} is caused by the OH stretching of the alcohol and carboxylic acid groups of PVA and lignin. This peak shifts towards a lower wavenumber after the addition of lignin with a growth in the width of the peaks. This might be explained by the development of strong hydrogen bonds resulting from the interaction of OH groups present in PVA and lignin (Korbag and Mohamed Saleh, 2016b). The small peak at 2924 cm^{-1} is associated with the characteristic CH_2 stretching vibration, and the peaks at 1654 cm^{-1} are related to the C=O stretching (Posoknistakul et al., 2020). The bands observed

at 1413 cm^{-1} and 1080 cm^{-1} were recognized as C−H bending in CH_3 and C–O, respectively (Suganthi et al., 2020). The peaks present in PVA were also found in the PVA/lignin films, showing that lignin incorporation at different proportions did not have a discernible effect on the PVA matrix's molecular structure.

5.4.2.2 XRD analysis

The XRD diffractogram of the neat and lignin-incorporated PVA films have been shown in **Fig. 5.9**. The peaks at 2θ = 19.4° and 26.35° are distinctive of PVA and can be attributed to the crystal planes of (101) and (200), correspondingly (Tang et al., 2015).

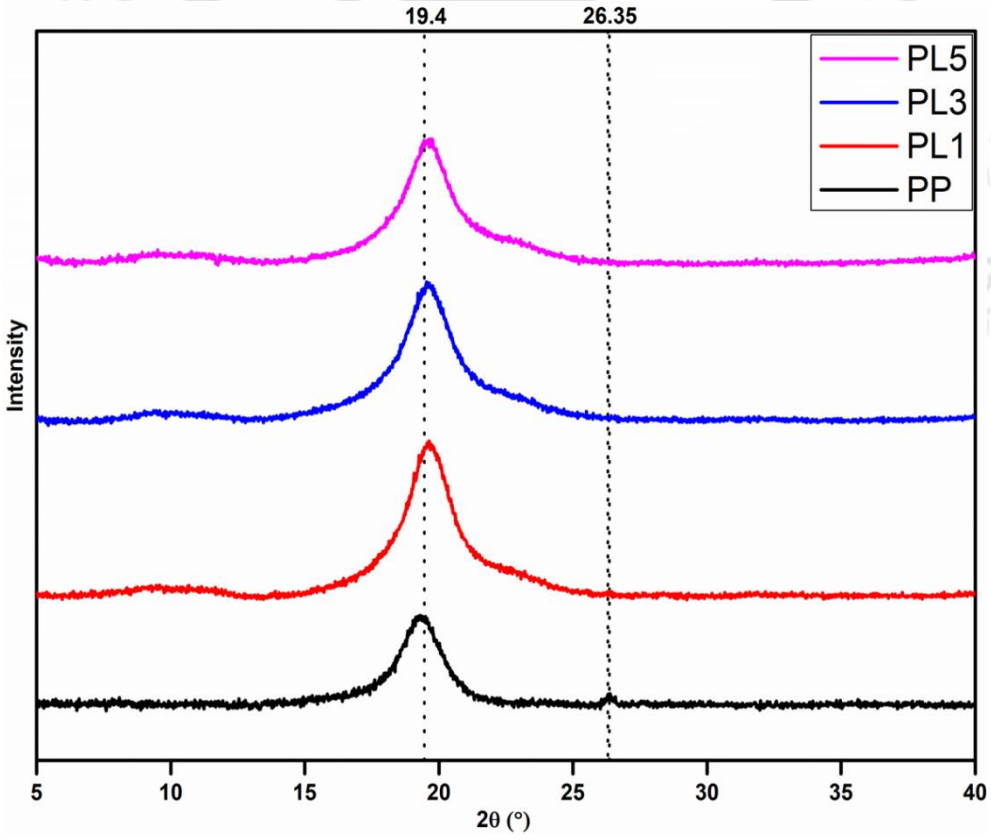

Figure 5.9 XRD diffractogram of the films. (PP: Pure PVA film; PL1: PVA+1% lignin; PL3: PVA+3% lignin; PL5: PVA+5% lignin).

The sharp peak at this position designates the semi-crystalline behaviour of PVA. Addition of amorphous lignin resulted in an enhanced peak width. This indicates that the

addition of lignin could probably affect the order of PVA arrangement in the crystalline region, due to the interaction between OH groups of PVA and lignin (Ye et al., 2016). This could lead to the reduced crystallinity of PVA films following lignin incorporation.

5.4.2.3 FESEM analysis

The morphology and dispersion of lignin into PVA films was visualized by FESEM images as shown in **Fig. 5.10.**

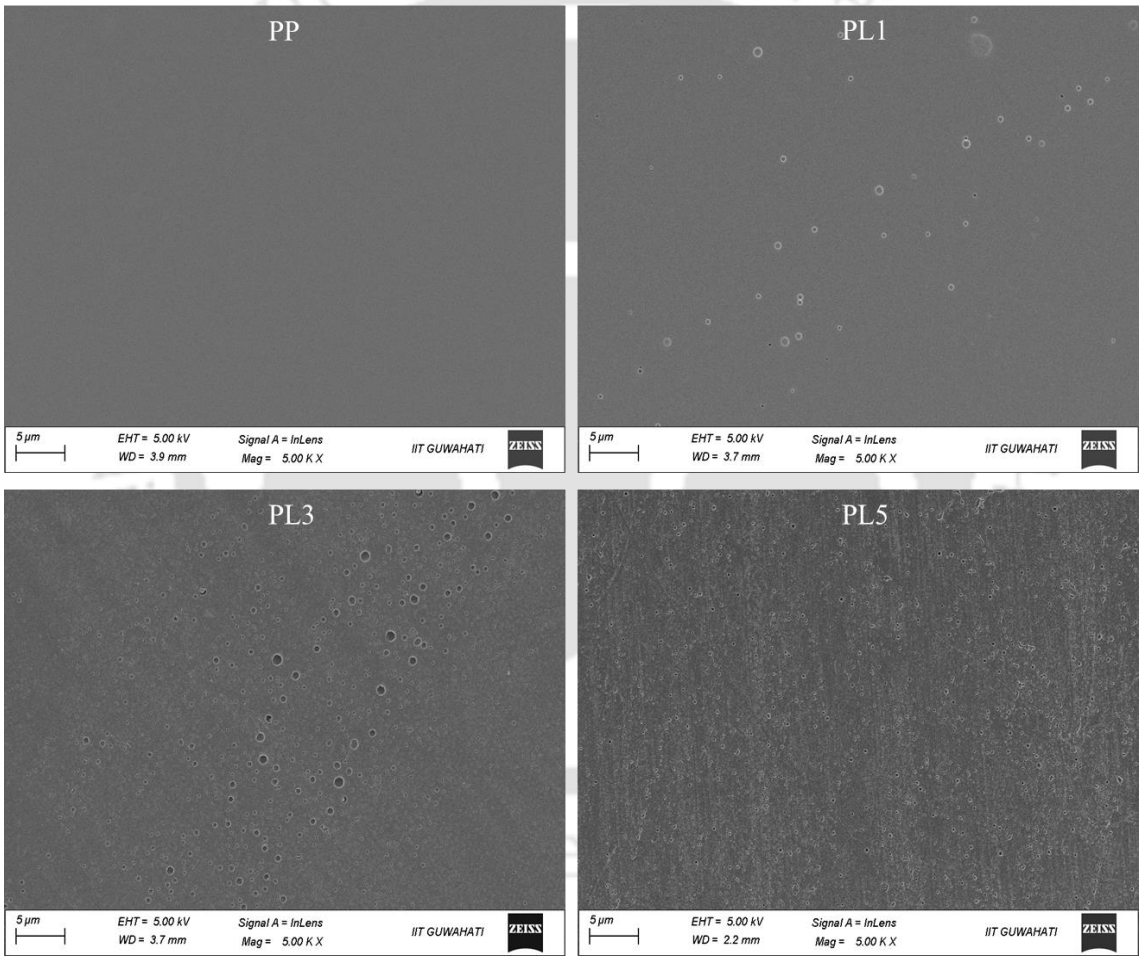

Figure 5.10 FESEM images of the films. (PP: Pure PVA film; PL1: PVA+1% lignin; PL3: PVA+3% lignin; PL5: PVA+5% lignin).

It was evident from the figure that the pure PVA film had a homogenous surface without any substantial blemish. This indicates a good film-forming ability of PVA through the

casting of its solution (Luzi et al., 2017). The incorporation of lignin affected the homogeneity of the PVA film regardless of the concentration. The roughness of the films surfaces increased with lignin content, resulting from the agglomeration of lignin particles.

5.4.2.4 AFM analysis

The AFM images of the neat and lignin – PVA films are given in **Fig. 5.11**. The incorporation of lignin visibly resulted in an increased roughness of the film surface proportionate to the concentration.

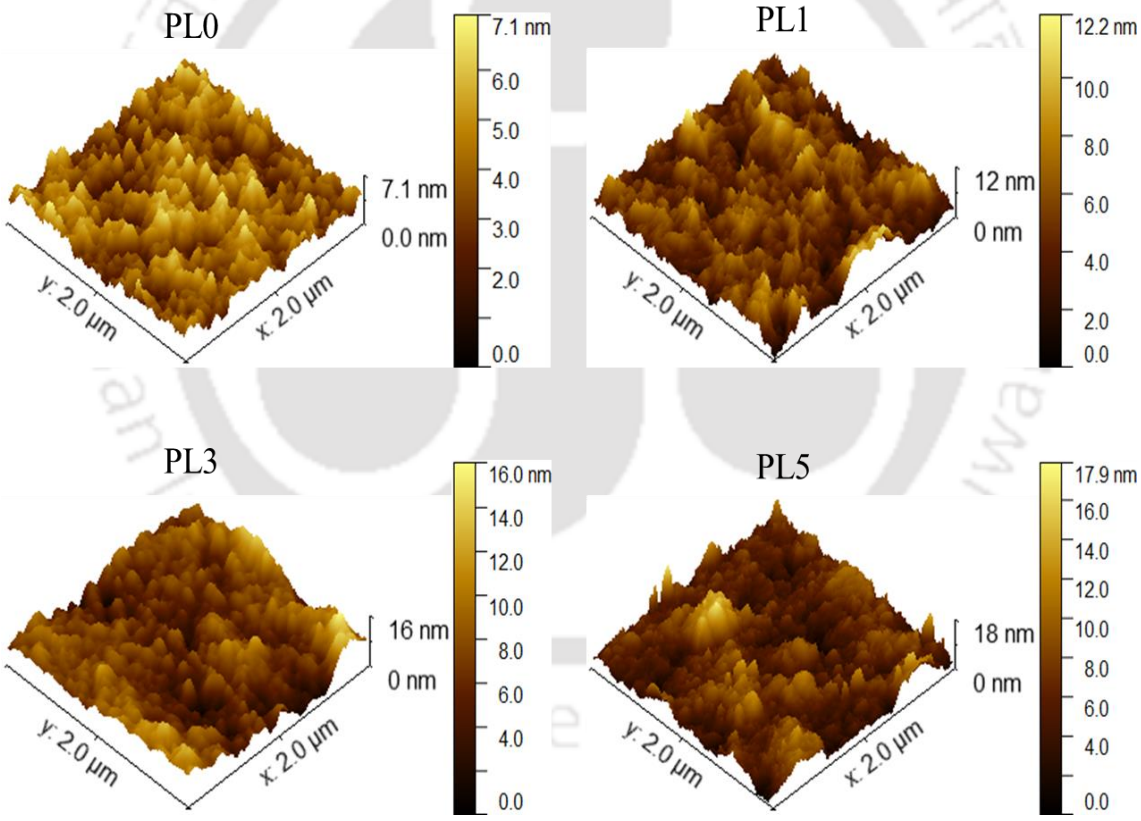

Figure 5.11 AFM images of the films. (PP: Pure PVA film; PL1: PVA+1% lignin; PL3: PVA+3% lignin; PL5: PVA+5% lignin).

When the concentration of lignin was low at 1%, there was a slight increase in the root mean square (RMS) roughness from 1.02 nm of the pure PVA film to 1.59 nm. This

suggests that in lower concentrations, the lignin and PVA matrix were uniformly mixed at the molecular level. Although, as the lignin content was raised to 3% and 5%, the RMS roughness amplified correspondingly to 2.15 nm and 2.29 nm, respectively. The increased roughness may be caused by the dispersion and aggregation of lignin (Kasai et al., 2018). Additionally, the vaporization of water from the non-homogenous portions might result in an increased roughness. The agglomeration of lignin could lead to macroscopic phase separation and this could substantially impact the barrier property blend films. The observations from AFM support the FESEM results (**Fig. 5.10**).

5.4.2.5 UV barrier property

The ability to shield UV light is desirable in a wide range of applications including food packaging. The transmission of UV light through PVA and lignin-incorporated PVA films is presented in **Fig. 5.12**.

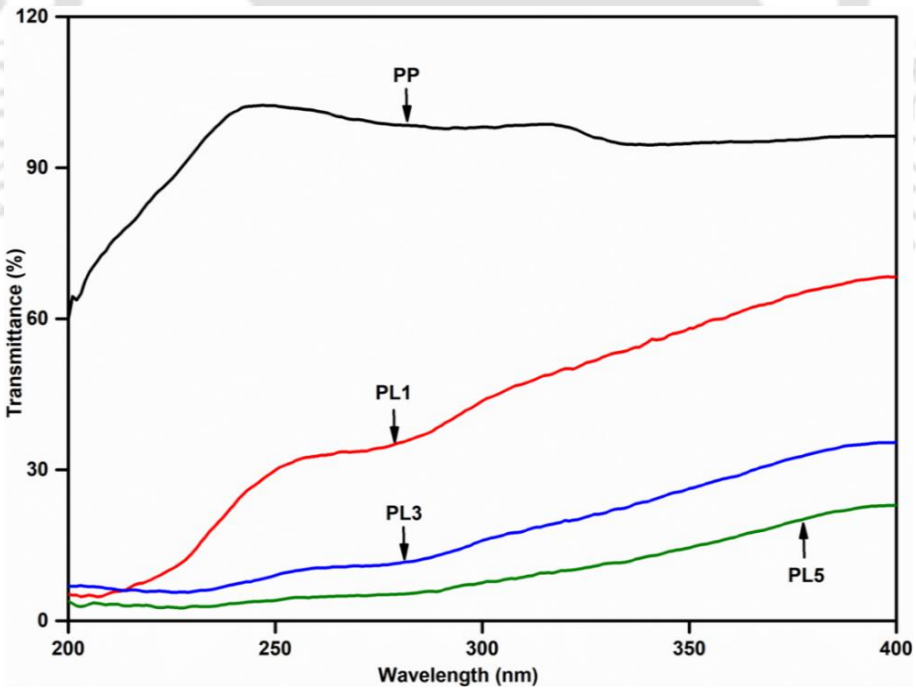

Figure 5.12 UV barrier property of films. (PP: Pure PVA film; PL1: PVA+1% lignin; PL3: PVA+3% lignin; PL5: PVA+5% lignin).

The neat PVA film displayed high transmittance of UV light, exhibiting minimal UV – barrier property. Lignin addition substantially reduces the transmission of UV light, compared to the neat PVA film. The observed shielding can be attributed to the large content of UV-absorbing groups and other chromophores in lignin (Posoknistakul et al., 2020). Even though the brownish colour of lignin slightly affected the transmission of visible light, the lignin – incorporated PVA films exhibited sufficient transparency which is a desirable property of food packaging systems.

5.4.2.6 Thermal analysis

The thermal property of lignin as well as the neat and lignin incorporated PVA films was evaluated using thermogravimetric analysis (**Fig. 5.13**). The weight loss of the lignin and film samples was initially brought on by the evaporation of free and bound water as indicated by a peak on the thermogravimetric (TG) and differential TG (DTG) curves up to around 150 °C **(Fig. 5.13(a))**.

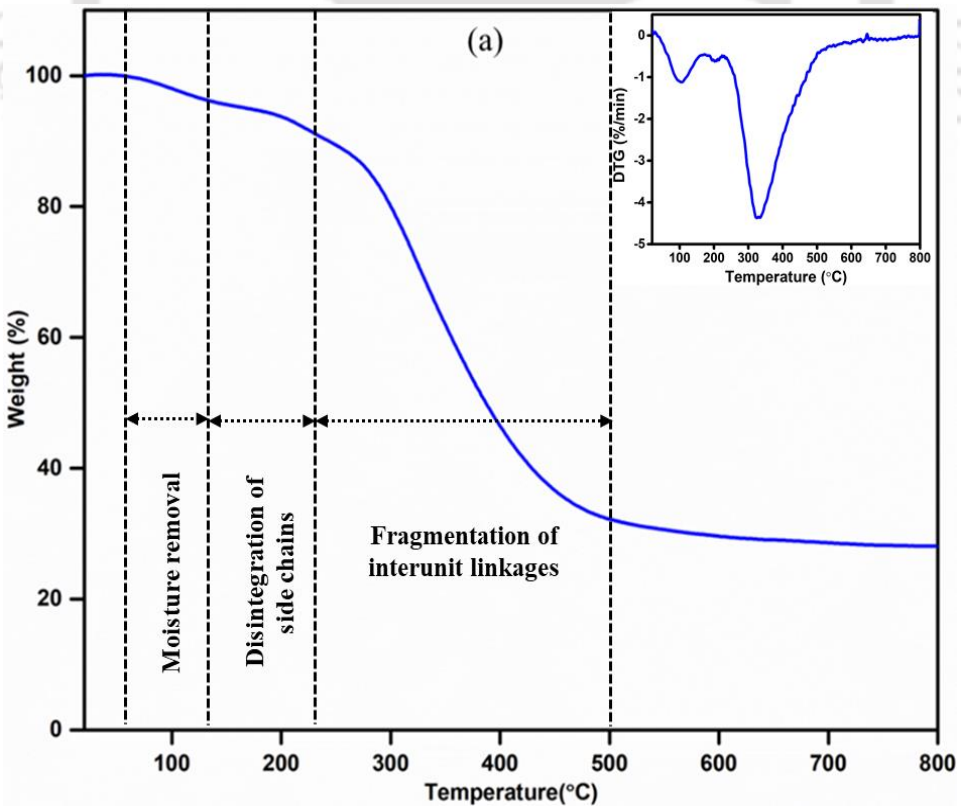

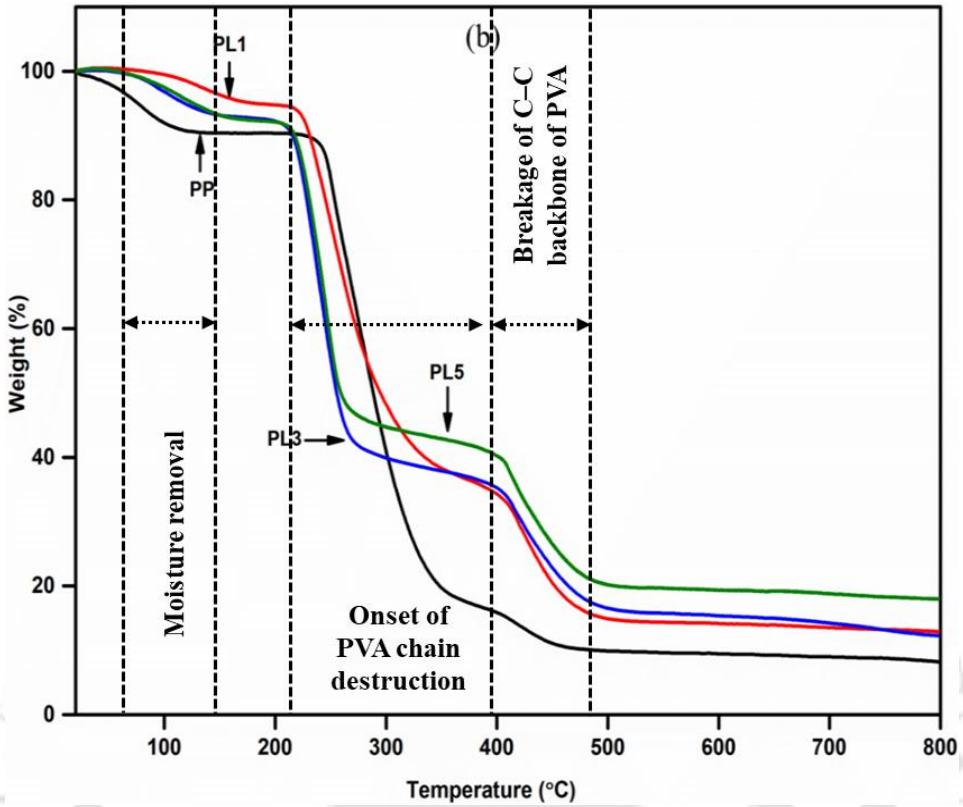

Figure 5.13 (a) TGA curve of lignin. Inset: DTG curve. (b) TGA curve of films. (PP: Pure PVA film; PL1: PVA+1% lignin; PL3: PVA+3% lignin; PL5: PVA+5% lignin).

The disintegration of side chains that releases volatiles caused mass loss in the 150 – 230 °C temperature range. The broad peak on the DTG curve indicates that the lignin sample degraded quickly between 240 and 500 °C. This decomposition process causes the interunit linkages to break down, releasing monomeric phenols and their derivatives into the vapor phase. The onset of the destruction of the PVA chain corresponds to the sharp mass loss between 220 – 380 °C (**Fig. 5.13 (b)**). The breakage of the C-C backbone of PVA corresponds to the final major thermal degradation (410 to 480 °C). The incorporation of lignin shifted the onset decomposition temperature to the higher side, implying an improvement in thermal stability. This improved stability can be explained by the establishment of aromatic units from lignin into PVA chains through stable hydrogen bonding (Liao et al., 2022).

5.4.2.7 Antioxidant property

The observations from the AA analysis of the films through DPPH assay are shown in **Fig. 5.14**. This analysis is based on the reduction of DPPH by the antioxidant compounds present in the films. The AA was found to be enhanced by increasing the lignin concentration. This antioxidant activity is primarily ascribed to the aromatic units of lignin, capable of preventing the oxidation processes induced by oxidizing species (Espinosa et al., 2019). The antioxidant activity increased from 11.99±1.29% for pure PVA to 33.53±1.98%, 42.01±1.01%, and 53.86±2.07% for PL1, PL3 and PL5, respectively. Hence, it may be conceived that the addition of lignin enhances the antioxidant activity of PVA films.

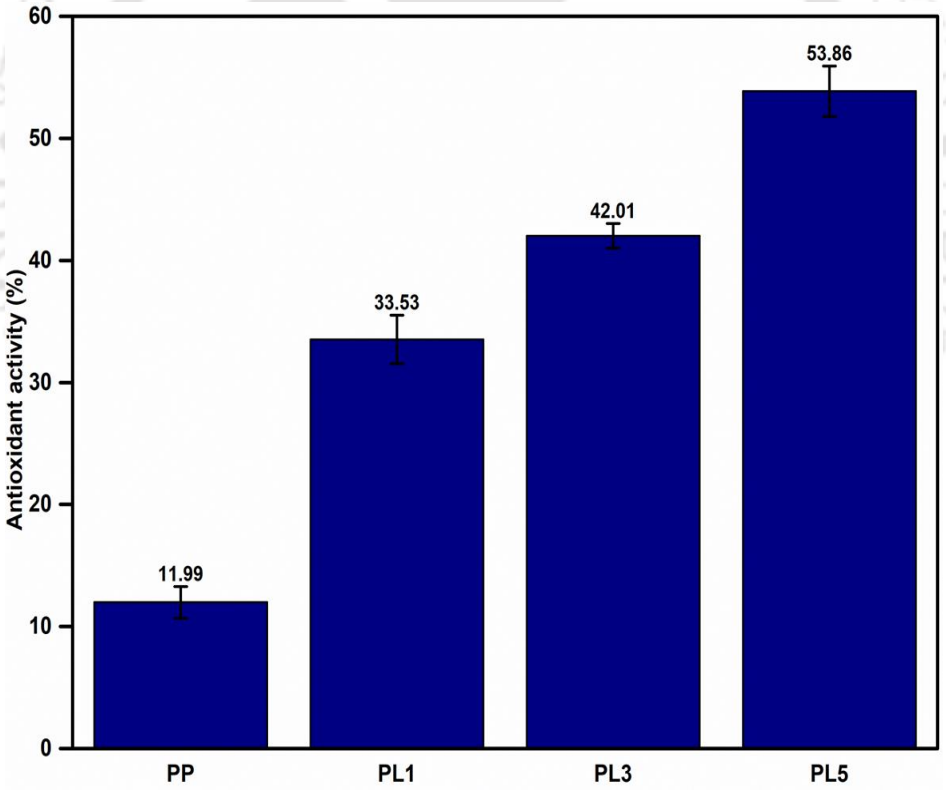

Figure 5.14 Antioxidant activity of the films. (PP: Pure PVA film; PL1: PVA+1% lignin; PL3: PVA+3% lignin; PL5: PVA+5% lignin).

5.4.2.8 Mechanical property

The mechanical properties in terms of the stress – strain curve as well as the tensile strength and elongation at break of the films has been shown in **Fig. 5.15 (a) and Fig. 5.15 (b)**, respectively. It was observed that the lignin incorporated PVA films exhibited a higher tensile strength than the pure PVA at all concentrations. The tensile strength increased from 18.96±0.07 MPa for PP to 25.47±1.37 MPa, 28.13±2.95 MPa, and 53.70±2.90 MPa for PL1, PL3, and PL5, respectively. The enhancement in tensile strength of PVA films following lignin incorporation can be ascribed to the characteristic chain toughness as well as the rigidity of lignin. The increase in tensile strength with increasing lignin can also be elucidated by the enhanced surface area of the lignin, improving the compatibility with PVA matrix, leading to better mechanical properties (Posoknistakul et al., 2020). Lignosulfonate and PVA blend films have also been reported to have improved mechanical performance than neat PVA owing to hydrogen bonding formation and the rigidity of lignin (Hu et al., 2016).

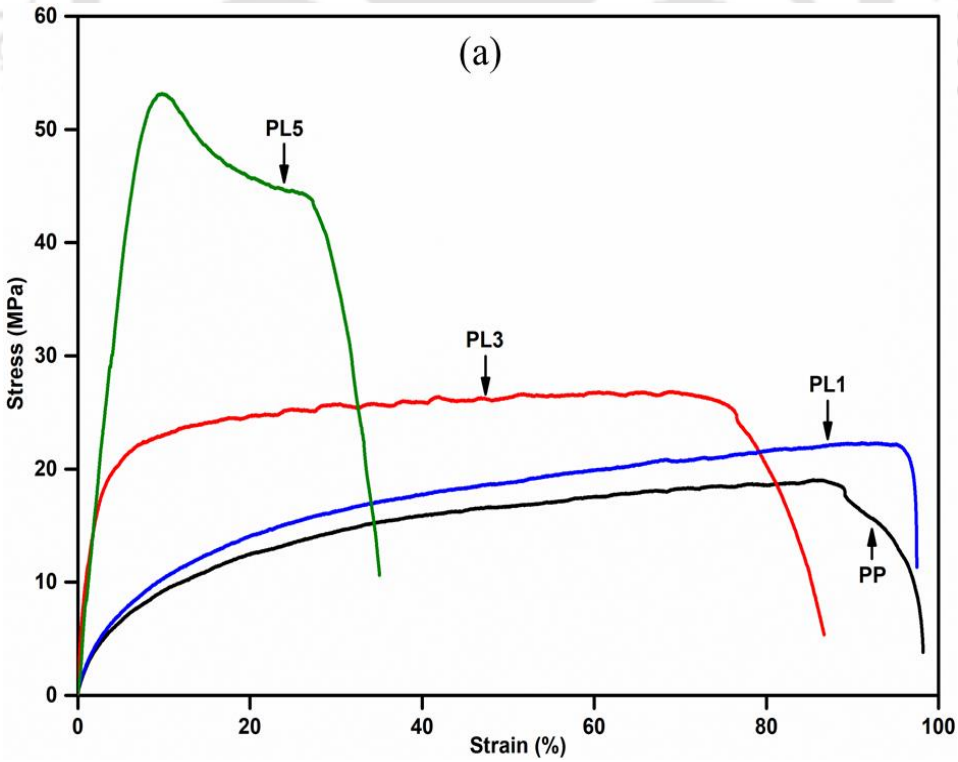

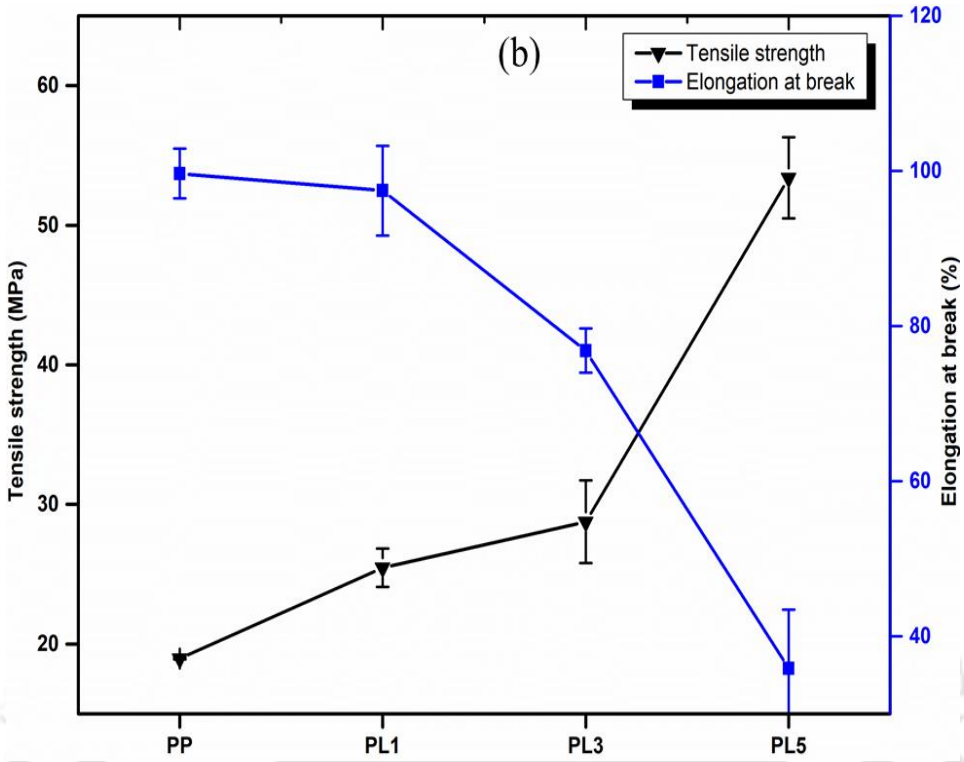

Figure 5.15 (a) Stress- strain curve and (b) Tensile strength and elongation at break of films. (PP: Pure PVA film; PL1: PVA+1% lignin; PL3: PVA+3% lignin; PL5: PVA+5% lignin).

Conversely, the elongation at break reduced from 100.33±3.2% for PP to 97±5.78%, 76±2.86%, and 35±7.60% for PL1, PL3 and PL5, respectively. This could be caused by the intermolecular hydrogen bonding between the OH groups present in lignin and PVA, resulting in increased stiffness as well as reduced elasticity (Espinosa et al., 2019).

5.4.2.9 Water barrier properties

The WS and WVP of packaging films are significant properties in analyzing the moisture transfer between a food being packed and the environment which further influences the quality and acceptability of a product wherein high water solubility shows a low water resistance. Lignin addition into PVA film resulted in a noticeable reduction in film solubility (≈78%), from 31.86% (neat PVA) to 7.14% (5% lignin) (**Table 5.3**). The reduced water solubility of PVA/lignin films can be elucidated by the high hydrophobicity and insolubility of lignin.

The WVP governs the competence of a package to capture moisture from the surrounding and transfer it into the food packed with the film. High moisture absorption can hasten the microbial growth and subsequent spoilage of commodities. The WVP was the least for PP and increased slightly with increase in lignin content (**Table 5.3**). The enhanced WVP might be caused by a rise in void volume resulting from the disturbance of the film network, which in turn is caused by the accumulation of lignin particles (Liu et al., 2021). This subsequently affects the path of moisture transport over the prepared films (Liao et al., 2022).

Table 5.3 Water solubility and water vapour permeability of the films

Film	**WS (%)**	**WVP ($\times 10^7$ g. Pa^{-1} h^{-1}m^{-1})**
PP	31.86 ± 3.06	3.85 ± 0.21
PL1	12.19 ± 3.13	3.92 ± 0.15
PL3	11.21 ± 2.67	5.16 ± 0.18
PL5	7.14 ± 1.94	7.84 ± 0.64

PP: Pure PVA film; PL1: PVA+1% lignin; PL3: PVA+3% lignin; PL5: PVA+5% lignin. The values are mean ± SD obtained from three replicates.

The findings can further be elucidated by the increased plasticization effect induced by moisture, reducing the density of the polymer and making it more permeable (Núñez-Flores et al., 2013). Neat PVA film is semi-crystalline in nature and the addition of amorphous lignin decreases this crystallinity. This reduction could also increase the amorphous regions through water diffused (Bumbudsanpharoke et al., 2022). The findings corroborate with the XRD (**Fig. 5.9**) and AFM (**Fig. 5.11**) results.

5.4.2.10 Antifogging property

Formation of fog inside a food package is undesirable as it can encourage the growth of spoilage microorganisms leading to spoilage of food. The appearance of a foggy layer also changes the material's optical characteristics and obscures the contents of the package. From the antifogging test results (**Fig. 5.16**), it can be seen that the uncoated part of the glass slides became covered with water droplets and became hazy when placed over hot water.

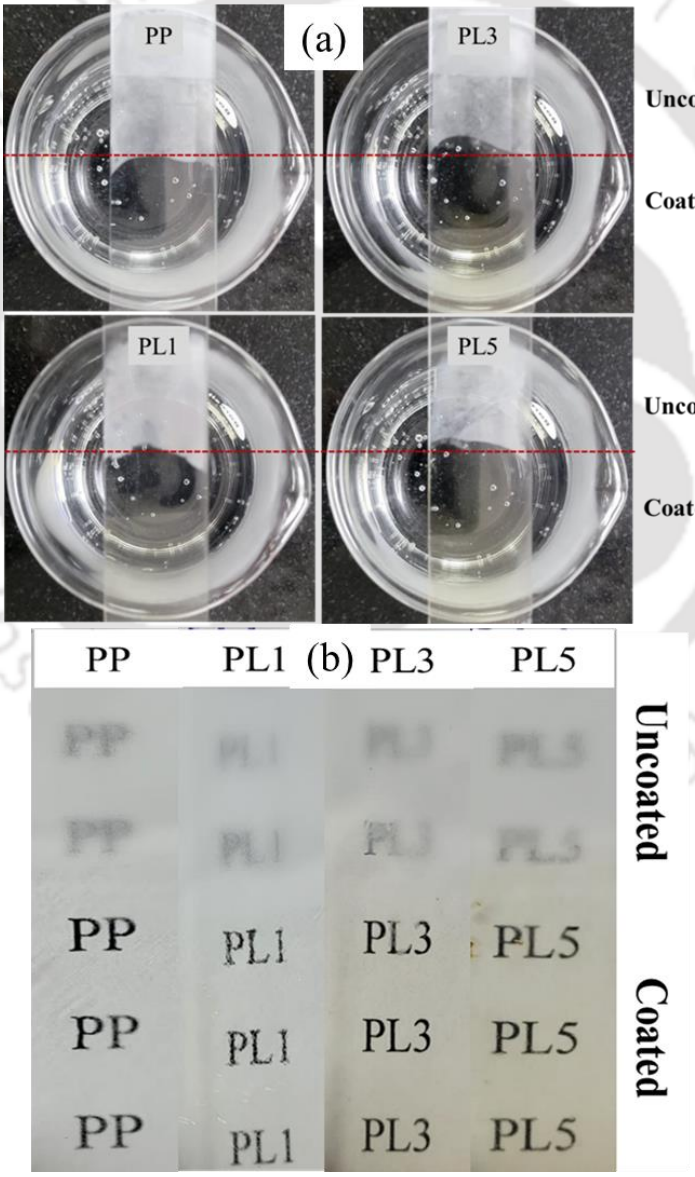

Figure 5.16 Antifogging property of films (a) Slides appearance within 5s of exposure to boiling water steam (b) Slides appearance within 5s after being transferred from freezer to ambient conditions (PP: Pure PVA film; PL1: PVA+1% lignin; PL3: PVA+3% lignin; PL5: PVA+5% lignin).

However, the coated parts of the slides remain fairly transparent at all concentrations of coating. The antifogging characteristic of the films may be accredited to the hydrophilicity and moisture absorption capacity of the coatings. The hydrophilic moieties of the coating adsorb the condensed moisture readily via hydrogen bond and dipole-dipole interactions, maintaining the transparency. On the other hand, the unadsorbed moisture on the bare side of the slide formed a thin layer, which resulted in the attenuation of the light scattering (Hu et al., 2018).

5.4.2.11 Leaching test

The study of migration of packaging components is important since the migrated conmpounds can interfere with and compromise the properties and quality of the food being packed. Leaching test was conducted to measure the quantity of leached out active components from films (**Fig. 5.17**). Among the three food stimulants taken, the films exhibited the highest leaching behaviour in distilled water, followed by 10% ethanol, and lowest in 3% acetic solution. The variation in solubility of PVA in the different stimulants might have influenced the leaching of film components. In all the stimulants taken, the highest leaching was exhibited by PL5 followed by PL3, PL1 and least in PP. This is probably correlated with the concentration of lignin in the films. Similar findings were observed for the leaching of active components in PVA – starch films (Mustafa et al., 2021). However, the prepared films are designed to be used for dry solid foods and there was no visible deposition of the film components into the samples being studied, signifying minimal leaching.

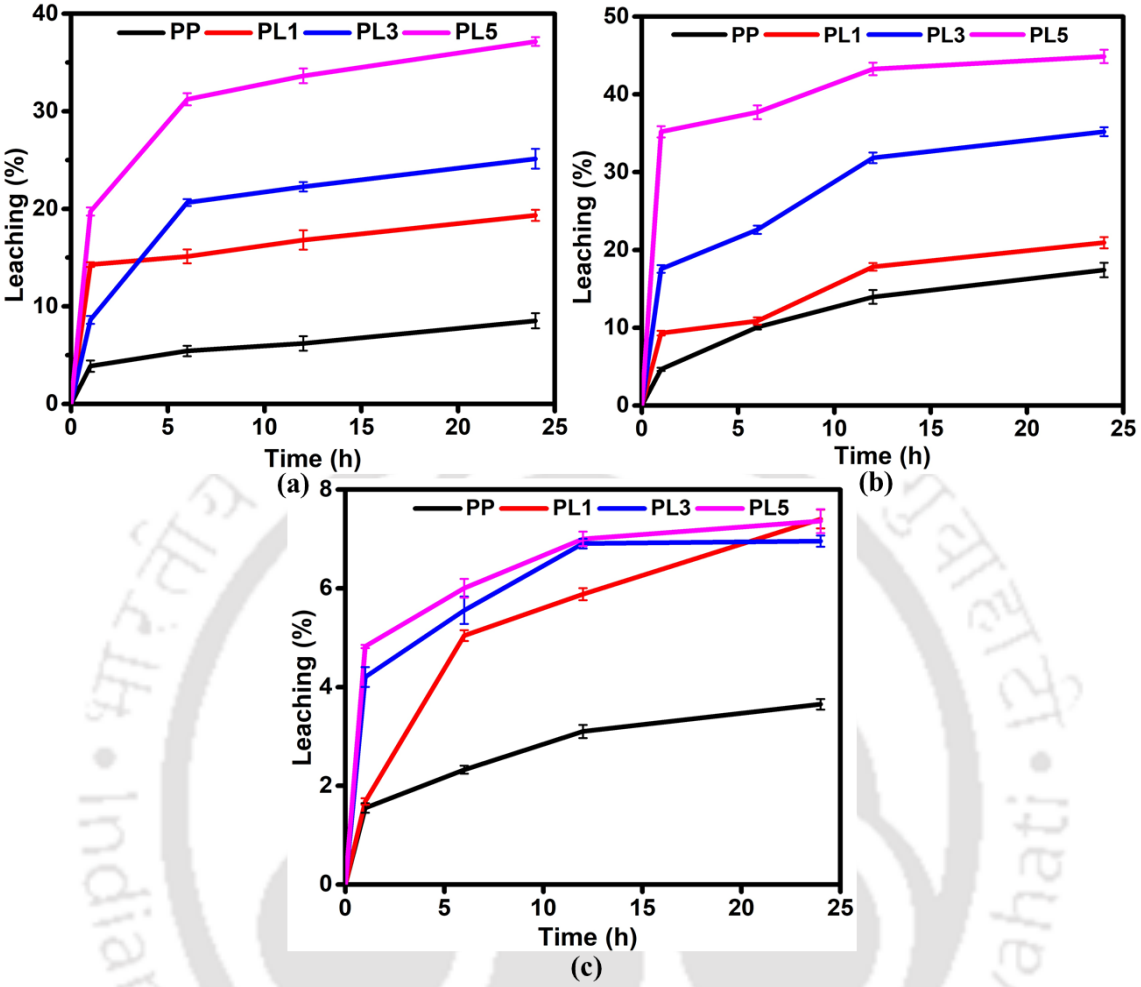

Figure 5.17 Leaching behaviour of the prepared films in (a) Distilled water (b) 10% ethanol and (c) 3% acetic acid. (PP: Pure PVA film; PL1: PVA+1% lignin; PL3: PVA+3% lignin; PL5: PVA+5% lignin).

5.4.3 Performance evaluation of the films for bread storage

The change in the bread appearance as a result of spoilage during storage is shown in **Table 5.4**. Lignin incorporation did not have any relevant impact on visibility of the samples. The bread samples packed in commercial packaging material started showing mold growth on the 3rd day and reached full growth on the 4th day. However, the growth was retarded till day 8 for all the samples packed using the prepared films and on the 9th day, PL3 and PL5 started showing small growth. The samples showed visually substantial

mold growth on the 12th day where growth shows in samples packed with PP. PL1 was able to retard the mold growth till 22nd day, when the first signs of growth appears. As seen from **Table 5.4**, the progression of mold growth was substantially slower in the prepared films. PVA is known to have a low oxygen permeability and this could positively impact the inhibition of mold growth by limiting the required oxygen for their growth (Idris et al., 2021). The combined effect of the low oxygen permeability with the antifungal and antioxidant properties of lignin could be the reason for the excellent performance of PL1. However, as the lignin content increased to 3% and 5%, the antifungal performance of the films declined. This might be due to an increased water and oxygen transmission though the films owing to the increased roughness brought about by lignin aggregation, as seen from the AFM results (**Fig. 5.10**).

Table 5.4 Progression of spoilage of bread packed with different packages at 25 °C

Day/ Sample	Commercial	PP	PL1	PL3	PL5
0					
3					
4	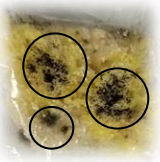				

Note: Arrows denote the start of mold growth and circles show the widespread growth on the samples. PP: Pure PVA film; PL1: PVA+1% lignin; PL3: PVA+3% lignin; PL5: PVA+5% lignin.

The study was also conducted at 30 °C and 35 °C to observe the effect of temperature on mold inhibition by the films during bread storage (**Tables 5.5 and 5.6**). It was found that the mold growth was fastest at 30 °C, where the spoilage of bread occurred within the shortest time as compared to 25 °C and 35 °C. As in the case of storage at 25 °C, the samples packed with commercial package started showing mold growth on the 3rd day and full growth by 4th day for both 30°C and 35 °C. All the samples attained full mold growth by the 9th day at 30 °C whereas the same was achieved by 11th day at 35 °C.

Among the three temperatures selected, mold growth was most enhanced at 30 °C, followed by 35 °C and least at 25 °C. Hence, it can be inferred that warmer and humid storage conditions favour the growth of mold in bread. In all the storage conditions, the prepared films performed better in inhibiting mold growth and there was minimum inhibition by the commercial packaging material.

Table 5.5 Progression of spoilage of bread packed with different packages at 30 °C

Day/ Sample	Commercial	PP	PL1	PL3	PL5
0					
3					
4					
7					

8			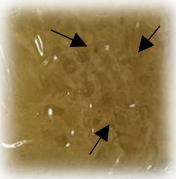	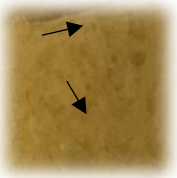	
9					

Note: Arrows denote the start of mold growth and circles show the widespread growth on the samples. PP: Pure PVA film; PL1: PVA+1% lignin; PL3: PVA+3% lignin; PL5: PVA+5% lignin.

Table 5.6 Progression of spoilage of bread packed with different packages at 35 °C

Day/ Sample	Commercial	PP	PL1	PL5	PL3
0					
3					
4					

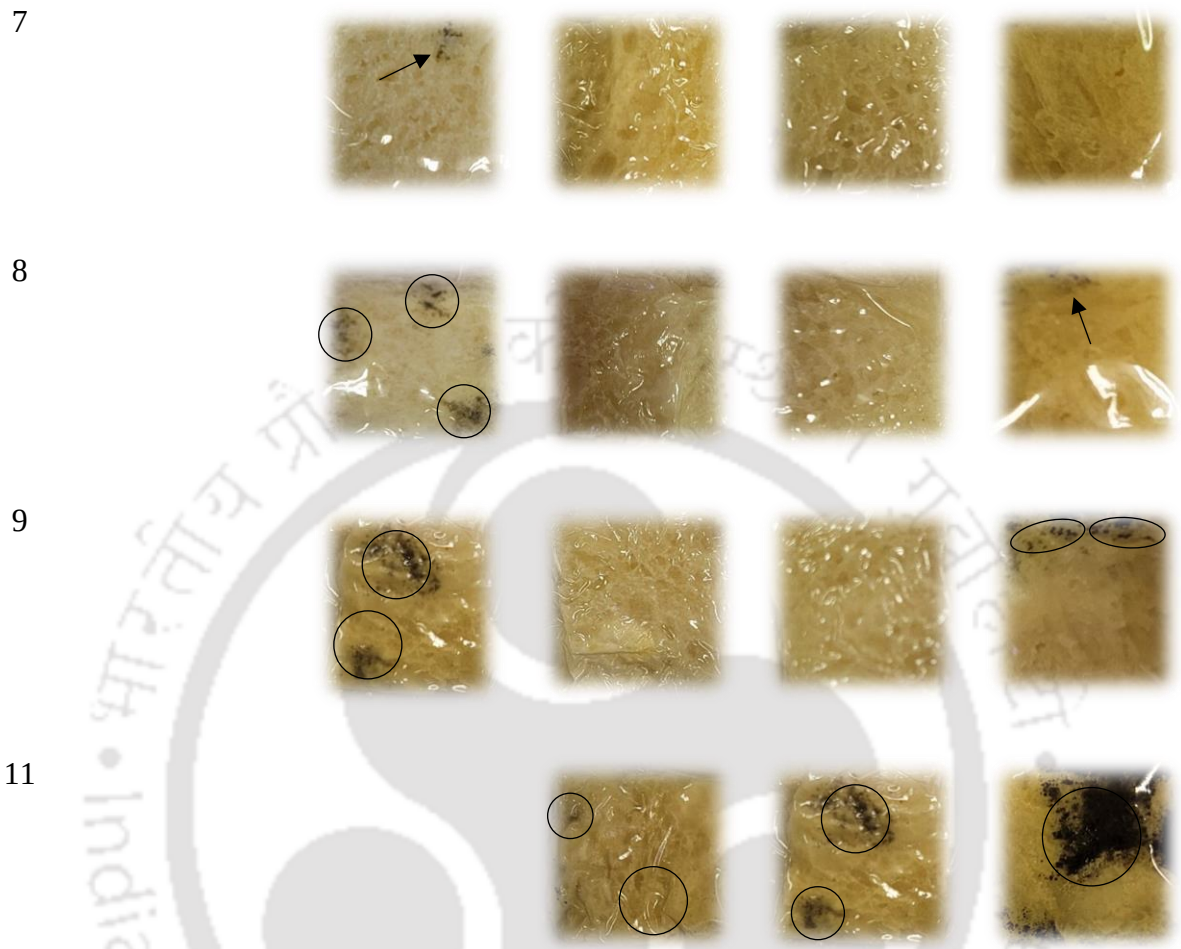

Note: Arrows denote the start of mold growth and circles show the widespread growth on the samples. PP: Pure PVA film; PL1: PVA+1% lignin; PL3: PVA+3% lignin; PL5: PVA+5% lignin.

5.5 Summary

This chapter explores the extraction of lignin from the waste leaves of *Ficus auriculata* obtained after extraction of gallic acid. The extracted lignin was incorporated into PVA films and the neat and blend films were characterized using different techniques. Although lignin caused led to slight browning of PVA film, the films retained sufficient transparency for use as packaging materials. Incorporation of lignin improved the thermal, mechanical, UV barrier and antioxidant activity of PVA films. All the prepared films exhibited good antifogging properties in both the methods considered. The water

solubility decreased and the WVP of films increased slightly with the incorporation of lignin. There was maximum leaching of film components of up to 44% in 24 h in distilled water, followed by 10% ethanol (37%) and minimum leaching in 3% acetic acid (7%). The performance evaluation of the prepared films for bread storage was carried out and compared with the commercially used packaging materials. The samples packed with commercial packages started showing mold growth on 3rd day during storage at 25 °C and attained full growth by the 4th day while one of the prepared films were able to inhibit the growth for 15 days. The samples packed with commercial package started showing mold growth on the 3rd day and full growth by 4th day for both 30°C and 35 °C. All the samples attained full mold growth by the 9th day at 30 °C whereas the same was achieved by 11th day at 35 °C. Among the three temperatures selected, mold growth was most enhanced at 30 °C, followed by 35 °C and least at 25 °C. The progression of spoilage was visibly slower in the samples packed with the prepared films. The results obtained from this study might be helpful in producing simple as well as eco-friendly packages for enhancing keeping quality of food products.

Chapter 6

Conclusions and scope of future work

Utilization of extract and by-products of *Ficus auriculata* leaves

Chapter 6

Conclusions and scope for future work

In this chapter, the main conclusions drawn from each objective and the possible scope for further research are reported. Gallic acid was extracted from F. auriculata leaves using ultrasound – assisted extraction. The extraction process was optimized by varying temperature, time, solvent solid ratio, pH and sonication power. The gallic acid – rich extract was used as an additive for PVA – based coating of banana for delayed ripening and the coatings were characterized. The extract was further used as the active ingredient in the preparation of antioxidant formulation which were formed into tablets. The waste leaves obtained after gallic acid extraction was used to synthesize lignin. The synthesized lignin was incorporated into PVA films and the films were studied for their potential use in bread packaging. The detailed conclusions are highlighted below, separately for each chapter.

❖ Introduction, Literature Review, Objectives and Organization of the Thesis

- The background of the thesis work, the state of art literature and possible scope of research are reported here.
- Based on the scopes, four research objectives are formulated.
- The organization of the thesis is briefly summarized

❖ Investigation of the ultrasound assisted extraction of gallic acid from *Ficus auriculata* leaves using green solvent

- Ultrasound assisted extraction using mildly alkaline water was able to efficiently extract gallic acid from *F. auriculata* leaves
- A combination of 50 °C, 50% of sonication level and 1:10 water – solid sample ratio and pH 8 resulted in the maximum extraction within 30 min of operation.

- Sonication bath was found to give 6.3% more of gallic acid as compared to probe sonicator.
- Maximum gallic acid was extracted using methanol but comparable results were observed for extraction using slightly alkaline water as the solvent resulting in yield of 329.5 and 312.92 mg/L, respectively. This indicates that water can be efficiently used for extraction as an environmentally friendly, cheap and safe solvent.
- The kinetics of extraction was studied by fitting the gallic acid extraction data into four mathematical models and Peleg model was found to best describe the gallic acid extraction process with the highest regression coefficient value (R^2>0.99).

❖ **Preparation and characterization of gallic acid (antioxidant) incorporated poly(vinyl alcohol) coating for delayed ripening of green bananas**

- The application of PVA-based coating was found potential to delay the ripening and increase the shelf stability of green bananas.
- The films exhibited low opacity of 0.86 ± 0.014 for pure PVA (PP) and 0.92 ± 0.019, 0.99 ± 0.020 and 1.18 ± 0.029 for PVA+1% extract (PE1), PVA+5% extract (PE5), and PVA+10% extract (PE10), respectively, signifying excellent transparency.
- The water solubility of the films increased from 33.19 ± 1.48% for PP to 37.59 ± 1.88%, 40.25 ± 1.33%, and 46.49 ± 2.39% for PE1, PE5, and PE10, respectively
- The WVP was the least for PP (1.99 ± 0.72 $\times 10^{-7}$ g.m.h^{-1}Pa^{-1}) while that of PE1, PE5, PE10 were 2.28 ± 0.08, 2.31 ± 0.17, and 2.35 ± 0.33 $\times 10^{-7}$ g.m.h^{-1}Pa^{-1}, respectively
- The fruits without any treatment attained complete maturity and thus commercial acceptability on the 9th day while the fruits coated with PP as

well as PE10 remained acceptable till day 15, and the ones with PE1 and PE5 reached full ripeness on day 18.

- There was continuous variation in the physicochemical properties during storage, however, coated samples exhibited slower change.

❖ Preparation and evaluation of antioxidant formulations containing gallic acid enriched extract

- Antioxidant formulations were prepared with gallic acid rich extract of *Ficus auriculata* leaves as the active ingredient.
- The formulations F2, F3, and F4 (Please refer to Chapter 4, Section 4.3) were found to have tendency to stick to one another due to the presence of higher amounts of hygroscopic sugar compounds and hence were not used for tablet preparation.
- F1, F5, and F6 (Please refer to Chapter 4, Section 4.3) were free flowing and had desirable angle of repose for tableting. The formulations were characterized and formed into tablets using a simple hand operated pellet maker.
- All the produced tablets had disintegration times lesser than 15 min
- The antioxidant activity of the tablets was found to be 83.78%, 33.51% and 78.92% for F1, F5, and F6, respectively.
- The tablets were completely stable under acidic and alkaline conditions for up to 2 h.

❖ Extraction of lignin from waste *Ficus auriculata* leaves and its potential application for bread packaging

- Lignin was extracted from the waste *F. auriculata* leaves obtained after the extraction of gallic acid and successfully incorporated into PVA films and characterized.

- The incorporation of lignin amended the thermal, mechanical, UV barrier and antioxidant activity of PVA films where the films retained sufficient transparency despite slight browning.
- The prepared films showed good antifogging properties.
- The water solubility of the films decreased from 31.86% for PP to 12.19, 11.21, and 7.14% for PL1, PL3, and PL5, respectively.
- The WVP of films increased slightly from 3.85×10^{-7} g.m.h^{-1}Pa^{-1} for PP to 3.92, 5.16, and 7.84 10^{-7} g.m.h^{-1}Pa^{-1}for PL1, PL3, and PL5, respectively.
- The prepared films were evaluated for their performance as a food packaging material during bread storage and compared with commercially used packaging material.
- The samples packed with commercial packages started showing mold growth on 3rd day and attained full growth by the 4th day.
- The prepared films inhibited mold growth fully till day 9 for PL3 and PL5, and upto day 12 for PP, while there was no growth in PL1 till the 15th day.
- The progression of spoilage was visibly slower in the samples packed with the prepared films.
- Fastest and maximum growth was observed at 30 °C, followed by 35 °C and 25 °C.

Recommendation for future works

Considering the observations reported in Chapters 2 to 5, the recommendations for further work are reported below for each chapter

Chapter 2

- Extraction of plant-based antioxidants using green solvent and hybrid-extraction methods.
- Encapsulation of extracted compounds using economical and safe wall materials and exploring their use in food and pharmaceutical industries.

Chapter 3

- Studies on effect of viscosity of the coating solution on the performance of fruit coating.
- Studies on different biodegradable polymer and antioxidant-based coatings on easy-spoiling fruits and vegetables.
- Study on the influence of different storage conditions on the performance of fruit coating.

Chapter 4

- Detailed stability study of formulations in gastrointestinal condition.
- In – vivo studies on effectiveness of antioxidant formulations.

Chapter 5

- Recovery of cellulose compounds from lignin-extracted biomass waste and studies on their utilization in food industries.
- Application of lignin as an additive in coating of existing food packaging materials.

References

Abdelaziz, O.Y., Hulteberg, C.P., 2017. Physicochemical Characterisation of Technical Lignins for Their Potential Valorisation. Waste and Biomass Valorization 8, 859–869. https://doi.org/10.1007/s12649-016-9643-9

Ahmed, Z.F.R., Palta, J.P., 2016. Postharvest dip treatment with a natural lysophospholipid plus soy lecithin extended the shelf life of banana fruit. Postharvest Biol. Technol. 113, 58–65. https://doi.org/10.1016/j.postharvbio.2015.10.016

Al Fishawy, A., Zayed, R., Afifi, S., 2011. Phytochemical and pharmacological studies of *Ficus auriculata* Lour. (Family Moraceae) cultivated in Egypt. Planta Med. 77. https://doi.org/10.1055/s-0031-1282654

Altemimi, A., Watson, D.G., Choudhary, R., Dasari, M.R., Lightfoot, D.A., 2016. Ultrasound assisted extraction of phenolic compounds from peaches and pumpkins. PLoS One 11, 1–20. https://doi.org/10.1371/journal.pone.0148758

Álvarez-Hernández, M.H., Artés-Hernández, F., Ávalos-Belmontes, F., Castillo-Campohermoso, M.A., Contreras-Esquivel, J.C., Ventura-Sobrevilla, J.M., Martínez-Hernández, G.B., 2018. Current Scenario of Adsorbent Materials Used in Ethylene Scavenging Systems to Extend Fruit and Vegetable Postharvest Life. Food Bioprocess Technol. 11, 511–525. https://doi.org/10.1007/s11947-018-2076-7

Anbalagan, K., Kumar, M.M., Ilango, K., Mohankumar, R., Priya, R.L., 2019. Prelusive scale extraction of mangiferin from *Mangifera indica* leaves: Assessing solvent competency, process optimization, kinetic study and diffusion modelling. Ind. Crops Prod. 140, 111703. https://doi.org/10.1016/j.indcrop.2019.111703

References

Andrade, J., González-Martínez, C., Chiralt, A., 2021. Effect of phenolic acids on the properties of films from Poly (vinyl alcohol) of different molecular characteristics. Food Packag. Shelf Life 29. https://doi.org/10.1016/j.fpsl.2021.100711

Archer, M. A., Kumadoh, D., Yeboah, G. N., Kyene, M. O., Kumatia, E. K., Antwi, S., & Appiah, A. A. (2020). Formulation and evaluation of capsules containing extracts of *Cassia sieberiana* for improved therapeutic outcome. *Scientific African*, *10*, e00609. https://doi.org/10.1016/j.sciaf.2020.e00609

Ardekani, P.S., Karimi, H., Ghaedi, M., Asfaram, A., Purkait, M.K., 2017. Ultrasonic assisted removal of methylene blue on ultrasonically synthesized zinc hydroxide nanoparticles on activated carbon prepared from wood of cherry tree: Experimental design methodology and artificial neural network. J. Mol. Liq. 229, 114–124. https://doi.org/10.1016/j.molliq.2016.12.028

Arvanitoyannis, I.S., Kotsanopoulos, K. V., 2014. Migration Phenomenon in Food Packaging. Food-Package Interactions, Mechanisms, Types of Migrants, Testing and Relative Legislation-A Review. Food Bioprocess Technol. 7, 21–36. https://doi.org/10.1007/s11947-013-1106-8

Asfaram, A., Ghaedi, M., Purkait, M.K., 2017. Novel synthesis of nanocomposite for the extraction of *Sildenafil Citrate* (Viagra) from water and urine samples: Process screening and optimization. Ultrason. Sonochem. 38, 463–472. https://doi.org/10.1016/j.ultsonch.2017.03.045

Athankar, K.K., Wasewar, K.L., Varma, M.N., Shende, D.Z., 2016. Reactive extraction of gallic acid with tri-n-caprylylamine. New J. Chem. 40, 2413–2417. https://doi.org/10.1039/c5nj03007b

Awad, M.A., Al-Qurashi, A.D., Mohamed, S.A., El-Shishtawy, R.M., Ali, M.A., 2017. Postharvest chitosan, gallic acid and chitosan gallate treatments effects on shelf life quality, antioxidant compounds, free radical scavenging capacity and enzymes activities of 'Sukkari' bananas. J. Food Sci. Technol. 54, 447–457. https://doi.org/10.1007/s13197-016-2481-8

Azmir, J., Zaidul, I.S.M., Rahman, M.M., Sharif, K.M., Mohamed, A., Sahena, F., Jahurul, M.H.A., Ghafoor, K., Norulaini, N.A.N., Omar, A.K.M., 2013. Techniques for extraction of bioactive compounds from plant materials: A review. J. Food Eng. 117, 426–436. https://doi.org/10.1016/j.jfoodeng.2013.01.014

Baite, T.N., Das, A.B., 2018. Extraction of glycyrrhizin from licorice using single screw extruder: Process kinetics and stimulus response modeling. Sep. Sci. Technol. 53, 449–457. https://doi.org/10.1080/01496395.2017.1391846

Baite, T.N., Mandal, B., Purkait, M.K., 2021. Ultrasound assisted extraction of gallic acid from *Ficus auriculata* leaves using green solvent. Food Bioprod. Process. 128, 1–11. https://doi.org/10.1016/j.fbp.2021.04.008

Baite, T.N., Mandal, B., Purkait, M.K., 2022. Antioxidant-Incorporated Poly(vinyl alcohol) Coating: Preparation, Characterization, and Influence on Ripening of Green Bananas. ACS Omega 7, 42320–42330. https://doi.org/10.1021/acsomega.2c05271

Barua, S., Rahi, T., Ullah, E., Ghosh, D., Ahmed, S., 2015. Delay in fruit ripening : a promising approach for reduction of spoilage and use of hazardous chemicals in Bangladesh. Int. J. Agron. Agric. Res. 6, 163–173.

Becerril-Bravo, E., Pablo Lamas, J., Sanchez-Prado, L., Lores, M., Garcia-Jares, C.,

Jimenez, B., Llompart, M., 2010. Ultrasound-assisted emulsification-microextraction of fragrance allergens in water. Chemosphere 81, 1378–1385. https://doi.org/10.1016/j.chemosphere.2010.09.028

Bucić-Kojić, A., Planinić, M., Tomas, S., Bilić, M., Velić, D., 2007. Study of solid-liquid extraction kinetics of total polyphenols from grape seeds. J. Food Eng. 81, 236–242. https://doi.org/10.1016/j.jfoodeng.2006.10.027

Bumbudsanpharoke, N., Wongphan, P., Promhuad, K., Leelaphiwat, P., Harnkarnsujarit, N., 2022. Morphology and permeability of bio-based poly(butylene adipate-co-terephthalate) (PBAT), poly(butylene succinate) (PBS) and linear low-density polyethylene (LLDPE) blend films control shelf-life of packaged bread. Food Control 132, 108541. https://doi.org/10.1016/j.foodcont.2021.108541

Cazón, P., Vázquez, M., Velázquez, G., 2020. Regenerated cellulose films with chitosan and polyvinyl alcohol: Effect of the moisture content on the barrier, mechanical and optical properties. Carbohydr. Polym. 236, 116031. https://doi.org/10.1016/j.carbpol.2020.116031

Chemat, F., Zill-E-Huma, Khan, M.K., 2011. Applications of ultrasound in food technology: Processing, preservation and extraction. Ultrason. Sonochem. 18, 813–835. https://doi.org/10.1016/j.ultsonch.2010.11.023

Chen, H., Zuo, Y., Deng, Y., 2001. Separation and determination of flavonoids and other phenolic compounds in cranberry juice by high-performance liquid chromatography. J. Chromatogr. A 913, 387–395. https://doi.org/10.1016/S0021-9673(00)01030-X

Chen, S., Lin, R., Lu, H., Wang, Q., Yang, J., Liu, J., Yan, C., 2020. Effects of phenolic acids on free radical scavenging and heavy metal bioavailability in *Kandelia obovata* under cadmium and zinc stress. Chemosphere 249, 126341. https://doi.org/10.1016/j.chemosphere.2020.126341

Chenwei, C., Zhipeng, T., Yarui, M., Weiqiang, Q., Fuxin, Y., Jun, M., Jing, X., 2018. Physicochemical, microstructural, antioxidant and antimicrobial properties of active packaging films based on poly(vinyl alcohol)/clay nanocomposite incorporated with tea polyphenols. Prog. Org. Coatings 123, 176–184. https://doi.org/10.1016/j.porgcoat.2018.07.001

Cheung, Y.C., Siu, K.C., Wu, J.Y., 2013. Kinetic Models for Ultrasound-Assisted Extraction of Water-Soluble Components and Polysaccharides from Medicinal Fungi. Food Bioprocess Technol. 6, 2659–2665. https://doi.org/10.1007/s11947-012-0929-z

Cláudio, A.F.M., Ferreira, A.M., Freire, C.S.R., Silvestre, A.J.D., Freire, M.G., Coutinho, J.A.P., 2012. Optimization of the gallic acid extraction using ionic-liquid-based aqueous two-phase systems. Sep. Purif. Technol. 97, 142–149. https://doi.org/10.1016/j.seppur.2012.02.036

Dastkhoon, M., Ghaedi, M., Asfaram, A., Ahmadi Azqhandi, M.H., Purkait, M.K., 2017. Simultaneous removal of dyes onto nanowires adsorbent use of ultrasound assisted adsorption to clean waste water: Chemometrics for modeling and optimization, multicomponent adsorption and kinetic study. Chem. Eng. Res. Des. 124, 222–237. https://doi.org/10.1016/j.cherd.2017.06.011

Dave, R.K., Ramana Rao, T. V., Nandane, A.S., 2017. Improvement of post-harvest

quality of pear fruit with optimized composite edible coating formulations. J. Food Sci. Technol. 54, 3917–3927. https://doi.org/10.1007/s13197-017-2850-y

Dávila, I., Gullón, P., Andrés, M.A., Labidi, J., 2017. Coproduction of lignin and glucose from vine shoots by eco-friendly strategies: Toward the development of an integrated biorefinery. Bioresour. Technol. 244, 328–337. https://doi.org/10.1016/j.biortech.2017.07.104

Deng, F., Zito, S.W., 2003. Development and validation of a gas chromatographic-mass spectrometric method for simultaneous identification and quantification of marker compounds including bilobalide, ginkgolides and flavonoids in *Ginkgo biloba* L. extract and pharmaceutical preparatio. J. Chromatogr. A 986, 121–127. https://doi.org/10.1016/S0021-9673(02)01921-0

Deng, Z., Jung, J., Simonsen, J., Zhao, Y., 2017. Cellulose nanomaterials emulsion coatings for controlling physiological activity, modifying surface morphology, and enhancing storability of postharvest bananas (*Musa acuminate*). Food Chem. 232, 359–368. https://doi.org/10.1016/j.foodchem.2017.04.028

Desai, S.D., Kundu, I., Swamy, N.P., Crull, G.B., Pan, D., Zhao, J., Shah, R.P., Venkatesh, C., Vig, B., Varia, S.A., Badawy, S.I.F., Desikan, S., Bhutani, H., 2020. Cross-linking of poly (vinyl alcohol) films under acidic and thermal stress. Eur. J. Pharm. Sci. 152, 105429. https://doi.org/10.1016/j.ejps.2020.105429

Devi, L.M., Lalnunthari, C., Badwaik, L.S., 2019. Direct Transformation of Muskmelon Seeds Meal into Biodegradable Films and Their Characterization. J. Polym. Environ. 27, 456–463. https://doi.org/10.1007/s10924-018-1361-x

Dhadge, V.L., Changmai, M., Purkait, M.K., 2019. Purification of catechins from

Camellia sinensis using membrane cell. Food Bioprod. Process. 117, 203–212. https://doi.org/10.1016/j.fbp.2019.07.010

Domínguez-Espinosa, M.E., Fuentes-Ruíz, A., Arreola-González, A., Jaime-Ornelas, T. de J., Morales-Ovando, M.A., Hernández-Méndez, J.M.E., Hernández-Cruz, M. del C., Cruz-Rodríguez, R.I., Romero-Cortés, T., Tirado-Gallegos, J.M., Cruz-Salomón, A., 2022. Edible coating based on banana starch and chitosan for postharvest conservation of guava. J. Food Process. Preserv. https://doi.org/10.1111/jfpp.16154

Dükkanci, M., Gündüz, G., 2006. Ultrasonic degradation of oxalic acid in aqueous solutions. Ultrason. Sonochem. 13, 517–522. https://doi.org/10.1016/j.ultsonch.2005.10.005

Dwivany, F.M., Aprilyandi, A.N., Suendo, V., Sukriandi, N., 2020. Carrageenan edible coating application prolongs Cavendish banana shelf life. Int. J. Food Sci. 2020. https://doi.org/10.1155/2020/8861610

Emani, S., Uppaluri, R., Purkait, M.K., 2013. Preparation and characterization of low cost ceramic membranes for mosambi juice clarification. Desalination 317, 32–40. https://doi.org/10.1016/j.desal.2013.02.024

Ena, A., Pintucci, C., Carlozzi, P., 2012. The recovery of polyphenols from olive mill waste using two adsorbing vegetable matrices. J. Biotechnol. 157, 573–577. https://doi.org/10.1016/j.jbiotec.2011.06.027

Esclapez, M.D., García-Pérez, J. V., Mulet, A., Cárcel, J.A., 2011. Ultrasound-Assisted Extraction of Natural Products. Food Eng. Rev. 3, 108–120. https://doi.org/10.1007/s12393-011-9036-6

References

Espinosa, E., Bascón-Villegas, I., Rosal, A., Pérez-Rodríguez, F., Chinga-Carrasco, G., Rodríguez, A., 2019. PVA/(ligno)nanocellulose biocomposite films. Effect of residual lignin content on structural, mechanical, barrier and antioxidant properties. Int. J. Biol. Macromol. 141, 197–206. https://doi.org/10.1016/j.ijbiomac.2019.08.262

Friedman, M., Jürgens, H.S., 2000. Effect of pH on the stability of plant phenolic compounds. J. Agric. Food Chem. 48, 2101–2110. https://doi.org/10.1021/jf990489j

Gaikwad, K.K., Singh, S., Negi, Y.S., 2020. Ethylene scavengers for active packaging of fresh food produce. Environ. Chem. Lett. 18, 269–284. https://doi.org/10.1007/s10311-019-00938-1

Gaire, B.P., Lamichhane, R., Sunar, C.B., Shilpakar, A., Neupane, S., Panta, S., 2011. Phytochemical screening and analysis of antibacterial and antioxidant activity of *Ficus auriculata* (Lour.) stem bark. Pharmacogn. J. 3, 49–55. https://doi.org/10.5530/pj.2011.21.8

Gallo, L., Ramírez-Rigo, M. V., Piña, J., Palma, S., Allemandi, D., & Bucalá, V. (2012). Valeriana officinalis dry plant extract for direct compression: Preparation and characterization. Scientia Pharmaceutica, *80*(4), 1013–1026. https://doi.org/10.3797/scipharm.1206-05

Garcia-Castello, E.M., Rodriguez-Lopez, A.D., Mayor, L., Ballesteros, R., Conidi, C., Cassano, A., 2015. Optimization of conventional and ultrasound assisted extraction of flavonoids from grapefruit (*Citrus paradisi* L.) solid wastes. Lwt 64, 1114–1122. https://doi.org/10.1016/j.lwt.2015.07.024

Gerke, I., Hamerski, F., Scheer, A., 2018. Solid–liquid extraction of bioactive compounds from yerba mate (*Ilex paraguariensis*) leaves: Experimental study, kinetics and modeling. J. Food Process Eng. 41.

Ghafoor, K., Choi, Y.H., Jeon, J.Y., Jo, I.H., 2009. Optimization of ultrasound-assisted extraction of phenolic compounds, antioxidants, and anthocyanins from grape (*Vitis vinifera*) seeds. J. Agric. Food Chem. 57, 4988–4994. https://doi.org/10.1021/jf9001439

Gol, N.B., Ramana Rao, T. V., 2011. Banana fruit ripening as influenced by edible coatings. Int. J. Fruit Sci. 11, 119–135. https://doi.org/10.1080/15538362.2011.578512

Golshan, T.A., Solaimani, D.N., Yasini, A.S.A., 2017. Physicochemical properties and applications of date seed and its oil. Int. Food Res. J. 24, 1399–1406.

Gomide, R.A.C., de Oliveira, A.C.S., Rodrigues, D.A.C., de Oliveira, C.R., de Assis, O.B.G., Dias, M.V., Borges, S.V., 2020. Development and Characterization of Lignin Microparticles for Physical and Antioxidant Enhancement of Biodegradable Polymers. J. Polym. Environ. 28, 1326–1334. https://doi.org/10.1007/s10924-020-01685-z

González-Centeno, M.R., Knoerzer, K., Sabarez, H., Simal, S., Rosselló, C., Femenia, A., 2014. Effect of acoustic frequency and power density on the aqueous ultrasonic-assisted extraction of grape pomace (*Vitis vinifera* L.) - A response surface approach. Ultrason. Sonochem. 21, 2176–2184. https://doi.org/10.1016/j.ultsonch.2014.01.021

González-Palma, I., Escalona-Buendía, H.B., Ponce-Alquicira, E., Téllez-Téllez, M.,

Gupta, V.K., Díaz-Godínez, G., Soriano-Santos, J., 2016. Evaluation of the antioxidant activity of aqueous and methanol extracts of *Pleurotus ostreatus* in different growth stages. Front. Microbiol. 7, 1–9. https://doi.org/10.3389/fmicb.2016.01099

Guan, Y., Shao, L., Dong, D., Wang, F., Zhang, Y., Wang, Y., 2016. Bio-inspired natural polyphenol cross-linking poly(vinyl alcohol) films with strong integrated strength and toughness. RSC Adv. 6, 69966–69972. https://doi.org/10.1039/c6ra08904f

Hajji, S., Younes, I., Affes, S., Boufi, S., Nasri, M., 2018. Optimization of the formulation of chitosan edible coatings supplemented with carotenoproteins and their use for extending strawberries postharvest life. Food Hydrocoll. 83, 375–392. https://doi.org/10.1016/j.foodhyd.2018.05.013

Haldar, D., Purkait, M.K., 2020. Thermochemical pretreatment enhanced bioconversion of elephant grass (*Pennisetum purpureum*): insight on the production of sugars and lignin. Biomass Convers. Biorefinery. https://doi.org/10.1007/s13399-020-00689-y

Harnly, J.M., Bhagwat, S., Lin, L.Z., 2007. Profiling methods for the determination of phenolic compounds in foods and dietary supplements. Anal. Bioanal. Chem. 389, 47–61. https://doi.org/10.1007/s00216-007-1424-7

Horikawa, Y., Hirano, S., Mihashi, A., Kobayashi, Y., Zhai, S., Sugiyama, J., 2019. Prediction of Lignin Contents from Infrared Spectroscopy: Chemical Digestion and Lignin/Biomass Ratios of *Cryptomeria japonica*. Appl. Biochem. Biotechnol. 188, 1066–1076. https://doi.org/10.1007/s12010-019-02965-8

Hossain, M.A., Rana, M.M., Kimura, Y., Roslan, H.A., 2014. Changes in biochemical

characteristics and activities of ripening associated enzymes in mango fruit during the storage at different temperatures. Biomed Res. Int. 2014. https://doi.org/10.1155/2014/232969

Hu, B., Chen, L., Lan, S., Ren, P., Wu, S., Liu, X., Shi, X., Li, H., Du, Y., Ding, F., 2018. Layer-by-layer assembly of polysaccharide films with self-healing and antifogging properties for food packaging applications. ACS Appl. Nano Mater. 1, 3733–3740. https://doi.org/10.1021/acsanm.8b01009

Hu, X.Q., Ye, D.Z., Tang, J.B., Zhang, L.J., Zhang, X., 2016. From waste to functional additives: Thermal stabilization and toughening of PVA with lignin. RSC Adv. 6, 13797–13802. https://doi.org/10.1039/c5ra26385a

Idris, A., Muntean, A., Mesic, B., Lestelius, M., Javed, A., 2021. Oxygen barrier performance of poly(Vinyl alcohol) coating films with different induced crystallinity and model predictions. Coatings 11. https://doi.org/10.3390/coatings11101253

Idumah, C.I., Hassan, A., Ihuoma, D.E., 2019. Recently emerging trends in polymer nanocomposites packaging materials. Polym. Technol. Mater. 58, 1054–1109. https://doi.org/10.1080/03602559.2018.1542718

Jin, L., Sun, S., Ryu, Y., Piao, Z.H., Liu, B., Choi, S.Y., Kim, G.R., Kim, H.S., Kee, H.J., Jeong, M.H., 2018. Gallic acid improves cardiac dysfunction and fibrosis in pressure overload-induced heart failure. Sci. Rep. 8, 1–11. https://doi.org/10.1038/s41598-018-27599-4

Kang, N., Lee, J.H., Lee, W.W., Ko, J.Y., Kim, E.A., Kim, J.S., Heu, M.S., Kim, G.H., Jeon, Y.J., 2015. Gallic acid isolated from Spirogyra sp. improves cardiovascular

disease through a vasorelaxant and antihypertensive effect. Environ. Toxicol. Pharmacol. 39, 764–772. https://doi.org/10.1016/j.etap.2015.02.006

Kasai, D., Chougale, R., Masti, S., Chalannavar, R., Malabadi, R.B., Gani, R., 2018. Influence of *Syzygium cumini* leaves extract on morphological, thermal, mechanical, and antimicrobial properties of PVA and PVA/chitosan blend films. J. Appl. Polym. Sci. 135. https://doi.org/10.1002/app.46188

Kasai, D., Chougale, R., Masti, S., Chalannavar, R., Malabadi, R.B., Gani, R., 2018. Influence of *Syzygium cumini* leaves extract on morphological, thermal, mechanical, and antimicrobial properties of PVA and PVA/chitosan blend films. J. Appl. Polym. Sci. 135. https://doi.org/10.1002/app.46188

Keller and Heckman, 2018. GRAS Notification for MonoSol's Use of Polyvinyl Alcohol (PVOH) as a Component in Edible Film. Https://Www.Fda.Gov/Food/Generally-Recognized-Safe-Gras/Gras-Notice-Inventory.

Korbag, I., Mohamed Saleh, S., 2016a. Studies on the formation of intermolecular interactions and structural characterization of polyvinyl alcohol/lignin film. Int. J. Environ. Stud. 73, 226–235. https://doi.org/10.1080/00207233.2016.1143700

Korbag, I., Mohamed Saleh, S., 2016b. Studies on the formation of intermolecular interactions and structural characterization of polyvinyl alcohol/lignin film. Int. J. Environ. Stud. 73, 226–235. https://doi.org/10.1080/00207233.2016.1143700

Leslie, C.A., Romani, R.J., 1988. Inhibition of ethylene biosynthesis by salicylic Acid. Plant Physiol. 88, 833–837. https://doi.org/10.1104/PP.88.3.833

Li, G., Li, X., Li, J., Lv, Z., Wang, H., Gao, R., Luo, L., 2021. Effect of natural green

coating materials on the postharvest quality of *Prunus salicina* Lindl. cv. 'Shazikongxinli fruit': A sustainable approach to prevent economic and food loss. Sustain. Chem. Pharm. 24, 100516. https://doi.org/10.1016/j.scp.2021.100516

Li, S., Chen, F., Jia, J., Liu, Z., Gu, H., Yang, L., Wang, F., Yang, F., 2016. Ionic liquid-mediated microwave-assisted simultaneous extraction and distillation of gallic acid, ellagic acid and essential oil from the leaves of *Eucalyptus camaldulensis*. Sep. Purif. Technol. 168, 8–18. https://doi.org/10.1016/j.seppur.2016.05.013

Li, S., Lundquist, K., 1994. A new method for the analysis of phenolic groups in lignins by ′H NMR spectrometry. Nord. Pulp Pap. Res. J. 9, 191–195. https://doi.org/10.3183/NPPRJ-1994-09-03-P191-195

Liao, J., Li, J., Wang, H., Zhu, Y., Essawy, H., Du, G., Zhou, X., 2022. Development of antioxidant packaging film based on chinese bayberry tannin extract and polyvinyl alcohol. J. Renew. Mater. 10, 19–31. https://doi.org/10.32604/JRM.2021.016152

Lin, C., Xia, G., Liu, S., 2017. Modeling and comparison of extraction kinetics of 8 catechins, gallic acid and caffeine from representative white teas. LWT - Food Sci. Technol. 83, 1–9. https://doi.org/10.1016/j.lwt.2017.04.028

Liu, C., Jin, T., Liu, W., Hao, W., Yan, L., Zheng, L., 2021. Effects of hydroxyethyl cellulose and sodium alginate edible coating containing asparagus waste extract on postharvest quality of strawberry fruit. Lwt 148, 111770. https://doi.org/10.1016/j.lwt.2021.111770

Liu, J., Yao, X., Yun, D., Zhang, M., Qian, C., Liu, Jun, 2021. Development of active packaging films based on quaternary ammonium chitosan, polyvinyl alcohol and

litchi (*Litchi chinensis* Sonn.) pericarp extract. Qual. Assur. Saf. Crop. Foods 13, 9–19. https://doi.org/10.15586/qas.v13iSP2.94

Liu, Juge, Yao, X., Yun, D., Zhang, M., Qian, C., Liu, Jun, 2021. Development of active packaging films based on quaternary ammonium chitosan, polyvinyl alcohol and litchi (*Litchi chinensis* Sonn.) pericarp extract. Qual. Assur. Saf. Crop. Foods 13, 9–19. https://doi.org/10.15586/qas.v13iSP2.94

Liu, Z., Chen, Z., Han, F., Kang, X., Gu, H., Yang, L., 2016. Microwave-assisted method for simultaneous hydrolysis and extraction in obtaining ellagic acid, gallic acid and essential oil from *Eucalyptus globulus* leaves using Brönsted acidic ionic liquid [HO3S(CH2)4mim]HSO4. Ind. Crops Prod. 81, 152–161. https://doi.org/10.1016/j.indcrop.2015.11.074

López, A.P., Gochicoa, M.T.N., Franco, A.R., 2010. Activities of antioxidant enzymes during strawberry fruit development and ripening. Biol. Plant. 54, 349–352. https://doi.org/10.1007/s10535-010-0061-8

Luque de Castro, M.D., Priego-Capote, F., Peralbo-Molina, A., 2011. The role of ultrasound in analytical derivatizations. J. Chromatogr. B Anal. Technol. Biomed. Life Sci. 879, 1189–1195. https://doi.org/10.1016/j.jchromb.2010.09.002

Luzi, F., Fortunati, E., Giovanale, G., Mazzaglia, A., Torre, L., Balestra, G.M., 2017. Cellulose nanocrystals from *Actinidia deliciosa* pruning residues combined with carvacrol in PVA_CH films with antioxidant/antimicrobial properties for packaging applications. Int. J. Biol. Macromol. 104, 43–55. https://doi.org/10.1016/j.ijbiomac.2017.05.176

Luzi, F., Pannucci, E., Santi, L., Kenny, J.M., Torre, L., Bernini, R., Puglia, D., 2019.

Gallic acid and quercetin as intelligent and active ingredients in poly(vinyl alcohol) films for food packaging. Polymers (Basel). 11, 1–20. https://doi.org/10.3390/polym11121999

Mansor, A.M., Lim, J.S., Ani, F.N., Hashim, H., Ho, W.S., 2019. Characteristics of cellulose, hemicellulose and lignin of MD2 pineapple biomass. Chem. Eng. Trans. 72, 79–84. https://doi.org/10.3303/CET1972014

Mariah, M.A.A., Vonnie, J.M., Erna, K.H., Nur'aqilah, N.M., Huda, N., Wahab, R.A., Rovina, K., 2022. The Emergence and Impact of Ethylene Scavengers Techniques in Delaying the Ripening of Fruits and Vegetables. Membranes (Basel). 12, 1–19. https://doi.org/10.3390/membranes12020117

Max, B., Salgado, J.M., Cortés, S., Domínguez, J.M., 2010. Extraction of phenolic acids by alkaline hydrolysis from the solid residue obtained after prehydrolysis of trimming vine shoots. J. Agric. Food Chem. 58, 1909–1917. https://doi.org/10.1021/jf903441d

Min, T., Zhu, Z., Sun, X., Yuan, Z., Zha, J., Wen, Y., 2020. Highly efficient antifogging and antibacterial food packaging film fabricated by novel quaternary ammonium chitosan composite. Food Chem. 308, 125682. https://doi.org/10.1016/j.foodchem.2019.125682

Miranda, K.W.E., Bresolin, J.D., Natarelli, C.V.L., Benevides, S.D., Bastos, M. do S.R., Mattoso, L.H.C., de Oliveira, J.E., 2021. Potential use of poly(lactic acid) nanofibers mats as Nano-sachets in postharvest of climacteric fruits and vegetables. J. Appl. Polym. Sci. 138. https://doi.org/10.1002/app.50735

Mokrani, A., Madani, K., 2016. Effect of solvent, time and temperature on the

extraction of phenolic compounds and antioxidant capacity of peach (*Prunus persica* L.) fruit. Sep. Purif. Technol. 162, 68–76. https://doi.org/10.1016/j.seppur.2016.01.043

Mondal, P., & Purkait, M. K. (2017). Green synthesized iron nanoparticle-embedded pH-responsive PVDF-co-HFP membranes: Optimization study for NPs preparation and nitrobenzene reduction. Separation Science and Technology (Philadelphia), *52*(14), 2338–2355. https://doi.org/10.1080/01496395.2016.1274759

Mushtaq, M., Sultana, B., Bhatti, H.N., Asghar, M., 2015. RSM based optimized enzyme-assisted extraction of antioxidant phenolics from underutilized watermelon (*Citrullus lanatus* Thunb.) rind. J. Food Sci. Technol. 52, 5048–5056. https://doi.org/10.1007/s13197-014-1562-9

Mustafa, P., Niazi, M.B.K., Jahan, Z., Rafiq, S., Ahmad, T., Sikander, U., Javaid, F., 2021. Improving functional properties of PVA/starch-based films as active and intelligent food packaging by incorporating propolis and anthocyanin. Polym. Polym. Compos. 29, 1472–1484. https://doi.org/10.1177/0967391120973503

Nandanwar, R.A., Chaudhari, A.R., Ekhe, J.D., 2016. Nitrobenzene Oxidation for Isolation of Value Added Products from Industrial Waste Lignin. J. Chem. Bio. Phy. Sci. Sec. D 6, 501–513.

Nawab, A., Alam, F., Hasnain, A., 2017. Mango kernel starch as a novel edible coating for enhancing shelf- life of tomato (*Solanum lycopersicum*) fruit. Int. J. Biol. Macromol. 103, 581–586. https://doi.org/10.1016/j.ijbiomac.2017.05.057

Nguyen, S. Van, Lee, B.K., 2022. PVA/CNC/TiO2 nanocomposite for food-packaging: Improved mechanical, UV/water vapor barrier, and antimicrobial properties.

Carbohydr. Polym. 298, 120064. https://doi.org/10.1016/j.carbpol.2022.120064

Núñez-Flores, R., Giménez, B., Fernández-Martín, F., López-Caballero, M.E., Montero, M.P., Gómez-Guillén, M.C., 2013. Physical and functional characterization of active fish gelatin films incorporated with lignin. Food Hydrocoll. 30, 163–172. https://doi.org/10.1016/j.foodhyd.2012.05.017

Othman, S.H., Amirah, S., Edwal, M., Risyon, N.P., Basha, R.K., Talib, R.A., 2017. Water sorption and water permeability properties of edible film made from potato peel waste. Food Sci. Technol. 37, 63–70. https://doi.org/https://doi.org/10.1590/1678-457X.30216

Pan, G., Yu, G., Zhu, C., Qiao, J., 2012. Optimization of ultrasound-assisted extraction (UAE) of flavonoids compounds (FC) from hawthorn seed (HS). Ultrason. Sonochem. 19, 486–490. https://doi.org/10.1016/j.ultsonch.2011.11.006

Parsafar, B., Ahmadi, M., Khaniki, G.J.J., Shariatifar, N., Foroushani, A.R., 2023. The impact of fruit and vegetable waste on economic loss estimation. Glob. J. Environ. Sci. Manag. 9, 871–884. https://doi.org/10.22035/gjesm.2023.04.14

Patel, M.K., Maurer, D., Feygenberg, O., Ovadia, A., Elad, Y., Oren-Shamir, M., Alkan, N., 2020. Phenylalanine: A promising inducer of fruit resistance to postharvest pathogens. Foods 9, 1–12. https://doi.org/10.3390/foods9050646

Peroni-Okita, F.H.G., Cardoso, M.B., Agopian, R.G.D., Louro, R.P., Nascimento, J.R.O., Purgatto, E., Tavares, M.I.B., Lajolo, F.M., Cordenunsi, B.R., 2013. The cold storage of green bananas affects the starch degradation during ripening at higher temperature. Carbohydr. Polym. 96, 137–147. https://doi.org/10.1016/j.carbpol.2013.03.050

Pham, B.T.T., Le, T.K.T., Nguyen, T.T., Van Tran, T., Van Nguyen, D., Bui, Q.T.P., Phung, T.K., 2022. Polyvinyl alcohol based functional coating incorporated with *Sonneratia ovata* extract: Preparation, characterization, and banana preservation. J. Appl. Polym. Sci. 1–13. https://doi.org/10.1002/app.52902

Pinho, E., Soares, G., Henriques, M., 2015. Cyclodextrin modulation of gallic acid in vitro antibacterial activity. J. Incl. Phenom. Macrocycl. Chem. 81, 205–214. https://doi.org/10.1007/s10847-014-0449-8

Plazzotta, S., Ibarz, R., Manzocco, L., Martín-Belloso, O., 2020. Optimizing the antioxidant biocompound recovery from peach waste extraction assisted by ultrasounds or microwaves. Ultrason. Sonochem. 63, 104954. https://doi.org/10.1016/j.ultsonch.2019.104954

Podsędek, A., Redzynia, M., Klewicka, E., & Koziołkiewicz, M. (2014). Matrix effects on the stability and antioxidant activity of red cabbage anthocyanins under simulated gastrointestinal digestion. *BioMed Research International*, *2014*. https://doi.org/10.1155/2014/365738

Posoknistakul, P., Tangkrakul, C., Chaosuanphae, P., Deepentham, S., Techasawong, W., Phonphirunrot, N., Bairak, S., Sakdaronnarong, C., Laosiripojana, N., 2020. Fabrication and characterization of lignin particles and their ultraviolet protection ability in PVA composite film. ACS Omega 5, 20976–20982. https://doi.org/10.1021/acsomega.0c02443

Purkait, M.K., 2011. Membrane Technologies and Applications. CRC Press. https://doi.org/10.1201/b11416

Purkait, M.K., DasGupta, S., De, S., 2006. Determination of design parameters for the

cloud point extraction of congo red and eosin dyes using TX-100. Sep. Purif. Technol. 51, 137–142. https://doi.org/10.1016/j.seppur.2005.12.027

Purkait, M.K., DasGupta, S., De, S., 2009. Determination of thermodynamic parameters for the cloud point extraction of different dyes using TX-100 and TX-114. Desalination 244, 130–138. https://doi.org/10.1016/j.desal.2008.04.042

Ramić, M., Vidović, S., Zeković, Z., Vladić, J., Cvejin, A., Pavlić, B., 2015. Modeling and optimization of ultrasound-assisted extraction of polyphenolic compounds from *Aronia melanocarpa* by-products from filter-tea factory. Ultrason. Sonochem. 23, 360–368. https://doi.org/10.1016/j.ultsonch.2014.10.002

Rooban, R., Shanmugam, M., Venkatesan, T., Tamilmani, C., 2016. Physiochemical changes during different stages of fruit ripening of climacteric fruit of mango (*Mangifera indica* L.) and non-climacteric of fruit cashew apple (Anacardium occidentale L.). J. Appl. Adv. Res. 1, 53–58. https://doi.org/10.21839/jaar.2016.v1i2.27

Rostagno, M.A., Palma, M., Barroso, C.G., 2003. Ultrasound-assisted extraction of soy isoflavones 1012, 119–128.

Rostami, H., Gharibzahedi, S.M.T., 2017. Mathematical Modeling of Mucilage Extraction Kinetic from the Waste Hydrolysates of Fruiting Bodies of *Zizyphus jujuba* Mill. J. Food Process. Preserv. 41. https://doi.org/10.1111/jfpp.13064

Rouhani, M., 2019. Modeling and optimization of ultrasound-assisted green extraction and rapid HPTLC analysis of stevioside from *Stevia Rebaudiana*. Ind. Crops Prod. 132, 226–235. https://doi.org/10.1016/j.indcrop.2019.02.029

Saidi, L., Duanis-Assaf, D., Galsarker, O., Maurer, D., Alkan, N., Poverenov, E., 2021.

Elicitation of fruit defense response by active edible coatings embedded with phenylalanine to improve quality and storability of avocado fruit. Postharvest Biol. Technol. 174, 111442. https://doi.org/10.1016/j.postharvbio.2020.111442

Saini, R., Garg, V., Dangwal, K., 2012. Comparative study of three wild edible fruits of Uttrakhand for antioxidant, antiproliferative activities and polyphenolic composition. Int. J. Pharma Bio Sci. 3, 158–167.

Saxena, R., De, M., 2021. Enhanced performance of supported Pd-Pt bimetallic catalysts prepared by modified electroless deposition for butane dehydrogenation. Appl. Catal. A Gen. 610, 117933. https://doi.org/10.1016/j.apcata.2020.117933

Segovia, F.J., Corral-Pérez, J.J., Almajano, M.P., 2016. Avocado seed: Modeling extraction of bioactive compounds. Ind. Crops Prod. 85, 213–220. https://doi.org/10.1016/j.indcrop.2016.03.005

Setyaningsih, W., Saputro, I.E., Carrera, C.A., Palma, M., 2019. Optimisation of an ultrasound-assisted extraction method for the simultaneous determination of phenolics in rice grains. Food Chem. 288, 221–227. https://doi.org/10.1016/j.foodchem.2019.02.107

Shahidi, F., Yeo, J.D., 2016. Insoluble-bound phenolics in food. Molecules 21. https://doi.org/10.3390/molecules21091216

Shi, Y.X., Xu, Y.K., Hu, H. Bin, Na, Z., Wang, W.H., 2011. Preliminary assessment of antioxidant activity of young edible leaves of seven Ficus species in the ethnic diet in Xishuangbanna, Southwest China. Food Chem. 128, 889–894. https://doi.org/10.1016/j.foodchem.2011.03.113

Shrestha, P.M., Dhillion, S.S., 2003. Medicinal plant diversity and use in the highlands

of Dolakha district, Nepal. J. Ethnopharmacol. 86, 81–96. https://doi.org/10.1016/S0378-8741(03)00051-5

Singh, M., Kamal, Y.T., Tamboli, E.T., Parveen, R., Siddiqui, K.M., Zaidi, S.M.A., Ahmad, S., 2012. Simultaneous estimation of gallic acid, ellagic acid, and ascorbic acid in *Emblica officinalis* and in unani polyherbal formulations by validated HPLC method. J. Liq. Chromatogr. Relat. Technol. 35, 2493–2502. https://doi.org/10.1080/10826076.2011.636468

Sinha, A., Gill, P.P.S., Jawandha, S.K., Kaur, P., Grewal, S.K., 2021. Chitosan-enriched salicylic acid coatings preserves antioxidant properties and alleviates internal browning of pear fruit under cold storage and supermarket conditions. Postharvest Biol. Technol. 182, 111721. https://doi.org/10.1016/j.postharvbio.2021.111721

Son, G. H., Lee, H. J., Na, Y. G., Lee, H. K., Kim, S. J., Huh, H. W., … Cho, C. W. (2019). Formulation and statistical analysis of an herbal medicine tablet containing *Morus alba* leaf extracts. *Journal of Pharmaceutical Investigation*, *49*(6), 625–634. https://doi.org/10.1007/s40005-018-00417-9

Soradech, S., Nunthanid, J., Limmatvapirat, S., Luangtana-anan, M., 2017. Utilization of shellac and gelatin composite film for coating to extend the shelf life of banana. Food Control 73, 1310–1317. https://doi.org/10.1016/j.foodcont.2016.10.059

Souza, M.C., Santos, M.P., Sumere, B.R., Silva, L.C., Cunha, D.T., Martínez, J., Barbero, G.F., Rostagno, M.A., 2020. Isolation of gallic acid, caffeine and flavonols from black tea by on-line coupling of pressurized liquid extraction with an adsorbent for the production of functional bakery products. Lwt 117, 108661. https://doi.org/10.1016/j.lwt.2019.108661

Suganthi, S., Vignesh, S., Kalyana Sundar, J., Raj, V., 2020. Fabrication of PVA polymer films with improved antibacterial activity by fine-tuning via organic acids for food packaging applications. Appl. Water Sci. 10, 1–11. https://doi.org/10.1007/s13201-020-1162-y

Suganthi, S., Vignesh, S., Kalyana Sundar, J., Raj, V., 2020. Fabrication of PVA polymer films with improved antibacterial activity by fine-tuning via organic acids for food packaging applications. Appl. Water Sci. 10, 1–11. https://doi.org/10.1007/s13201-020-1162-y

Sun, X., Wang, Z., Kadouh, H., Zhou, K., 2014. The antimicrobial, mechanical, physical and structural properties of chitosan-gallic acid films. LWT - Food Sci. Technol. 57, 83–89. https://doi.org/10.1016/j.lwt.2013.11.037

Sun, Z., Zhao, L., Zuo, L., Qi, C., Zhao, P., Hou, X., 2014. A UHPLC-MS/MS method for simultaneous determination of six flavonoids, gallic acid and 5,8-dihydroxy-1,4-naphthoquinone in rat plasma and its application to a pharmacokinetic study of Cortex Juglandis Mandshuricae extract. J. Chromatogr. B Anal. Technol. Biomed. Life Sci. 958, 55–62. https://doi.org/10.1016/j.jchromb.2014.03.013

Tang, C.M., Tian, Y.H., Hsu, S.H., 2015. Poly(vinyl alcohol) nanocomposites reinforced with bamboo charcoal nanoparticles: Mineralization behavior and characterization. Materials (Basel). 8, 4895–4911. https://doi.org/10.3390/ma8084895

Tang, C.M., Tian, Y.H., Hsu, S.H., 2015. Poly(vinyl alcohol) nanocomposites reinforced with bamboo charcoal nanoparticles: Mineralization behavior and characterization. Materials (Basel). 8, 4895–4911.

https://doi.org/10.3390/ma8084895

Teller, C., Holweg, C., Reiner, G., Kotzab, H., 2018. Retail store operations and food waste. J. Clean. Prod. 185, 981–997. https://doi.org/10.1016/j.jclepro.2018.02.280

Terzioğlu, P., Güney, F., Parın, F.N., Şen, İ., Tuna, S., 2021. Biowaste orange peel incorporated chitosan/polyvinyl alcohol composite films for food packaging applications. Food Packag. Shelf Life 30. https://doi.org/10.1016/j.fpsl.2021.100742

Thakur, R., Pristijono, P., Bowyer, M., Singh, S.P., Scarlett, C.J., Stathopoulos, C.E., Vuong, Q. V., 2019. A starch edible surface coating delays banana fruit ripening. Lwt 100, 341–347. https://doi.org/10.1016/j.lwt.2018.10.055

Thingbaijam, R., Dutta, B.K., Paul, S.B., 2012. Phytochemical screening and antibacterial studies of the leaf extract of *Eurya japonica* Thunb. and *Ficus auriculata* Lour. J. Pure Appl. Microbiol. 4, 4–7.

Tromp, S.O., Haijema, R., Rijgersberg, H., van der Vorst, J.G.A.J., 2016. A systematic approach to preventing chilled-food waste at the retail outlet. Int. J. Prod. Econ. 182, 508–518. https://doi.org/10.1016/j.ijpe.2016.10.003

Turhan, M., Sayar, S., Gunasekaran, S., 2002. Application of Peleg model to study water absorption in chickpea during soaking. J. Food Eng. 53, 153–159. https://doi.org/10.1016/S0260-8774(01)00152-2

Vadivel, V., Brindha, P., 2015. Antioxidant property of solvent extract and acid/alkali hydrolysates from rice hulls. Food Biosci. 11, 85–91. https://doi.org/10.1016/j.fbio.2015.06.002

Variya, B.C., Bakrania, A.K., Patel, S.S., 2020. Antidiabetic potential of gallic acid

from *Emblica officinalis*: Improved glucose transporters and insulin sensitivity through PPAR-γ and Akt signaling. Phytomedicine 73, 152906. https://doi.org/10.1016/j.phymed.2019.152906

Vieira, G.S., Cavalcanti, R.N., Meireles, M.A.A., Hubinger, M.D., 2013. Chemical and economic evaluation of natural antioxidant extracts obtained by ultrasound-assisted and agitated bed extraction from jussara pulp (*Euterpe edulis*). J. Food Eng. 119, 196–204. https://doi.org/10.1016/j.jfoodeng.2013.05.030

Vu, C.H.T., Won, K., 2013. Novel water-resistant UV-activated oxygen indicator for intelligent food packaging. Food Chem. 140, 52–56. https://doi.org/10.1016/j.foodchem.2013.02.056

Vuong, Q. V., Hirun, S., Roach, P.D., Bowyer, M.C., Phillips, P.A., Scarlett, C.J., 2013. Effect of extraction conditions on total phenolic compounds and antioxidant activities of Carica papaya leaf aqueous extracts. J. Herb. Med. 3, 104–111. https://doi.org/10.1016/j.hermed.2013.04.004

Wantat, A., Rojsitthisak, P., Seraypheap, K., 2021. Inhibitory effects of high molecular weight chitosan coating on 'Hom Thong' banana fruit softening. Food Packag. Shelf Life 29, 100731. https://doi.org/10.1016/j.fpsl.2021.100731

Xia, E.Q., Yu, Y.Y., Xu, X.R., Deng, G.F., Guo, Y.J., Li, H. Bin, 2012. Ultrasound-assisted extraction of oleanolic acid and ursolic acid from *Ligustrum lucidum* Ait. Ultrason. Sonochem. 19, 772–776. https://doi.org/10.1016/j.ultsonch.2011.11.014

Xie, J., Wang, R., Li, Y., Ni, Z., Situ, W., Ye, S., Song, X., 2022. A novel Ag2O-TiO2-Bi2WO6/polyvinyl alcohol composite film with ethylene photocatalytic degradation performance towards banana preservation. Food Chem. 375, 131708.

https://doi.org/10.1016/j.foodchem.2021.131708

Xiong, X., Sun, J., Hu, D., Xiao, C., Wang, J., Zhuo, Q., Qin, C., Dai, L., 2020. Fabrication of polyvinyl alcohol hydrogels with excellent shape memory and ultraviolet-shielding behaviorviathe introduction of tea polyphenols. RSC Adv. 10, 35226–35234. https://doi.org/10.1039/d0ra06053d

Yang, W., Fortunati, E., Dominici, F., Giovanale, G., Mazzaglia, A., Balestra, G.M., Kenny, J.M., Puglia, D., 2016a. Effect of cellulose and lignin on disintegration, antimicrobial and antioxidant properties of PLA active films. Int. J. Biol. Macromol. 89, 360–368. https://doi.org/10.1016/j.ijbiomac.2016.04.068

Yang, W., Owczarek, J.S., Fortunati, E., Kozanecki, M., Mazzaglia, A., Balestra, G.M., Kenny, J.M., Torre, L., Puglia, D., 2016b. Antioxidant and antibacterial lignin nanoparticles in polyvinyl alcohol/chitosan films for active packaging. Ind. Crops Prod. 94, 800–811. https://doi.org/10.1016/j.indcrop.2016.09.061

Yang, Z., Zhai, X., Zhang, C., Shi, J., Huang, X., Li, Z., Zou, X., Gong, Y., Holmes, M., Povey, M., Xiao, J., 2022. Agar/TiO2/radish anthocyanin/neem essential oil bionanocomposite bilayer films with improved bioactive capability and electrochemical writing property for banana preservation. Food Hydrocoll. 123, 107187. https://doi.org/10.1016/j.foodhyd.2021.107187

Yavari, Saba, Kamyab, H., Binti Abd Manan, T.S., Chelliapan, S., Asadpour, R., Yavari, Sara, Sapari, N. Bin, Baloo, L., Sidik, A.B.C., Kirpichnikova, I., 2022. Bio-efficacy of imidazolinones in weed control in a tropical paddy soil amended with optimized agrowaste-derived biochars. Chemosphere 303, 134957. https://doi.org/10.1016/j.chemosphere.2022.134957

Ye, D.Z., Jiang, L., Hu, X.Q., Zhang, M.H., Zhang, X., 2016. Lignosulfonate as reinforcement in polyvinyl alcohol film: Mechanical properties and interaction analysis. Int. J. Biol. Macromol. 83, 209–215. https://doi.org/10.1016/j.ijbiomac.2015.11.064

Youssef, H.F., El-naggar, M.E., Fouda, F.K., Youssef, A.M., 2019. Antimicrobial packaging film based on biodegradable CMC / PVA-zeolite doped with noble metal cations. Food Packag. Shelf Life 22, 100378. https://doi.org/10.1016/j.fpsl.2019.100378

Yu, S.H., Tsai, M.L., Lin, B.X., Lin, C.W., Mi, F.L., 2015. Tea catechins-cross-linked methylcellulose active films for inhibition of light irradiation and lipid peroxidation induced β-carotene degradation. Food Hydrocoll. 44, 491–505. https://doi.org/10.1016/j.foodhyd.2014.10.022

Zanela, J., Bilck, A.P., Casagrande, M., Grossmann, M.V.E., Yamashita, F., 2018. Polyvinyl alcohol (PVA) molecular weight and extrusion temperature in starch/PVA biodegradable sheets. Polimeros 28, 256–265. https://doi.org/10.1590/0104-1428.03417

Zhai, X., Sun, Y., Cen, S., Wang, Xinyu, Zhang, J., Yang, Z., Li, Y., Wang, Xin, Zhou, C., Arslan, M., Li, Z., Shi, J., Huang, X., Zou, X., Gong, Y., Holmes, M., Povey, M., 2022. Anthocyanins-encapsulated 3D-printable bigels: A colorimetric and leaching-resistant volatile amines sensor for intelligent food packaging. Food Hydrocoll. 133, 107989. https://doi.org/10.1016/j.foodhyd.2022.107989

Zhang, Q.A., Shen, H., Fan, X.H., Shen, Y., Wang, X., Song, Y., 2015. Changes of gallic acid mediated by ultrasound in a model extraction solution. Ultrason.

Sonochem. 22, 149–154. https://doi.org/10.1016/j.ultsonch.2014.06.010

Zhu, X., Shen, L., Fu, D., Si, Z., Wu, B., Chen, W., Li, X., 2015. Effects of the combination treatment of 1-MCP and ethylene on the ripening of harvested banana fruit. Postharvest Biol. Technol. 107, 23–32. https://doi.org/10.1016/j.postharvbio.2015.04.010